

THE CROSSFIELD CURRENT-DRIVEN ION ACOUSTIC  
INSTABILITY IN A TWO-ION PLASMA

by

*Jagathesan Govender*

Submitted in partial fulfilment of the requirements for the degree  
of Master of Science in the Department of Physics in the Faculty of  
Science at the University of Durban-Westville.

Supervisor: Dr R. Bharuthram

Date Submitted: November 1987

(ii)

TO SHAMLA

|  |
|--|
| <b>UNIVERSITY OF DURBAN-</b><br><b>WESTVILLE LIBRARY</b> |
| BRN <u>121573</u>  |
| CLASS No. <u>530.44 GOV</u>                              |

ACKNOWLEDGEMENTS

The presentation of this thesis would not have been possible without the important contributions from the following people:

Dr R. Bharuthram, whose expert guidance, availability and encouragement is most gratefully appreciated;

Professor M.A. Hellberg, for many helpful discussions;

Mr S. Baboolal, for his assistance in the computing;

Professor K. Bharuth-Ram, for his interest and encouragement;

Mr L. Subramony, for his assistance in the preparation of this thesis;

Mrs P.V. Subramony, for her painstaking typing of this thesis;

My colleagues at Springfield College of Education, especially those in the Science and Computer Science Departments, for their concern and assistance;

Finally, I am especially grateful to my wife, Shamla, for her patience and encouragement;

To all of the above and many other well wishers, my sincerest thanks and appreciation.

ABSTRACT

The behaviour of the crossfield current-driven ion acoustic instability in a plasma containing two ion species is theoretically examined. In our model the electrons are assumed to be hot and the ions cold, i.e.  $T_e \gg T_i$  ( $\sim 0$ ), where both ion species are given the same temperature. The length and time scales are such that the electrons are magnetized and the ions unmagnetized.

The linearised Vlasov equation is used to set up a dispersion relation for electrostatic waves for Maxwellian equilibrium velocity distributions of the electrons and ions. For the ion acoustic wave, a study is made of the dependence of the critical electron drift velocity ( $V_0^C$ ) required to excite an instability on several parameters. The parameters include light ion fraction, heavy to light ion mass ratio, magnetic field strength and the propagation angle. In general the maximum value of  $V_0^C$  is found to be smaller than that for an unmagnetized plasma. Approximate analytic solutions of the dispersion relation are used to make comparisons with solutions from the full dispersion relation.

The effect of drifts due to inhomogeneities in external magnetic field, perpendicular electron temperature and electron density on the growth rate of the ion acoustic instability are investigated in the ion rest frame.

Finally, in a reference frame in which the electrons are stationary, both ion species are given external drifts. The effects of the ion drift velocities (both equal and unequal), electron to ion temperature ratio, light ion fraction, and heavy to light ion mass ratio on the growth rate of the ion acoustic instability are then studied.

C O N T E N T S

|   | PAGE |
|---|------|
| CHAPTER ONE : INTRODUCTION  | 1    |
| 1.1 ION ACOUSTIC WAVES  | 1    |
| 1.2 OUTLINE OF THIS THESIS  | 3    |
| CHAPTER TWO : LITERATURE SURVEY OF THE CROSSFIELD ION<br>ACOUSTIC INSTABILITY   | 4    |
| 2.1 ION ACOUSTIC INSTABILITY IN A SINGLE-ION<br>PLASMA  | 4    |
| 2.2 ION ACOUSTIC WAVES IN A TWO-ION PLASMA  | 7    |
| CHAPTER THREE : THE PLASMA DISPERSION RELATION FOR<br>CROSSFIELD CURRENT-DRIVEN ION ACOUSTIC<br>WAVES IN A TWO-ION PLASMA | 12   |
| 3.1 INTRODUCTION  | 12   |
| 3.2 THE ELECTRON TERM   | 13   |
| 3.3 THE ION TERMS   | 20   |
| 3.4 THE DISPERSION RELATION   | 21   |
| 3.5 THE APPROXIMATE DISPERSION RELATION FOR<br>MARGINAL STABILITY OF ION ACOUSTIC WAVES                                   | 25   |
| 3.6 MARGINAL STABILITY STUDIES USING BOTH THE<br>FULL AND APPROXIMATE DISPERSION RELATIONS                                | 29   |
| 3.6.1 Variation of $V_0^C$ with Light Ion Fraction (f)  | 29   |
| 3.6.2 Variation of the Wave Phase Speed with<br>Light Ion Fraction (f)  | 37   |
| 3.6.3 Variation of $(V_0^C)_{\max}$ with Heavy to Light<br>Ion Mass Ratio (M)   | 39   |
| 3.6.4 Variation of $(V_0^C)_{\max}$ with Magnetic Field<br>Strength   | 45   |
| 3.6.5 Variation of $(V_0^C)_{\max}$ with Propagation Angle  | 45   |

|  | PAGE |
|--|------|
| CHAPTER FOUR : THE EFFECT OF INHOMOGENEITIES ON THE<br>CROSSFIELD CURRENT-DRIVEN ION ACOUSTIC<br>INSTABILITY IN A TWO-ION PLASMA | 49   |
| 4.1 DERIVATION OF THE ELECTRON TERM IN THE<br>LINEAR DISPERSION RELATION   | 49   |
| 4.2 THE GENERAL DISPERSION RELATION  | 60   |
| 4.3 THE APPROXIMATE DISPERSION RELATION  | 60   |
| 4.4 NUMERICAL ANALYSIS OF THE FULL AND<br>APPROXIMATE DISPERSION RELATIONS   | 65   |
| 4.4.1 Effect of the Normalised $\vec{E} \times \vec{B}$ Drift<br>( $V_0/c_e$ )   | 66   |
| 4.4.2 Effect of Increasing $\theta = T_e/T_i$  | 69   |
| 4.4.3 Effect of Varying the Light Ion Fraction, $f$  | 71   |
| 4.4.4 Effect of Inhomogeneities  | 71   |
| 4.4.5 Effect of Varying Propagation Angle ( $k_z/k$ )  | 74   |
| 4.4.6 Effect of Magnetic Field   | 78   |
| CHAPTER FIVE : THE CROSSFIELD ION ACOUSTIC INSTABILITY<br>IN A TWO-ION PLASMA WITH DRIFTING IONS                                 | 82   |
| 5.1 THE PLASMA DISPERSION RELATION FOR<br>DRIFTING IONS  | 82   |
| 5.2 NUMERICAL ANALYSIS   | 84   |
| CHAPTER SIX : SUMMARY AND CONCLUSION   | 99   |
| REFERENCES   | 104  |

LIST OF SYMBOLS

|               |   |
|---------------|---|
| b             | argument of modified Bessel functions = $k_{\perp}^2 c_e^2 / \Omega_e^2$  |
| $\vec{B}$     | magnetic field vector   |
| c             | speed of light  |
| $c_e$         | electron thermal speed = $\sqrt{T_e / m_e}$   |
| $c_{L(H)}$    | light (heavy) ion thermal speed = $\sqrt{T_{L(H)} / M_{L(H)}}$  |
| $c_{SL(H)}$   | light (heavy) ion sound speed = $\sqrt{T_e / M_{L(H)}}$   |
| $d\vec{V}$    | volume element<br>in velocity space } = $dV_x dV_y dV_z$ (cartesian)<br>$V_{\perp} dV_{\perp} dV_z d\theta$ (cylindrical) |
| $\vec{E}$     | electric field vector   |
| e             | magnitude of electronic charge  |
| f             | fraction of light ions = $n_{oL} / n_{oe}$  |
| $f_j$         | velocity distribution function of particles of type j   |
| $f_j^{(o)}$   | equilibrium distribution of particles of type j   |
| H             | subscript referring to heavy ions   |
| i             | imaginary number = $\sqrt{-1}$  |
| $I_{\ell}$    | modified Bessel function of first kind of order $\ell$  |
| $I_m(\omega)$ | imaginary part of complex quantity $\omega$   |
| $J_p$         | Bessel function of first kind of order p  |
| $\vec{k}$     | wave propagation vector   |
| $k_{\perp}$   | component of $\vec{k}$ perpendicular to $\vec{B} = \sqrt{k_x^2 + k_y^2}$  |
| $k_D$         | inverse electron Debye length = $\lambda_D^{-1}$  |
| L             | subscript referring to light ions   |
| $M_{L(H)}$    | mass of light (heavy) ion   |
| M             | heavy to light ion mass ratio = $M_H / M_L$   |
| $m_e$         | mass of electron  |

|                               |   |
|-------------------------------|---|
| $\bar{m}$                     | heavy ion to electron mass ratio = $M_H/m_e$  |
| $n_j$                         | density of particles of type j  |
| $n_{oj}$                      | equilibrium density of particles of type j  |
| $\vec{r}$                     | position vector = (x, y, z)   |
| $r_e$                         | electron gyroradius   |
| $r_{L(H)}$                    | light (heavy) ion gyroradius  |
| $R_e(\omega)$                 | real part of complex quantity $\omega$  |
| $T_e$                         | Boltzmann's constant x electron temperature   |
| $T_{L(H)}$                    | Boltzmann's constant x light (heavy) ion temperature  |
| $T_i$                         | Boltzmann's constant x ion temperature  |
| $\vec{V}$                     | velocity vector   |
| $\vec{V}_B$                   | magnetic field gradient drift velocity = $(\epsilon V_{\perp}^2 / 2\Omega_e) \hat{y}$           |
| $\vec{V}_n$                   | density gradient drift velocity = $(\alpha T_{e0} / m_e \Omega_e) \hat{y}$                      |
| $\vec{V}_O$                   | $\vec{E} \times \vec{B}$ drift velocity = $(eE_0 / B_0) \hat{y}$                                |
| $\vec{V}_T$                   | perpendicular temperature gradient drift velocity<br>= $(\delta T_{e0} / m_e \Omega_e) \hat{y}$ |
| $V_{\phi}$                    | wave phase velocity   |
| $(\hat{x}, \hat{y}, \hat{z})$ | set of cartesian unit vectors   |
| $Z(\lambda)$                  | plasma dispersion function with argument $\lambda$  |
| $Z'(\lambda)$                 | first derivative of plasma dispersion function  |
| $\alpha^{-1}$                 | scale length of non-uniformity of electron density  |
| $\gamma$                      | imaginary part of complex frequency $\omega$  |
| $\delta^{-1}$                 | scale length of non-uniformity of perpendicular electron temperature                            |
| $\epsilon^{-1}$               | scale length of non-uniformity of magnetic field  |
| $\theta$                      | electron to ion temperature ratio = $T_e/T_i$   |
| $\lambda$                     | wavelength  |



|                     |   |
|---------------------|---|
| $\lambda_D$         | electron Debye length = $(T_e/4\pi n_e e^2)$  |
| $\rho$              | $(1 + k^2 \lambda_D^2)^{-\frac{1}{2}}$  |
| $\varphi$           | propagation angle = $\cos^{-1} (k_z/k)$   |
| $\phi$              | electric potential  |
| $\omega$            | complex frequency   |
| $\omega_R$          | real part of complex frequency $\omega$   |
| $\omega_{pe}$       | electron plasma frequency = $(4\pi n_e e^2/m_e)^{1/2}$  |
| $\omega_{pi}$       | ion plasma frequency = $(4\pi n_i e^2/M_i)^{1/2}$   |
| $\Gamma_p$          | $e^{-b} I_p(b)$   |
| $\Phi$              | angle between $k_x$ and $k_{\perp}$ components of $\vec{k}$   |
| $\Omega_e$          | electron gyrofrequency = $eB/m_e c$   |
| $\Omega_i$          | ion gyrofrequency = $eB/M_i c$  |
| $\nabla$            | differential operator = $\frac{\partial}{\partial x} \hat{x} + \frac{\partial}{\partial y} \hat{y} + \frac{\partial}{\partial z} \hat{z}$ |
| $\nabla B$          | magnetic field gradient   |
| $\nabla n$          | electron density gradient   |
| $\nabla T_{e\perp}$ | perpendicular electron temperature gradient   |

## CHAPTER ONE

### INTRODUCTION

Experimental measurements in magnetically confined plasmas, especially in fusion-oriented devices such as tokamaks and stellarators, indicate anomalous particle and energy transport across the confining magnetic field. It is widely suggested that such observations are due to turbulence associated with plasma waves and instabilities. In this regard, of particular interest are the electrostatic instabilities since they have faster growth rates in most cases. Of such modes, the low frequency ion acoustic wave (and associated instability) has received much experimental and theoretical investigation.

#### 1.1 ION ACOUSTIC WAVES

When the frequency of an incoming signal in a plasma is decreased to that of the ion plasma frequency, the massive ions respond to the signal and are set into vibration. As the frequency is decreased below the ion plasma frequency, the ion oscillations become more coherent and ion acoustic waves are set up.

Ion acoustic waves in a plasma were first observed by Wong et al. (1964) in a Q-machine. The phase velocity of such waves in a single ion plasma can be found by the use of fluid theory (see, e.g., Chen, 1974), and is given by

$$\frac{\omega}{k} = \left( \frac{T_e}{M_i} \frac{1}{1 + k^2 \lambda_D^2} + \frac{\gamma_i T_i}{M_i} \right)^{1/2} \quad (1.1.1)$$

where  $T_e(T_i)$  is the electron (ion) temperature,  $M_i$  the ion mass,  $\gamma_i$  the ratio of the specific heats for the ion,  $\lambda_D = (T_e/4\pi n_0 e^2)^{1/2}$ , the electron Debye length, with  $n_0$  being the equilibrium plasma density. For most experimental parameters,  $k\lambda_D \ll 1$  and  $T_e \gg T_i (\sim 0)$ . Then the phase velocity can be written as

$$\frac{\omega}{k} = \left( \frac{T_e}{M_i} \right)^{1/2} \equiv c_s \quad (1.1.2)$$

where  $c_s$  is the ion sound speed. It can thus be seen that the ion acoustic wave is basically a constant-velocity wave and exists only when there is thermal motion. This can be explained by noting that the electrons are dragged along with the oscillating ions and as a result tend to shield out the electric fields arising from the bunching of the ions. This shielding, however, is not perfect because of the thermal motion of the electrons. The resulting electric field (proportional to  $T_e$ ) exerts a restoring force on the ions. But the ions overshoot their equilibrium position because of their inertia. This sets up ion acoustic waves in the plasma.

Ion acoustic waves have been thoroughly investigated in single-ion plasmas, both experimentally and theoretically. More recent attention has been given to their behaviour in two-ion plasmas. While much work has been done in unmagnetized plasmas, the study of ion acoustic waves in magnetized plasmas is incomplete. Here, we examine the behaviour of the ion acoustic instability in a magnetized two-ion plasma with crossfield drifts acting as the driving mechanism.

## 1.2 OUTLINE OF THIS THESIS

The studies in this thesis are based on the linear theory of the electrostatic instabilities in a collisionless magnetized two-ion plasma. Chapter Two presents a literature survey of both theoretical and experimental investigations of the ion acoustic instability. The linear dispersion relation for a model consisting of drifting Maxwellian electrons and stationary ions is established in Chapter Three. Series and asymptotic expansions of the plasma dispersion function are used to obtain approximate solutions to the dispersion relation. Marginal stability studies are made to show the dependence of the critical external electron drift speed required to excite the instability on the fraction of light ions. The dependence on other parameters, such as heavy to light ion mass ratio, strength of magnetic field and propagation angle are also examined.

The effect of inhomogeneities in electron temperature, electron density and external magnetic field on the instability growth rate is studied in Chapter Four. In Chapter Five, we adopt a model in which the electrons are stationary and both the ion species given external drifts. The effect of the ion drift velocities (both equal and unequal), electron to ion temperature ratio, light ion fraction and heavy to light ion mass ratio on the ion acoustic instability growth rate are studied.

The main results of this thesis are summarised in Chapter Six. Conclusions are also drawn and possible extensions to the work presented are discussed.

## CHAPTER TWO

### LITERATURE SURVEY OF THE CROSSFIELD ION ACOUSTIC INSTABILITY

The crossfield current-driven ion acoustic instability (Gary, 1970) is one of a set of low frequency electrostatic instabilities generated when a current flows across a magnetic field  $\vec{B}_0$ . The instability is characterised by  $(m_e/M_i)^{1/2} < (k_z/k_\perp) < 1$  with  $V_0 > c_s$  and  $T_e > T_i$ , where  $m_e$  is the electron mass and  $k_z(k_\perp)$  is the component of the wave vector parallel (perpendicular) to the magnetic field.

#### 2.1 ION ACOUSTIC INSTABILITY IN A SINGLE-ION PLASMA

This section is included not only for completeness but also since the effect of gradients on the growth rate of the ion acoustic instability in a two-ion plasma is similar to that in a single-ion plasma. We present a brief survey of studies undertaken.

Krall and Book (1969) conducted an initial theoretical investigation of the ion acoustic instability propagating across a magnetic field  $\vec{B}$ . Spatial gradients in the magnetic field  $\vec{B}$  and electron density  $n$  were used to drive the instability. They found that the growth rates for the crossfield mode and the field free modes were comparable.

Priest and Sanderson (1972) made a theoretical study of the effect of temperature, density and magnetic field gradients on the ion acoustic instability in perpendicular shocks. Making the assumptions  $(k_y \rho_e)^2 \gg 1$  and  $(k_z \rho_e)^2 \gg 1$  with  $\vec{k} = (0, \vec{k}_y, \vec{k}_z)$  and  $\rho_e$  being the electron gyroradius, they derived an expression for the growth rate

via the Gordeyev integral. It was found that a large temperature gradient in strong shocks considerably increased the growth rate of the ion acoustic instability and this effect was explained in terms of a distortion in the electron velocity distribution function. (For a more detailed explanation, see Chapter Four of this thesis). The effect of the density gradient was found to be small, while the magnetic field gradient only produced a slight correction to the growth rate.

Lashmore-Davies and Martin (1973) made a study of the linear theory of all fast growing ( $\gamma > \Omega_i$ ) electrostatic instabilities which occur when a current flows perpendicular to a magnetic field, for the temperature ranges  $T_e \gg T_i$ ,  $T_e = T_i$  and  $T_i = 10 T_e$ . Although they worked with a homogenous plasma, their findings, especially the establishment of an upper limit for the propagation of the modified two-stream instability is important to our work. This limit was found to be  $(k_z/k) \sim (m_e/M_i)^{1/2}$ . As  $(k_z/k)$  increases, the modified two-stream instability changes into the ion acoustic instability. They also found that the effect of the magnetic field was to enhance the growth rate.

Bharuthram and Hellberg (1974) made a numerical study of the role of weak gradients in density, perpendicular electron temperature and magnetic field on the crossfield current-driven ion acoustic instability. In their model the dominant drift,  $\vec{V}_0$ , was either an external beam or an  $\vec{E} \times \vec{B}$  drift. The destabilizing effect of the temperature gradient (Priest and Sanderson, 1972) was only observed for the regime  $k_{\perp} \rho_e \gtrsim 1$ , with  $k_z \neq 0$ . On the other hand, the density gradient always had a stabilising effect.

Hirose et al. (1972) have reported experimental observations of the ion acoustic instability in a toroidal turbulent-heating machine. For  $T_e/T_i \gtrsim 40$ , they found that the wave propagated across the field in a direction opposite to that of the electron diamagnetic current. The growth rate was observed to be greater in the presence of a temperature gradient than for an  $\vec{E} \times \vec{B}$  or  $\nabla n$  drift.

Hayzen and Barrett (1977) used a double-plasma device to study the crossfield current-driven ion acoustic instability driven by an ion beam. The growth rate of the ion acoustic instability was investigated as a function of  $k_{\perp} \rho_e$  and the magnetic field angle  $\theta$ . Allowing for the finiteness of the plasma and the effect of ion-neutral collisions, the authors found good agreement between the measured growth rates and the equivalent theoretical estimates.

We conclude this section by making a brief review of some of the more recent research on ion acoustic waves in a single-ion plasma. Much of this research has been on non-linear aspects such as the propagation of solitons. Lonngren et al. (1982) have performed a series of experiments to investigate the propagation of grid launched linear and non-linear ion acoustic waves. They suggested that a soliton or a dispersing "Airy function" response could be used as a diagnostic tool to determine the plasma density. Gabl et al. (1984) interpreted the ion acoustic wave excitation in terms of "klystron bunching" using a water bag model. A condition for optimum excitation of planar solitons was also derived by these authors. In another study on grid launched linear and non-linear ion acoustic waves, Raychaudhuri et al. (1984) observed that spherical ion acoustic solitons could be launched from a small planar grid.

In other non-linear investigations, Bharuthram and Hellberg (1982), have used quasilinear theory to study the saturation of the cross-field current-driven ion acoustic instability. Majeski et al. (1984) have observed the suppression of the current-driven ion acoustic instability in a single-ended Q-machine. This occurred as a result of non-linear coupling produced by pondermotive effects arising from the introduction of a large amplitude lower hybrid wave. Sekar and Saxena (1985) have demonstrated the formation of ion acoustic double layers in a laboratory plasma, starting from the linear growth of ion acoustic instabilities in a current-carrying plasma.

## 2.2 ION ACOUSTIC WAVES IN A TWO-ION PLASMA

Plasmas containing more than one ion species play an important part in the study of the upper ionosphere and fusion plasmas as well as in the study of laboratory plasmas.

The ion Landau damping of ion acoustic waves in a two-ion plasma was first observed by Alexeff et al. (1967) in their now classic experiment. The addition of a small concentration (about 0.3%) of light ions was found to sharply damp the growth rate of the ion acoustic instability, although the effective ion mass (and hence the phase velocity) was almost unchanged.

Hirose et al. (1970) have experimentally investigated the effects of magnetic fields and propagation angle on the ion Landau damping in a helium-xenon plasma. Fluid theory was used to make comparisons between theoretical and experimental results. The ion Landau damping for propagation parallel to the magnetic field was found to be



similar to that without a field (as investigated by Alexeff et al., 1967). The angular dependence of the "contaminant" Landau damping was also investigated and results showed that the damping vanished for propagation almost perpendicular to the external magnetic field.

Fried et al. (1971) have used kinetic theory to make a detailed study of the "contaminant" damping. The linear dispersion relation was derived for a multispecies plasma and solutions to this equation displayed in the complex phase velocity plane. Comparisons were also made with the approximate solutions of the dispersion relation (derived by using asymptotic expansions for both ion terms). The authors found that there are two important modes associated with the two ion species in the plasma, each with different phase velocities - the principal heavy ion mode and the principal light ion mode. The principal heavy ion mode is significantly affected by the addition of a small concentration of light ions (the "contaminant" damping). The principal modes were investigated as a function of  $\theta = T_e/T_i$  and light ion fraction,  $f$ . Figure 2.1, taken from their paper, shows the damping rate as a function of  $f$  for an argon-helium plasma.

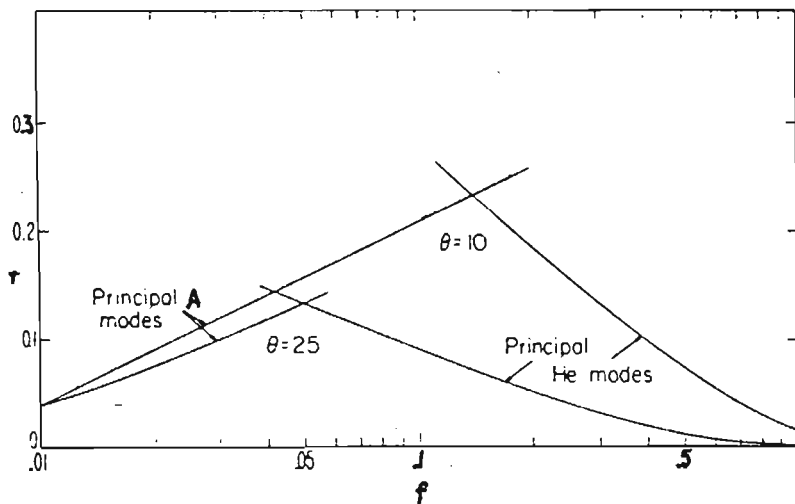


FIG. 2.1. Damping rate  $r$  vs light ion fraction  $f$  (from Fried et al., 1971).

The experimental findings of Nakamura et al. (1975) on changes of damping rate with light fraction in an argon-helium plasma confirmed the theoretical work of Fried et al. (1971). The damping rate was found to be a maximum for  $f \approx 0.08$ . Furthermore, only a single wave was detected for the range  $21 < \theta < 26$ , where  $\theta = T_e/T_i$ . In a subsequent paper, Nakamura et al. (1976b) investigated the temperature range  $\theta = 10$  to  $15$ . Although they detected a single mode in an argon-neon plasma, two modes were detected in an argon-helium plasma. On the basis of their results, Nakamura et al. (1976a) used fluid theory to suggest that two-wave behaviour will occur for  $\theta < 2M$  ( $M$  being the heavy to light ion mass ratio) in a two-ion plasma, which implies that only a single mode will be observed for  $\theta > 2M$ .

Similar results were found by Tran and Coquerand (1975a and b) who observed two simultaneous modes in an argon-helium plasma ( $M = 10$ ) for  $\theta = 9$ . In a later paper (Tran and Coquerand, 1976), they used real  $\omega$  and complex  $k$  to draw the dispersion curves for  $\theta = 25$  and  $\theta = 10$  in an argon-helium plasma. For the case  $\theta = 10$ , the existence of two simultaneous modes was clearly shown, while  $\theta = 25$  yielded a single mode.

Lambert et al. (1976) used Nyquist diagrams to illustrate the behaviour of the roots of the dispersion relation for a two-ion plasma. They conclude that the light ion "contaminant" damping occurs for the range  $5 \lesssim \theta \lesssim 100$ . The width of this interval depends on both the heavy to light ion mass ratio and the light ion concentration. Lambert et al. continued their investigations in a second paper (1977) and studied the effect of such parameters as ion mass

ratio and temperature ratio on the "contaminant" damping in an argon-helium plasma.

Gledhill (1982) used the saddle point technique to make a comprehensive study of the effects of  $\theta$ ,  $M$  and  $f$  on the behaviour of the various ion acoustic modes in a two-ion plasma. In their kinetic treatment, Gledhill and Hellberg (1987), confirmed the findings of Nakamura et al. (1976a) by establishing the criteria for the existence of two simultaneous modes in a two-ion plasma as  $\theta < \theta^*$  where  $\theta^* = 2.1 M$  for  $M > 10$ .

Dell (1984) continued with the saddle point technique of Gledhill. Some of his studies focussed on the effect of an electron beam on the ion acoustic instability in an unmagnetized two-ion plasma. The presence of the electron beam was found to modify the conditions necessary for the coexistence of two weakly damped waves.

Yagura et al. (1985) experimentally studied the ion acoustic instability in a two-ion plasma in the presence of two-ion beams. The ion acoustic instability was found to be excited by the coupling of the ion acoustic wave associated with the background plasma and the slow space charge wave of the heavy ion beam. Experimental measurements were found to agree quite closely with the theoretical results. The ion beam energies required to produce instability were found to depend upon both the light ion fraction  $f$  and the heavy to light ion mass ratio  $M$ .

Gary and Omidi (1987) have solved the linear dispersion relation for ion-acoustic-like instabilities in a plasma consisting of counter

streaming ion components. Some of the results found were: (i) the instability undergoes a transition from fluid-like to beam resonant as the beam-background ion relative temperature ratio approaches unity; (ii) when the beam-background temperature ratio is of order unity, the threshold core (background ions) drift speed for the electron-ion acoustic instability is larger than that for the ion-ion acoustic instability for a very wide range of plasma parameters; (iii) anisotropies in the electron temperature,  $T_{\perp e}/T_{\parallel e} > 1$  enhances the ion-ion acoustic instability at oblique propagations; (iv) the effect of an external magnetic field is to either increase or decrease the growth rate of the instability for large beam-background ion drift speeds. The authors then use their results to make comparisons with the findings of other authors on the ion acoustic instability in space plasmas.

In a recent theoretical study of ion acoustic behaviour in two-ion plasmas, Jackson (1986) investigated the propagation of ion acoustic instabilities in a deuterium-tritium plasma and their significance in controlling thermonuclear reactions. The SASER (Sound Amplification by Stimulated Emission of (Acoustic) Radiation) effect is discussed.

CHAPTER THREE

THE PLASMA DISPERSION RELATION FOR CROSSFIELD CURRENT-DRIVEN ION  
ACOUSTIC WAVES IN A TWO-ION PLASMA

3.1 INTRODUCTION

The plasma dispersion relation used in this thesis is based on kinetic theory. It has been derived for crossfield ion acoustic waves by Gary and Sanderson (1970), but the following derivation of the relation is based closely on the more detailed approach of Bharuthram (1974).

We consider electrostatic waves in a collisionless Vlasov plasma consisting of two species of stationary ions and Maxwellian electrons drifting perpendicular to an external magnetic field. The derivation of the plasma relation is based on the following two assumptions:

- (a) The time scale ( $\tau$ ) and length scale ( $L$ ) of the perturbations satisfy the following conditions:

$$\Omega_i < \tau^{-1} < |\Omega_e|$$

$$r_e < L < r_i$$

where  $\Omega_i$  ( $\Omega_e$ ) is the ion (electron) gyrofrequency and  $r_i$  ( $r_e$ ) is the ion (electron) gyroradius.

Under such conditions the ions may be considered unmagnetized.

- (b) We use the electrostatic approximation, i.e. magnetic field perturbations are neglected. Then  $\vec{E}^{(1)} = -\nabla\phi^{(1)}$  where  $\vec{E}^{(1)}$  ( $\phi^{(1)}$ ) is the perturbation electric field (potential). It then follows

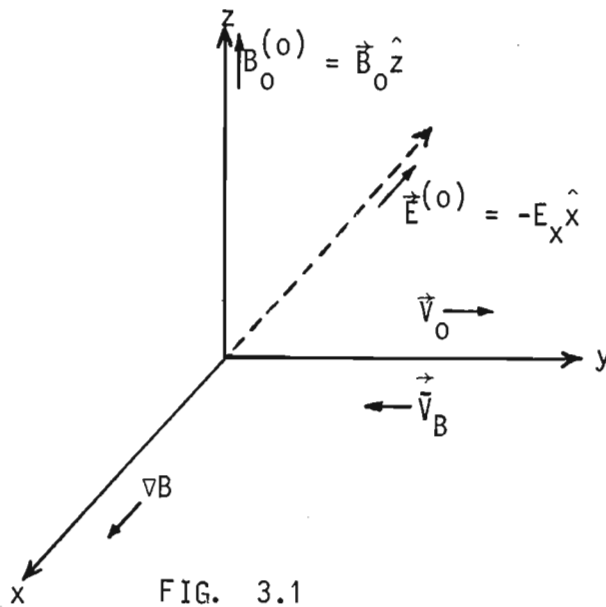
from Maxwell's equations that for harmonic variations of the form  $\exp i(\vec{k} \cdot \vec{r} - \omega t)$ ,  $\vec{k}$  is parallel to  $\vec{E}^{(1)}$ . Thus electrostatic waves are longitudinal in nature. To ensure that electromagnetics effects are always negligible we require the wave phase speed  $V_\phi$  to be much smaller than the speed of light, i.e.  $V_\phi \ll c$ .

In the next section we describe our model and then obtain the electron contribution to the dispersion relation.

### 3.2 THE ELECTRON TERM

We consider a collisionless two-ion plasma embedded in external electric and magnetic fields:

$$\begin{aligned} \vec{E}^{(0)} &= -E_x \hat{x} \\ \vec{B}^{(0)} &= B_0 (1 + \epsilon x) \hat{z} \end{aligned} \tag{3.2.1}$$



Since the electrons are magnetized and the ions not, the former have an  $\vec{E}^{(0)} \times \vec{B}^{(0)}$  drift relative to the latter,

$$\vec{V}_0 = \frac{c \vec{E}^{(0)} \times \vec{B}^{(0)}}{B_0^2} \tag{3.2.2}$$

in the y-direction. The drift velocity of the electrons due to the inhomogeneity in the magnetic field,  $\vec{V}_B$ , is in the negative y-direction and is given by. (Boyd and Sanderson, 1969)

$$\vec{V}_B = \frac{\frac{1}{2} m_e V_{\perp} c (\vec{B} \times \nabla) \vec{B}}{(-e) B^3} \quad (3.2.3)$$

Substituting for  $\vec{B}^{(0)}$  from eqn (3.1.1), we have

$$|\vec{V}_B| = \frac{\epsilon V_{\perp}^2}{2\Omega_e}$$

Effects of gradients in plasma temperature and density are neglected here, but will be studied later in Chapter Four.

Since we are considering magnetized electrons and unmagnetized ions, the scale length of nonuniformity of  $\vec{B}^{(0)}$  is restricted by

$$r_e \ll |1/\epsilon| \ll r_i$$

The equation of motion for the electrons is given by

$$\begin{aligned} \frac{m_e d\vec{V}}{dt} &= e \left( \vec{E}^{(0)} + \frac{\vec{V} \times \vec{B}^{(0)}}{c} \right) \\ &= e [-E_x \hat{x} + \vec{V} \times \{B_0 (1+\epsilon x)/c\} \hat{z}], \end{aligned}$$

which leads to

$$\left. \begin{aligned} \ddot{x} &= \frac{eE_x}{m_e} - \Omega_e (1+\epsilon x) V_y \\ \ddot{y} &= \Omega_e (1+\epsilon x) V_x \\ \ddot{z} &= 0. \end{aligned} \right\} \quad (3.2.5)$$

Two constants of motion (to order  $\epsilon$ ) can be constructed by the use of eqn (3.2.5). These are  $V_z$  and  $V_{\perp}^2 = V_x^2 + (V_y - V_0)^2$ .

The Vlasov equation for the electrons,

$$\frac{\partial f_e}{\partial t} + \vec{v} \cdot \nabla f_e + \frac{e}{m_e} \left( \vec{E} + \frac{\vec{v} \times \vec{B}}{c} \right) \cdot \nabla_{\vec{v}} f_e = 0, \quad (3.2.6)$$

is satisfied by the equilibrium Maxwellian velocity distribution

$$f_e^{(0)} = n_0 (2\pi c_e^2)^{-3/2} \exp\left\{-\frac{V_x^2 + (V_y - V_0)^2 + V_z^2}{2c_e^2}\right\} \quad (3.2.7)$$

where  $m_e$  is the electron mass and  $c_e = \sqrt{T_e/m_e}$  the electron thermal speed.

Allowing for small perturbations in the equilibrium quantities, viz.

$$f_e = f_e^{(1)} + f_e^{(0)} \quad (|f_e^{(1)}| \ll |f_e^{(0)}|)$$

and 
$$\vec{E} = \vec{E}^{(1)} + \vec{E}^{(0)} \quad (|E^{(1)}| \ll |E^{(0)}|)$$

where the superscript (1) indicates the perturbations, we substitute in eqn (3.2.6), and linearize to obtain

$$\begin{aligned} \frac{\partial f_e^{(1)}}{\partial t} + \vec{v} \cdot \frac{\partial f_e^{(1)}}{\partial \vec{r}} - \frac{e}{m_e} \left( \vec{E}^{(0)} + \frac{\vec{v} \times \vec{B}^{(0)}}{c} \right) \cdot \frac{\partial f_e^{(1)}}{\partial \vec{v}} \\ = \frac{e}{m_e} \left( \vec{E}^{(1)} + \frac{\vec{v} \times \vec{B}^{(1)}}{c} \right) \cdot \frac{\partial f_e^{(0)}}{\partial \vec{v}}, \end{aligned} \quad (3.2.8)$$

which may be rewritten as

$$\left[ \frac{df_e^{(1)}}{dt} \right]_0 = - \frac{e}{m_e} \nabla \phi \cdot \frac{\partial f_e^{(0)}}{\partial \vec{v}}$$

where  $\vec{B}^{(1)} = 0$  for the electrostatic case, and the left hand side represents the rate of change following an unperturbed orbit (as defined by  $\vec{E}^{(0)}$  and  $\vec{B}_0^{(0)}$ ) in phase space. Upon integrating along the unperturbed orbits, we obtain

$$f_e^{(1)}(\vec{r}, \vec{v}, t) = - \frac{e}{m_e} \int_{-\infty}^t \nabla \phi^{(1)} \cdot \frac{\partial f_e^{(0)}}{\partial \vec{v}} dt', \quad (3.2.9)$$



where

$$\left. \begin{aligned} \frac{d\vec{r}'}{dt'} &= \vec{v}', \vec{r}'(0) = \vec{r}, \vec{v}'(0) = \vec{v} \\ \frac{d\vec{v}'}{dt'} &= -\frac{e}{m_e} (\vec{E}(0) + \frac{\vec{v}' \times \vec{B}(0)}{c}) \\ \vec{E}^{(1)} &= -\nabla\phi^{(1)} \end{aligned} \right\} (3.2.10)$$

and where we have taken the lower limit of the integration  $t' = -\infty$  under the assumption that the plasma is undisturbed in the infinite past.

Assuming  $f_e^{(1)}$  and  $\phi^{(1)}$  to vary harmonically in space and time we may write,

$$f_e^{(1)}(\vec{r}, \vec{v}, t) = f_e^{(1)}(\vec{v}) \exp\{i(\vec{k} \cdot \vec{r} - \omega t)\} \quad (3.2.11)$$

$$\phi^{(1)}(\vec{r}, t) = \phi_{k\omega}^{(1)} \exp\{i(\vec{k} \cdot \vec{r} - \omega t)\} \quad (3.2.12)$$

Inserting the eqns (3.2.11) and (3.2.12) into (3.2.9), we obtain

$$\begin{aligned} f_e^{(1)}(\vec{r}, \vec{v}, t) &= f_e^{(1)}(\vec{v}) \exp\{i(\vec{k} \cdot \vec{r} - \omega t)\} \\ &= -\frac{e}{m_e} \frac{f_e^{(0)}}{c_e^2} \left[ \int_{-\infty}^t -\vec{v}' \cdot \nabla\phi^{(1)} dt' + \int_{-\infty}^t \vec{v}'_0 \cdot \nabla\phi^{(1)} dt' \right] \end{aligned} \quad (3.2.13)$$

where the result  $\frac{\partial f_e^{(0)}}{\partial \vec{v}'} = [-\vec{v}' + \vec{v}'_0] \frac{f_e^{(0)}(\vec{v}')}{c_e^2}$  (from eqn 3.2.7)

has been used.

Now

$$\int_{-\infty}^t \nabla\phi^{(1)} \cdot \vec{v}' dt' = \int_{-\infty}^t \frac{\partial\phi^{(1)}}{\partial \vec{r}'} \cdot \frac{\partial \vec{r}'}{\partial t'} dt' = \int_{-\infty}^t \left( \frac{d\phi^{(1)}}{dt'} - \frac{\partial\phi^{(1)}}{\partial t'} \right) dt',$$

which on using eqn (3.2.12) and the boundary condition at  $t' = -\infty$  yields

$$\int_{-\infty}^t \nabla \phi^{(1)} \cdot \vec{V}' dt' = [\phi^{(1)}]_{t'=t} + i\omega \int_{-\infty}^t \phi_{k\omega}^{(1)} \exp\{i(\vec{k} \cdot \vec{r}' - \omega t')\} dt'. \quad (3.2.14)$$

With the aid of eqn (3.2.12), one gets

$$\int_{-\infty}^t \nabla \phi^{(1)} \cdot \vec{V}'_0 dt' = i\vec{k} \cdot \vec{V}'_0 \int_{-\infty}^t \phi_{k\omega}^{(1)} \exp\{i(\vec{k} \cdot \vec{r}' - \omega t')\} dt' \quad (3.2.15)$$

Combining eqns (3.2.13), (3.2.14) and (3.2.15), one finds

$$\begin{aligned} & f_e^{(1)}(\vec{V}) \exp\{i(\vec{k} \cdot \vec{r} - \omega t)\} \\ &= \frac{ef_e^{(0)}}{m_e c^2} \left[ [\phi_{k\omega}^{(1)} \exp\{i(\vec{k} \cdot \vec{r}' - \omega t')\}]_{t'=t} \right. \\ & \quad \left. + i(\omega - \vec{k} \cdot \vec{V}'_0) \int_{-\infty}^t \phi_{k\omega}^{(1)} \exp\{i(\vec{k} \cdot \vec{r}' - \omega t')\} dt' \right] \end{aligned}$$

Evaluating this equation at  $t = 0$  with  $\vec{r}'(0) = \vec{r}, \vec{V}'(0) = \vec{V}$ , we obtain

$$f_e^{(1)}(\vec{V}) = \frac{ef_e^{(0)}}{T_e} \phi_{k\omega}^{(1)} \left[ 1 + i(\omega - \vec{k} \cdot \vec{V}'_0) \int_{-\infty}^0 \exp\{i(\vec{k} \cdot \vec{r}' - \omega t')\} dt' \right] \quad (3.2.16)$$

where the relation  $c_e^2 = T_e/m_e$  has been used.

Now if  $\vec{V}'(0) = \vec{V} = (V_{\perp} \cos \phi, V_{\perp} \sin \phi, V_z)$  and  $\vec{r}'(0) = \vec{r} = (x_0, y_0, z_0)$

the approximate solution to the electron orbit equations are

$$\begin{aligned} \vec{r}'(t') &= (x_0 + \frac{V_{\perp}'}{\Omega_e} \{\sin(\Omega_e t' + \phi) - \sin \phi\}, \\ & \quad y_0 - \frac{V_{\perp}'}{\Omega_e} \{\cos(\Omega_e t' + \phi) - \cos \phi\} + \left( V_0 - \frac{eV_{\perp}'^2}{2\Omega_e} \right) t', \\ & \quad z_0 + V_z' t'). \end{aligned} \quad (3.2.17)$$

If we now write

$$\vec{k} = (k_x, k_y, k_z) = (k_{\perp} \cos \psi, k_{\perp} \sin \psi, k_z),$$

the integral in eqn (3.2.16) becomes, with the aid of eqn (3.2.17),

$$\int_{-\infty}^0 \exp i \left[ k_z V'_z + k_y \left( V_0 - \frac{\epsilon V_{\perp}^2}{2\Omega_e} \right) - \omega \right] t' \\ + \frac{k_{\perp} V_{\perp}}{\Omega_e} \{ \sin(\Omega_e t' + \phi - \psi) - \sin(\phi - \psi) \} dt'$$

The above integration can be performed with the aid of the following identity (Watson, 1944):

$$\exp(i \alpha \sin \beta) = \sum_{\ell=-\infty}^{+\infty} \exp(i \ell \beta) J_{\ell}(\alpha), \quad (3.2.18)$$

where  $J_{\ell}(\alpha)$  is the Bessel function of order  $\ell$ .

Equation (3.2.16) can then be written as

$$f_e^{(1)}(\vec{V}) = \frac{e f_e^{(0)}}{T_e} \phi_{k\omega}^{(1)} \left[ 1 + (\omega - \vec{k} \cdot \vec{V}_0) \times \right. \\ \left. \sum_{p=-\infty}^{+\infty} \sum_{q=-\infty}^{+\infty} \frac{J_p \left( \frac{k_{\perp} V_{\perp}}{\Omega_e} \right) J_q \left( \frac{k_{\perp} V_{\perp}}{\Omega_e} \right) \exp\{i(p-q)(\phi - \psi)\}}{\left\{ k_z V'_z + k_y \left( V_0 - \frac{\epsilon V_{\perp}^2}{2\Omega_e} \right) - \omega + p\Omega_e \right\}} \right] \quad (3.2.19)$$

The perturbed electron density is then given by

$$n_e^{(1)}(\vec{r}, t) = n_{ek\omega}^{(1)} \exp\{i(\vec{k} \cdot \vec{r} - \omega t)\} = \int f_e^{(1)}(\vec{r}', \vec{V}', t') d^3 V' \\ = \int f_e^{(1)}(\vec{V}') \exp\{i(\vec{k} \cdot \vec{r}' - \omega t)\} d^3 V'.$$

Using eqn (3.2.19), with  $f_e^{(0)}$  given by eqn (3.2.7) and  $V_{\perp}^2 = V_x^2 + (V_y - V_0)^2$ , we obtain

$$n_{ek\omega}^{(1)} = \int \frac{e \phi_{k\omega}^{(1)}}{T_e} \left\{ \bar{n}_0 (2\pi c_e^2)^{-3/2} \exp \left( \frac{-V_{\perp}^2 + V_z^2}{2c_e^2} \right) \right\} \left[ 1 + (\omega - \vec{k} \cdot \vec{V}_0) \right.$$

$$\begin{aligned}
 & \times \int_{p=-\infty}^{+\infty} \int_{q=-\infty}^{+\infty} \frac{J_p \left( \frac{k_{\perp} V'_{\perp}}{\Omega_e} \right) J_q \left( \frac{k_{\perp} V'_{\perp}}{\Omega_e} \right) \exp \{ i(p-q) (\phi-\psi) \}}{\left\{ k_z V'_z + k_y \left( V_0 - \frac{\epsilon V'^2_{\perp}}{2\Omega_e} \right) - \omega + p\Omega_e \right\}} d^3 V' \\
 & = \frac{n_0 e \phi_{k\omega}^{(1)}}{T_e} \left[ 1 + \frac{\omega - \vec{k} \cdot \vec{V}_0}{(2\pi c_e^2)^{3/2}} 2\pi \int_{p=-\infty}^{+\infty} \int_0^{\infty} \frac{\exp\left(-\frac{V'^2_z}{2c_e^2}\right) dV'_z}{\left[ k_z V'_z - \left\{ \omega - k_y \left( V_0 - \frac{\epsilon V'^2_{\perp}}{2\Omega_e} \right) - p\Omega_e \right\} \right]} \right. \\
 & \left. \times J_p^2 \left( \frac{k_{\perp} V'_{\perp}}{\Omega_e} \right) \exp\left(-\frac{V'^2_{\perp}}{2c_e^2}\right) V'_{\perp} dV'_{\perp} \right] \quad (3.2.20)
 \end{aligned}$$

where we have used cylindrical coordinates  $(V'_{\perp}, \phi, V'_z)$  in velocity space and have performed the angular integration using the result:

$$\int_0^{2\pi} \exp\{i(p-q)\phi\} d\phi = \begin{cases} 0 & \text{if } p \neq q \\ 2\pi & \text{if } p = q \end{cases} \quad (3.2.21)$$

Using the plasma dispersion function (Fried and Conte, 1961),

$$Z(\lambda) = \pi^{-1/2} \int_{-\infty}^{\infty} \frac{e^{-x^2}}{(x-\lambda)} dx \quad \text{for } \text{Im}(\lambda) > 0, \quad (3.2.22)$$

the term

$$\int_{-\infty}^{\infty} \frac{\exp\left(-\frac{V'^2_z}{2c_e^2}\right) dV'_z}{\left[ \frac{V'_z}{\sqrt{2}c_e} - \left\{ \frac{\omega - k_y \left( V_0 - \frac{\epsilon V'^2_{\perp}}{2\Omega_e} \right) - p\Omega_e}{\sqrt{2}k_z c_e} \right\} \right]} \sqrt{2}k_z c_e$$

may be rewritten as

$$\frac{\pi^{1/2}}{k_z} Z \left\{ \frac{\omega - k_y \left( V_0 - \frac{\epsilon V'^2_{\perp}}{2\Omega_e} \right) - p\Omega_e}{\sqrt{2}k_z c_e} \right\}$$

Equation (3.2.20) then reduces to

$$n_{ek\omega}^{(1)} = \frac{n_0 e \phi_{k\omega}^{(1)}}{T_e} \left[ 1 + \frac{(\omega - \vec{k} \cdot \vec{V}_0)}{\sqrt{2} k_z c_e^3} \sum_{p=-\infty}^{+\infty} \int_0^{\infty} J_p^2 \left( \frac{k_{\perp} V_{\perp}'}{\Omega_e} \right) \exp \left( - \frac{V_{\perp}'^2}{2c_e^2} \right) \right. \\ \left. \times Z \left\{ \frac{\omega - k_y \left( V_0 - \frac{\epsilon V_{\perp}'^2}{2\Omega_e} \right) - p\Omega_e}{\sqrt{2} k_z c_e} \right\} \right] \quad (3.2.23)$$

### 3.3 THE ION TERMS

The time and length scales are assumed to be such that both the light ions (denoted by the subscript L) and the heavy ions (denoted by the subscript H) in our two-ion plasma are unmagnetized. In addition, due to their inertia, both ion species are assumed not to react to the electric field. Thus the equation of motion of each ion is of the type

$$\ddot{\vec{r}} = 0,$$

with the solution

$$\vec{r}' - \vec{r} = \vec{V}' t' \quad (3.3.1)$$

For the equilibrium plasma, the densities of the species are related by

$$n_{oe} = n_{oL} + n_{oH} \quad (3.3.2)$$

We shall first derive the perturbed ion distribution for light ions. As for the electrons, we integrate along the unperturbed orbits to obtain

$$f_L^{(1)}(\vec{r}, \vec{V}, t) = e/M_L \int_{-\infty}^t \nabla \phi^{(1)} \cdot \frac{\partial f_L^{(0)}}{\partial \vec{V}'} dt', \quad (3.3.3)$$

where  $M_L$  is the light ion mass. With the equilibrium light ion velocity distribution given by

$$f_L^{(0)}(\vec{V}) = \frac{n_{oL}}{(2\pi c_L^2)^{3/2}} \exp\left(-\frac{V^2}{2c_L^2}\right), \quad (3.3.4)$$

(where  $c_L = \sqrt{T_L/M_L}$  is the light ion thermal speed)

we follow the procedure outlined in section 3.2 for the electrons to obtain

$$n_{Lk\omega}^{(1)} = -\frac{en_{oL}}{T_L} \phi_{k\omega}^{(1)} \left[ 1 + \frac{\omega}{(2\pi c_L^2)^{3/2}} \int_{-\infty}^{\infty} \frac{\exp\left(-\frac{V'^2}{2c_L^2}\right)}{\vec{k} \cdot \vec{V}' - \omega} d^3V' \right] \quad (3.3.5)$$

The integration in the above equation is performed by moving the axis into the ion rest frame and then rotating the axis such that one of the axes points in the  $\vec{k}$  direction. It then turns out that the light ion perturbed density is given by

$$n_{Lk\omega}^{(1)} = \frac{en_{oL}\phi_{k\omega}^{(1)}}{2T_L} Z' \left( \frac{\omega}{\sqrt{2}kc_L} \right) \quad (3.3.6)$$

where  $Z'(\lambda)$ , the first derivative of the plasma dispersion function is given by (Fried and Conte, 1961)

$$Z'(\lambda) = -2[1 + \lambda Z(\lambda)]. \quad (3.3.7)$$

In a similar manner for the heavy ions we find

$$n_{Hk\omega}^{(1)} = \frac{en_{oH}\phi_{k\omega}^{(1)}}{2T_H} Z' \left( \frac{\omega}{\sqrt{2}kc_H} \right) \quad (3.3.8)$$

### 3.4 THE DISPERSION RELATION

In the electrostatic approximation, Maxwell's equations are replaced by Poisson's equation:

$$\nabla^2 \phi = - 4\pi \sum_j q_j n_j, \quad (3.4.1)$$

from which we obtain

$$\phi_{k\omega}^{(1)} = \frac{4\pi e}{k^2} (n_{Lk\omega}^{(1)} + n_{Hk\omega}^{(1)} - n_{ek\omega}^{(1)}) \quad (3.4.2)$$

for harmonic variations.

Upon substituting for the perturbed densities from eqns (3.2.23), (3.3.6) and (3.3.8), we obtain

$$\begin{aligned} 1 + \frac{4\pi e}{T_e k^2} \left[ - \frac{n_{oL} e T_e}{2T_L} Z' \left( \frac{\omega}{\sqrt{2} k c_L} \right) - \frac{n_{oH} e T_e}{2T_H} Z' \left( \frac{\omega}{\sqrt{2} k c_H} \right) \right. \\ \left. + n_{oe} \left\{ 1 + \frac{\omega - \vec{k} \cdot \vec{V}_0}{\sqrt{2} k_z c_e^3} \sum_{p=-\infty}^{\infty} \int_0^{\infty} J_p^2 \left( \frac{k_{\perp} V_{\perp}'}{\Omega_e} \right) \exp \left( - \frac{V_{\perp}'^2}{2c_e^2} \right) \right. \right. \\ \left. \left. \times Z \left( \frac{\omega - k_y \left( V_0 - \frac{\epsilon V_{\perp}'^2}{2\Omega_e} \right) - p\Omega_e}{\sqrt{2} k_z c_e} \right) V_{\perp}' dV_{\perp}' \right\} \right] = 0 \end{aligned} \quad (3.4.3)$$

which can be written as

$$1 + K_L + K_H + K_e = 0 \quad (3.4.4)$$

where

$$K_L = - \frac{k_D^2}{k^2} \left( \frac{n_{oL}}{n_{oe}} \right) \left( \frac{T_e}{2T_L} \right) Z' \left( \frac{\omega}{\sqrt{2} k c_L} \right), \quad (3.4.5)$$

$$K_H = - \frac{k_D^2}{k^2} \left( \frac{n_{oH}}{n_{oe}} \right) \left( \frac{T_e}{2T_H} \right) Z' \left( \frac{\omega}{\sqrt{2} k c_H} \right), \quad (3.4.6)$$

$$K_e = \frac{k_D^2}{k^2} \left[ 1 + \left( \frac{\omega - \vec{k} \cdot \vec{V}_0}{\sqrt{2} k_z c_e^3} \right) \sum_{p=-\infty}^{+\infty} \int_0^{\infty} J_p^2 \left( \frac{k_{\perp} V_{\perp}'}{\Omega_e} \right) \exp \left( - \frac{V_{\perp}'^2}{2c_e^2} \right) \right. \\ \left. \times Z \left( \frac{\omega - k_y \left( V_0 - \frac{\epsilon V_{\perp}'^2}{2\Omega_e} \right) - p\Omega_e}{\sqrt{2} k_z c_e} \right) V_{\perp}' dV_{\perp}' \right], \quad (3.4.7)$$

and  $k_D$  is the inverse of the electron Debye length

$$\lambda_D = \left( \frac{T_e}{4\pi n_{0e} e^2} \right)^{\frac{1}{2}}.$$

For a uniform magnetic field,  $\epsilon = 0$ . Then the Z function in eqn (3.4.7) is independent of  $V_{\perp}'$  and may be taken outside the integral sign, yielding

$$K_e = \frac{k_D^2}{k^2} \left[ 1 + \left( \frac{\omega - \vec{k} \cdot \vec{V}_0}{\sqrt{2} k_z c_e^3} \right) \sum_{p=-\infty}^{+\infty} Z \left( \frac{\omega - k_y V_0 - p\Omega_e}{\sqrt{2} k_z c_e} \right) \right. \\ \left. \times \int_0^{\infty} J_p^2 \left( \frac{k_{\perp} V_{\perp}'}{\Omega_e} \right) \exp \left( - \frac{V_{\perp}'^2}{2c_e^2} \right) V_{\perp}' dV_{\perp}' \right] \\ = \frac{k_D^2}{k^2} \left[ 1 + \left( \frac{\omega - \vec{k} \cdot \vec{V}_0}{\sqrt{2} k_z c_e^3} \right) \sum_{p=-\infty}^{+\infty} \exp \left( - \frac{k_{\perp}^2 c_e^2}{\Omega_e^2} \right) I_p \left( \frac{k_{\perp}^2 c_e^2}{\Omega_e^2} \right) Z \left( \frac{\omega - k_y V_0 - p\Omega_e}{\sqrt{2} k_z c_e} \right) \right] \quad (3.4.8)$$

where we have used the relation (Watson, 1944)

$$\int_0^{\infty} \exp(-\alpha x^2) J_p^2(\beta x) x dx = \frac{1}{2\alpha} \exp \left( - \frac{\beta^2}{2\alpha} \right) I_p \left( \frac{\beta^2}{2\alpha} \right). \quad (3.4.9)$$

$I_p$  is the modified Bessel function of order p.



It thus follows that the dispersion relation for electrostatic waves in a uniform plasma with magnetized electrons and two species of unmagnetized ions can be written as

$$1 + \frac{k^2}{k_D^2} - \left(\frac{n_{oL}}{n_{oe}}\right) \left(\frac{T_e}{2T_L}\right) Z'(z_L) - \left(\frac{n_{oH}}{n_{oe}}\right) \left(\frac{T_e}{2T_H}\right) Z'(z_H) + \left(\frac{\omega - \vec{k} \cdot \vec{V}_o}{\sqrt{2} k_z c_e}\right) \sum_{p=-\infty}^{+\infty} Z(z_{pe}) \Gamma_p = 0 \quad (3.4.10a)$$

where

$$\begin{aligned} z_L &= \frac{\omega}{\sqrt{2} k c_L}, \\ z_H &= \frac{\omega}{\sqrt{2} k c_H}, \\ z_{pe} &= \frac{\omega - k_y V_o - p \Omega_e}{\sqrt{2} k_z c_e}, \end{aligned} \quad (3.4.10b)$$

and  $\Gamma_p = e^{-b} I_p(b)$ , with  $b = \frac{k_{\perp}^2 c_e^2}{\Omega_e^2}$ .

If one is interested in low frequency modes with  $\omega < \Omega_e$ , then

$Z_p = -Z_{-p}$ , and only the  $p = 0$  term contributes in eqn (3.4.8). Then

$$\begin{aligned} k_e &= \frac{k_D^2}{k^2} \left[ 1 + \left(\frac{\omega - \vec{k} \cdot \vec{V}_o}{\sqrt{2} k_z c_e}\right) \exp\left(-\frac{k_{\perp}^2 c_e^2}{\Omega_e^2}\right) I_0\left(-\frac{k_{\perp}^2 c_e^2}{\Omega_e^2}\right) Z\left(\frac{\omega - k_y V_o}{\sqrt{2} k_z c_e}\right) \right] \\ &= \frac{k_D^2}{k^2} [1 + z_{oe} Z(z_{oe}) \cdot \Gamma_0] \end{aligned} \quad (3.4.11)$$

Letting  $f = n_{oL}/n_{oe}$ ,  $\theta_j = T_e/T_j$  ( $j = L, H$ ), the full dispersion relation, eqn (3.4.10a), then finally becomes

$$\frac{k^2}{k_D^2} + 1 + z_{oe} Z(z_{oe}) \cdot \Gamma_0 - f \frac{\theta_L}{2} Z'(z_L) - (1 - f) \frac{\theta_H}{2} Z'(z_H) = 0 \quad (3.4.12)$$

### 3.5 THE APPROXIMATE DISPERSION RELATION FOR MARGINAL STABILITY OF ION ACOUSTIC WAVES

We consider the marginal stability of low frequency ion acoustic waves in a two-ion magnetized plasma. For such modes the dispersion relation given by eqn (3.4.12) is applicable. It is assumed that the ion and electron temperatures are such that  $T_e \gg T_j$  ( $j = L, H$ ). Then ion Landau damping is small and the arguments  $z_{oe}$ ,  $z_L$ ,  $z_H$  in eqn (3.4.12) satisfy

$$|z_j| = \left| \frac{\omega}{\sqrt{2}kc_j} \right| \gg 1 \quad (j = L, H)$$

and

$$|z_{oe}| = \left| \frac{\omega - \vec{k} \cdot \vec{V}_0}{\sqrt{2}k_z c_e} \right| \ll 1 .$$

Physically,  $|z_{oe}| \ll 1$  means that the doppler-shifted wave phase speed along  $\vec{B}_0$  is much smaller than the electron thermal speed, while for  $|z_j| \gg 1$  ( $j = L, H$ ) the wave phase speed  $V_\phi = |\omega/k|$  is much larger than the thermal speeds of the two ion species.

Asymptotic and power series expansions of the plasma dispersion function may then be used to simplify the dispersion relation, eqn (3.4.12). These are given by (Fried and Conte, 1961):

(1)  $|z| \gg 1$

$$Z(z) = i\sqrt{\pi}\delta \exp(-z^2) - \frac{1}{z} \left[ 1 + \frac{1}{2z^2} + \frac{3}{4z^4} + \dots \right] \quad (3.5.1)$$

where

$$\delta = \begin{cases} 0 & \text{if } \text{Im}(z) > 0 \\ 1 & \text{if } \text{Im}(z) = 0 \\ 2 & \text{if } \text{Im}(z) < 0 \end{cases}$$

(2)  $|z| \ll 1$

$$Z(z) = i\sqrt{\pi} \exp(-z^2) - 2z \left[ 1 - \frac{2z^2}{3} + \frac{4z^4}{15} - \dots \right] \quad (3.5.2)$$

For marginal stability ( $\gamma = 0$ ),  $\delta = 1$  in eqn (3.5.1) and the light ion term in eqn (3.4.12), for  $\theta_L = \theta_H = \theta$ , becomes

$$K_L = f \frac{\theta}{2} \left[ 2i\sqrt{\pi} z_L \exp(-z_L^2) - \frac{1}{z_L^2} \right] \quad (3.5.3)$$

Similarly the heavy ion term in eqn (3.4.12) becomes

$$K_H = (1 - f) \frac{\theta}{2} \left[ 2i\sqrt{\pi} z_H \exp(-z_H^2) - \frac{1}{z_H^2} \right] \quad (3.5.4)$$

The electron term in eqn (3.4.12), to lowest order, reduces with the aid of eqn (3.5.2) to

$$\begin{aligned} K_e &\approx 1 + z_{oe} (i\sqrt{\pi} - 2z_{oe}) \Gamma_0 \\ &\approx 1 + i\sqrt{\pi} z_{oe} \Gamma_0, \end{aligned} \quad (3.5.5)$$

since  $\left| \frac{2z_{oe}}{i\sqrt{\pi}} \right| = \frac{|z_{oe}|}{(\pi/4)^{1/2}} \ll 1$  for  $|z_{oe}| \ll 1$ .

Inserting eqns (3.5.3), (3.5.4) and (3.5.5) into eqn (3.4.12), the approximate dispersion relation for marginal stability (of ion acoustic waves as we shall shortly see) is

$$\begin{aligned} \frac{k^2}{k_D^2} + \left[ 1 + i\sqrt{\pi} \left( \frac{\omega - \vec{k} \cdot \vec{v}_0}{\sqrt{2} k_z c_e} \right) \Gamma_0 + f \frac{\theta}{2} \left\{ 2i\sqrt{\pi} \left( \frac{\omega}{\sqrt{2} k c_L} \right) \exp \left\{ - \left( \frac{\omega}{\sqrt{2} k c_L} \right)^2 \right\} \right. \right. \\ \left. \left. - \frac{2k^2 c_L^2}{\omega^2} \right\} + (1 - f) \frac{\theta}{2} \left\{ 2i\sqrt{\pi} \left( \frac{\omega}{\sqrt{2} k c_H} \right) \exp \left\{ - \left( \frac{\omega}{\sqrt{2} k c_H} \right)^2 \right\} - \frac{2k^2 c_H^2}{\omega^2} \right\} \right] = 0 \end{aligned} \quad (3.5.6)$$

where we have used eqns (3.4.10b).

At change over from stable to unstable behaviour the imaginary part of the wave frequency  $\omega$  is zero. Setting  $\omega = \omega_R$  ( $\omega_R$  being the real part of the frequency), we equate the real part of eqn (3.5.6) to zero:

$$\frac{k^2}{k_D^2} + 1 + f \frac{\theta\left(-\frac{2k^2 c_L^2}{\omega_R^2}\right)}{2} + (1 - f) \frac{\theta\left(-\frac{2k^2 c_H^2}{\omega_R^2}\right)}{2} = 0 \quad ,$$

which can easily be manipulated to yield

$$\omega_R^2 = k^2 \{f c_{SL}^2 + (1 - f) c_{SH}^2\} (1 + k^2 \lambda_D^2)^{-1} \quad (3.5.7)$$

where  $c_{SL(H)} = \sqrt{T_e/M_{L(H)}}$ , is the light (heavy) ion sound speed.

Equation (3.5.7) gives the real frequency for ion acoustic waves in a two-ion plasma. In the limits  $f = 0$  (only heavy ions present) and  $f = 1$  (only light ions present) it reduces to the well-known results for single-ion plasmas (Chen, 1974).

In the long wavelength approximation,  $\lambda \gg \lambda_D$ ,  $k^2 \lambda_D^2 \ll 1$ . Then from eqn (3.5.7), the wave phase speed is given by

$$V_\phi = \omega_R/k = \{f c_{SL}^2 + (1 - f) c_{SH}^2\}^{1/2} \quad (3.5.8a)$$

and when normalised with respect to  $c_{SH}$  we have

$$\hat{V}_\phi = V_\phi/c_{SH} = \{1 + (M - 1) f\}^{1/2} \quad , \quad (3.5.8b)$$

where  $M = M_H/M_L$ , the heavy to light ion mass ratio.

Setting  $\omega = \omega_R$  and equating the imaginary part of eqn (3.5.6) to zero, we obtain

$$\sqrt{\pi} \left( \frac{\omega_R - \vec{k} \cdot \vec{V}_0}{\sqrt{2} k_z c_e} \right) \Gamma_0 + f \theta \sqrt{\pi} \left( \frac{\omega_R}{\sqrt{2} k c_L} \right) \exp \left\{ - \frac{\omega_R^2}{2 k c_L^2} \right\} \\ + (1 - f) \theta \sqrt{\pi} \left( \frac{\omega_R}{\sqrt{2} k c_H} \right) \exp \left\{ - \frac{\omega_R^2}{2 k c_H^2} \right\} = 0 ,$$

from which we obtain

$$\vec{k} \cdot \vec{V}_0 = \omega_R + f \theta \frac{k_z}{k} \left( \frac{c_e}{c_L} \right) \frac{\omega_R}{\Gamma_0} \exp \left\{ - \left( \frac{\omega_R}{\sqrt{2} k c_L} \right)^2 \right\} \\ + (1 - f) \theta \frac{k_z}{k} \left( \frac{c_e}{c_H} \right) \frac{\omega_R}{\Gamma_0} \exp \left\{ - \left( \frac{\omega_R}{\sqrt{2} k c_H} \right)^2 \right\}$$

Since in our model  $\vec{V}_0$  is the  $\vec{E} \times \vec{B}$  drift with  $\vec{V}_0 = V_0 \hat{y}$ , it follows that  $\vec{k} \cdot \vec{V}_0 = k_y V_0$ . Solving for the critical electron drift speed  $V_0^C$  for marginal stability, one gets

$$\frac{V_0^C}{c_e} = \frac{k}{k_y} \frac{\hat{V}_\phi}{\sqrt{\bar{m}}} \left[ 1 + f \sqrt{\theta^3 \bar{m}} \left( \frac{k_z}{k} \cdot \frac{1}{\Gamma_0} \right) \exp \left( - \frac{\hat{V}_\phi^2 \theta}{2 \bar{M}} \right) \right. \\ \left. + (1 - f) \sqrt{\theta^3 \bar{m}} \left( \frac{k_z}{k} \cdot \frac{1}{\Gamma_0} \right) \exp \left( - \frac{\hat{V}_\phi^2 \theta}{2} \right) \right] \quad (3.5.9)$$

where  $V_0^C$  has been normalised with respect to the electron thermal speed;  $\bar{m} = M_H/m_e$  is the heavy ion to electron mass ratio and  $\hat{V}_\phi$  is the normalised wave phase speed given by eqn (3.5.8b).

### 3.6 MARGINAL STABILITY STUDIES USING BOTH THE FULL AND APPROXIMATE DISPERSION RELATIONS

In this section solutions from the full dispersion relation, eqn (3.4.12), (without any expansions for the Z-functions) are compared with the values of  $V_0^C$  calculated from the approximate eqns (3.5.8) and (3.5.9). The standard values of the parameters used for the results presented here are:

$$\bar{m} = M_H/m_e = 73326;$$

$$k = \pi \text{ cm}^{-1}; \quad k_z/k = 0.0316;$$

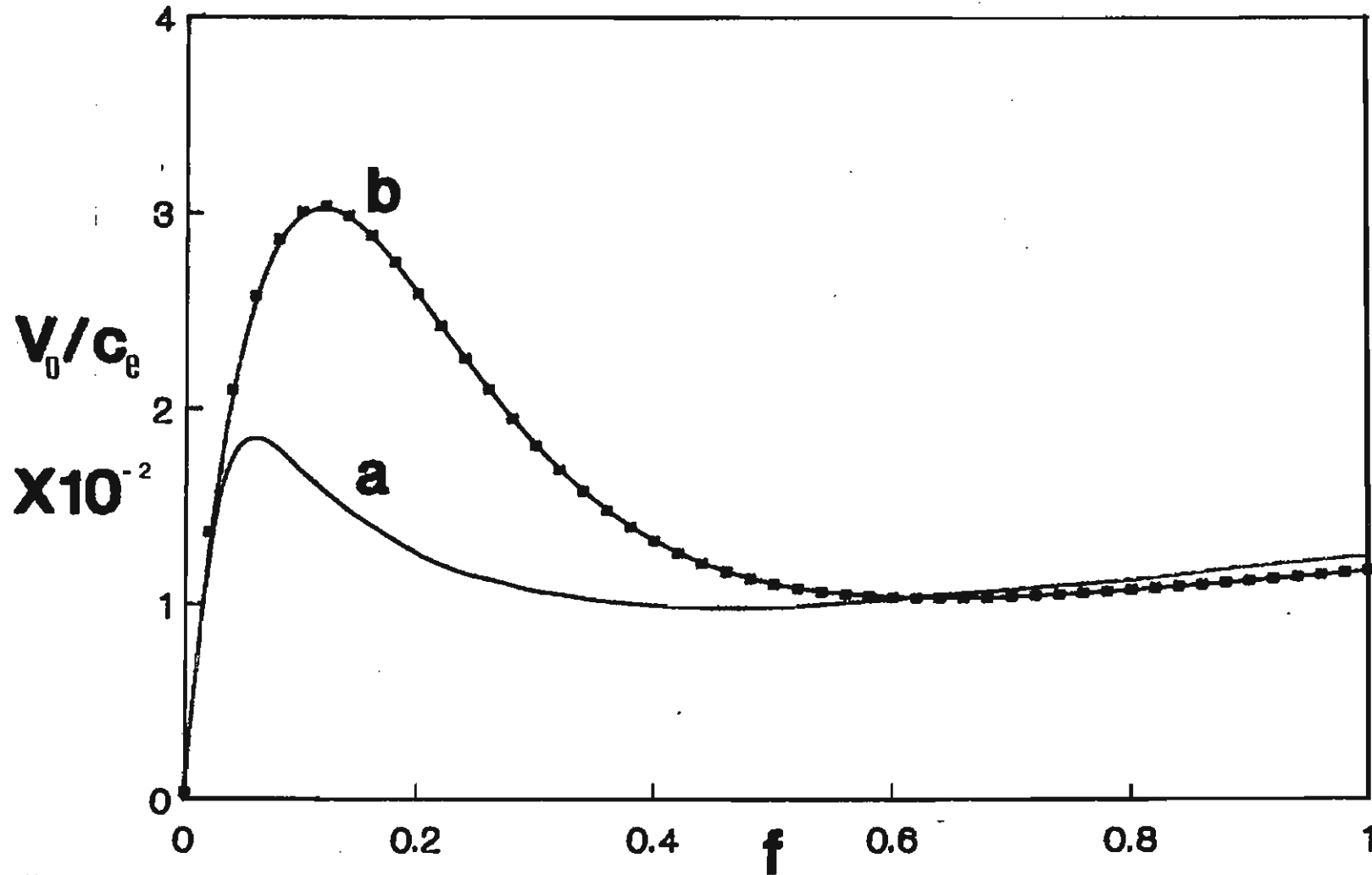
$$b = k_{\perp}^2 c_e^2 / \Omega_e^2 = 0.5 \Rightarrow \Gamma_0(b) = 0.64504.$$

Thus the heavy ion species is chosen to be argon. Except for the results in section 3.6.5, wave propagation is restricted to almost perpendicular (to  $\vec{B}_0$ ) propagation, as is experimentally observed (Barrett et al., 1972; Hayzen and Barrett, 1977).

#### 3.6.1 Variation of $V_0^C$ with Light Ion Fraction (f)

Figure 3.2 represents the relationship between  $f$  (the light ion fraction) and the critical electron drift velocity  $V_0^C$  (normalised with respect to the electron thermal speed,  $c_e$ ). Curve a (—) has been obtained from the full dispersion relation, eqn (3.4.12), whereas curve b (—) is from the approximate eqns (3.5.8) and (3.5.9). In both cases we have set the electron to (common) ion temperature ratio  $\theta = 25$  and the heavy to light ion mass ratio  $M = 10$  (corresponding to the light ion being helium).

# Fig 3.2



Marginal stability curves for  $M = 10$ ,  $\theta = 25$ . Curve (a) is from the full dispersion relation, eqn (3.4.12) while curve (b) is from the approximate dispersion relation, eqn (3.5.9).

The shapes of the curves are similar to those found by Dell (1984) for an unmagnetized plasma. Furthermore, the values of  $f$  (0.055 for the full dispersion curve and 0.12 for the approximate curve) at which  $V_0^C$  attains a maximum value are the same as those found by Dell. This behaviour is consistent with the "contaminant damping" effect of a small fraction of light ions as theoretically discussed by Fried *et al.* (1971), Lambert *et al.* (1976, 1977), Gledhill (1982) and Dell (1984), and experimentally observed by Alexeff *et al.* (1967), Hirose *et al.* (1970), Tran and Coquerand (1975a, 1975b) and Nakamura *et al.* (1975, 1976a, 1976b). In Figure 3.3 we present a plot of damping rate versus real frequency from the work of Fried *et al.* (1971) for an unmagnetized, stable two-ion plasma.

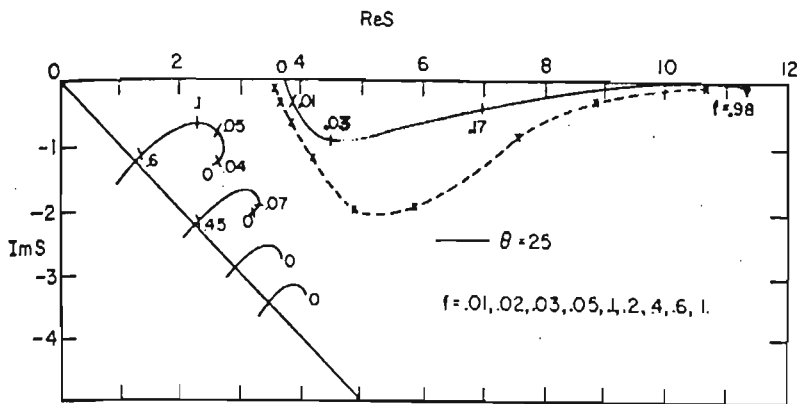


FIG. 3.3. (from Fried *et al.*, 1971). Crosses indicate use of approximate expression for dispersion relation.

It is seen that the damping is largest for a light ion fraction of  $\approx 0.1$  (approximate dispersion relation) and 0.03 (full dispersion relation). Therefore to overcome the damping prior to producing an instability, it follows that the available free energy (and thus the critical drift  $V_0^C$ ) must reach the maximum threshold value for values



of  $f$  near the above values. A possible explanation for this behaviour is given below.

For large  $\theta$  and small  $f$ , the phase velocity,  $V_\phi$ , given by eqn (3.5.8a), is approximately equal to  $(T_e/M_f)^{1/2}$ , where the effective mass  $M_f$  is given by

$$\frac{1}{M_f} = \frac{1}{M_H} (1 - f) + \frac{1}{M_L} f \quad (3.6.1)$$

As helium is added, the phase velocity increases slightly because of the initial decrease in effective mass. Damping at first increases sharply as more light ions become available to resonate with the wave. (Figure 3.4a shows the position of the phase velocity relative to the velocities of the plasma particles in this case).

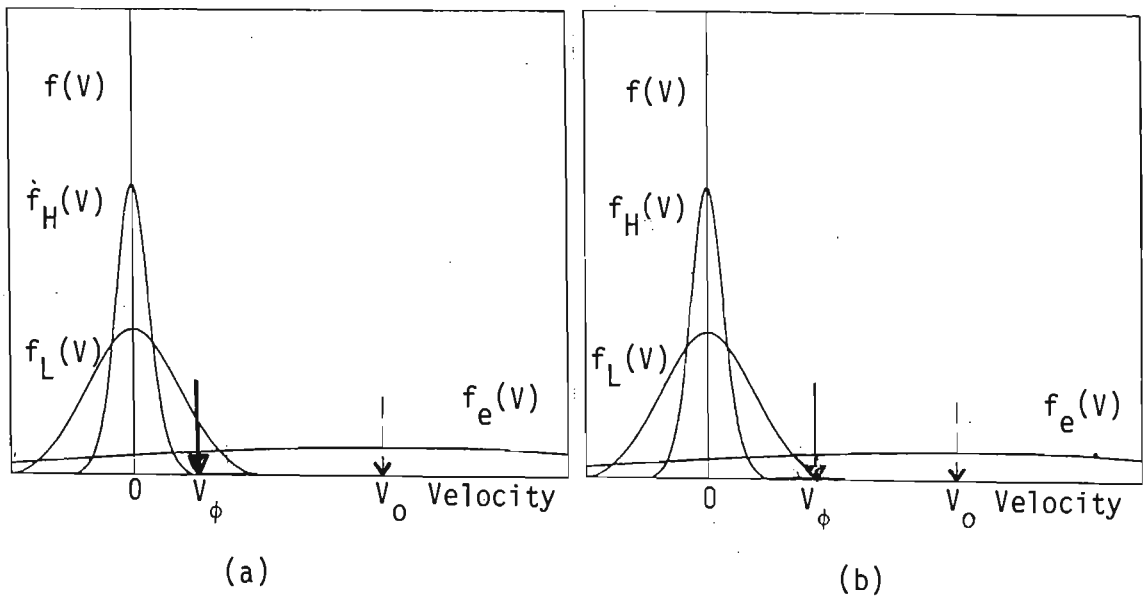


FIG. 3.4

However, as the percentage of light ions increases, the effective ion mass decreases sharply and the phase velocity increases such that very few light ions are available for resonance with the wave (Figure 3.4b). The damping rate decreases and the phase velocity approaches the pure helium value.

The values of  $f$  for  $(V_0^C)_{\max}$  are in reasonable agreement with the condition  $f \sim M^{-1}$  as found by Lambert et al. (1976).

When  $f = 0$  (a pure argon (heavy ion) plasma), Figure 3.2 shows  $V_0^C/c_e = 0.0037$ . Then  $V_0^C = 0.0037 c_e = 0.0037 \sqrt{T_e/M_H} \cdot \sqrt{M_H/m_e} = 1.002 c_{SH}$ , i.e., the critical drift satisfies  $V_0^C \gtrsim c_{SH}$ , which is in agreement with the condition for instability in a plasma with a single ion species (Bharuthram, 1974). Similarly for  $f = 1$ , only helium is present, and  $V_0^C/c_e = 0.012 \Rightarrow V_0^C \gtrsim c_{SL}$ . We also note that  $V_0^C/c_e \ll 1$ , which is in agreement with the criterion,  $c_S < V_0 < c_e$ , of Gary and Biskamp (1971) for the excitation of unstable modes.

For  $f \lesssim 2\%$  and  $f \gtrsim 50\%$  the full dispersion curve and the approximate dispersion curve in Figure 3.2 agree quite closely.

For intermediate values of  $f$ , the approximate dispersion eqns (3.5.8) and (3.5.9) give a larger damping (by as much as a factor of 1.6) than the full dispersion relation, eqn (3.4.12). This is probably due to the assumption  $V_0/c_e \ll 1$  (used in deriving the approximate dispersion equations) being only valid for small  $V_0$ .

We now compare Figure 3.2 with the results obtained by Dell (1984), represented in Figure 3.5. We note that the maximum critical drift speed required for instability in a field-free plasma (Figure 3.5) is approximately 10 times greater than that in a magnetized plasma (Figure 3.2). This difference in peak drift velocity can be explained (Hayzen, 1976; Bharuthram, 1979) with the aid of the following Figures 3.6a and b.

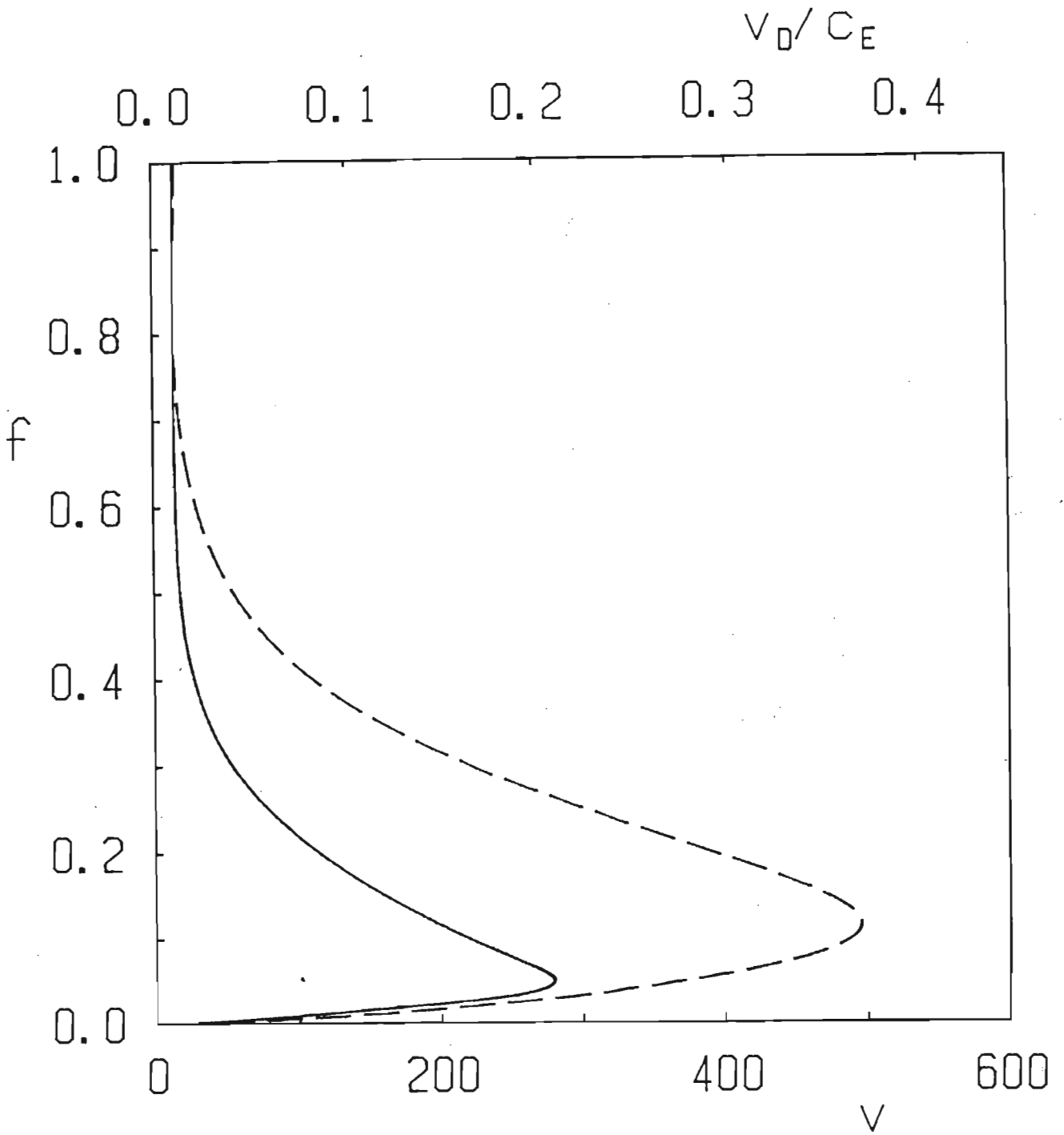


FIG. 3.5 (Fig. 5.3a from Dell, 1984). Marginal stability curves for an unmagnetized two-ion plasma.  $M = 10$  and  $\theta = 25$ . The curve represented by broken lines was obtained from the approximate expression for the dispersion relation.

In the absence of a magnetic field, the electrons, because of their small mass, move rapidly to neutralize any potential perturbations produced by the ions. However, for  $\vec{B} \neq 0$ , the electrons, being magnetized, are tied to the field lines and are only free to accelerate along  $\vec{B}_0$ . In Figure 3.6a below, an electron at point P will travel a distance PQ in the field free case to neutralize the perturbation in the potential. In a magnetized plasma, the electron, being forced to accelerate along  $\vec{B}_0$  travels the longer distance RQ. This longer distance travelled allows the perturbations to grow to a larger amplitude. It can be seen in Figure 3.6a that  $RQ/PQ = k/k_z$ . On the other hand, Figure 3.6b on the next page can be used to explain the increase in growth rate in terms of the velocity distribution functions.

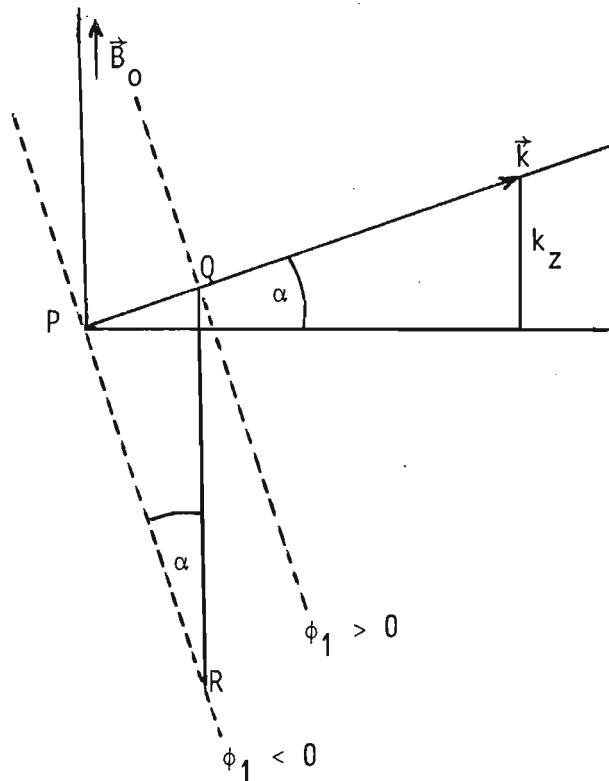


FIG. 3.6a

Since the electron thermal motion is restricted along  $\vec{B}_0$  in the magnetized plasma, its projection along the wave vector  $\vec{k}$  gives an effective distribution with the thermal speed diminished by  $k_z/k$ .

Consequently, even for small drift velocities

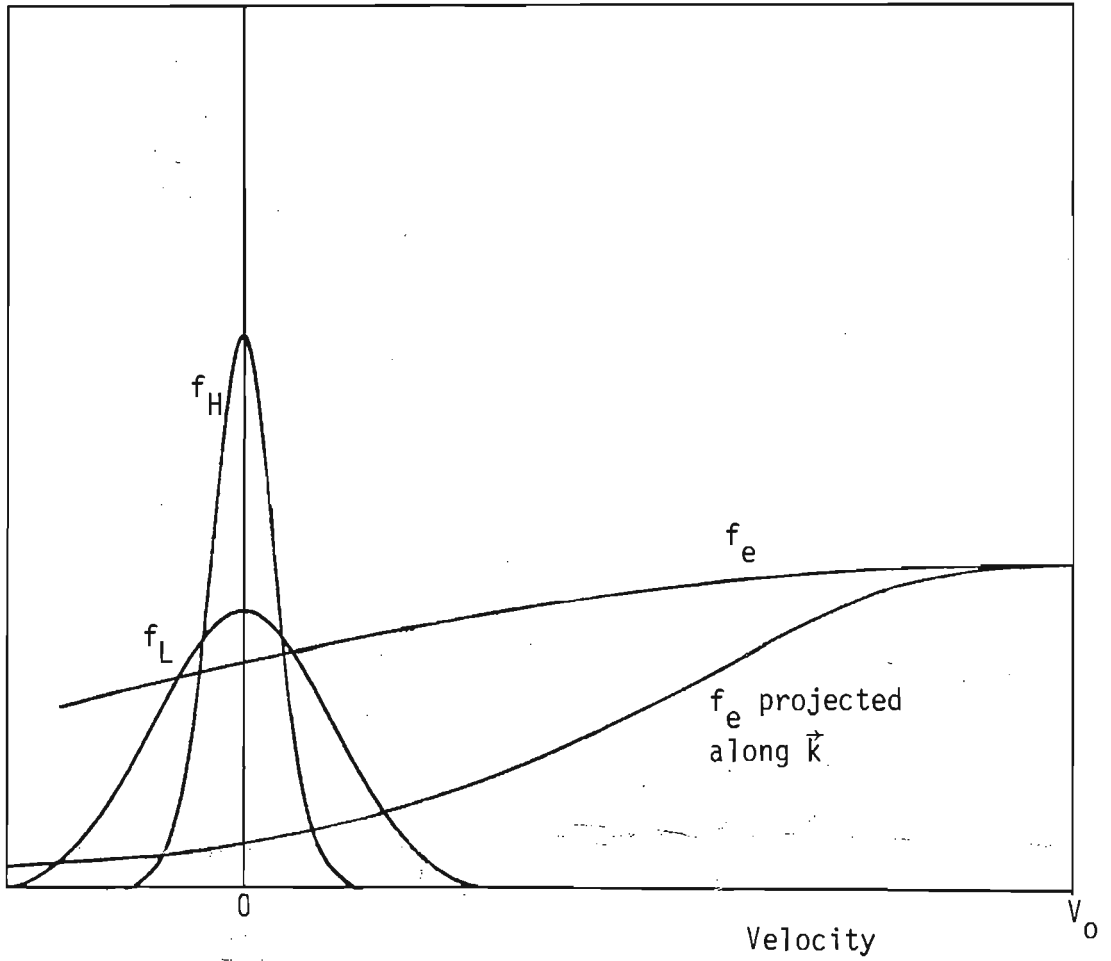


FIG. 3.6b. Effect of magnetic field on the velocity distribution functions of the plasma particles.

$$V_0 \geq \{f c_{SL}^2 + (1 - f) c_{SH}^2\}^{1/2},$$

the phase velocity

$$V_\phi = \{f c_{SL}^2 + (1 - f) c_{SH}^2\}^{1/2} / (1 + k^2 \lambda_D^2)^{1/2}$$

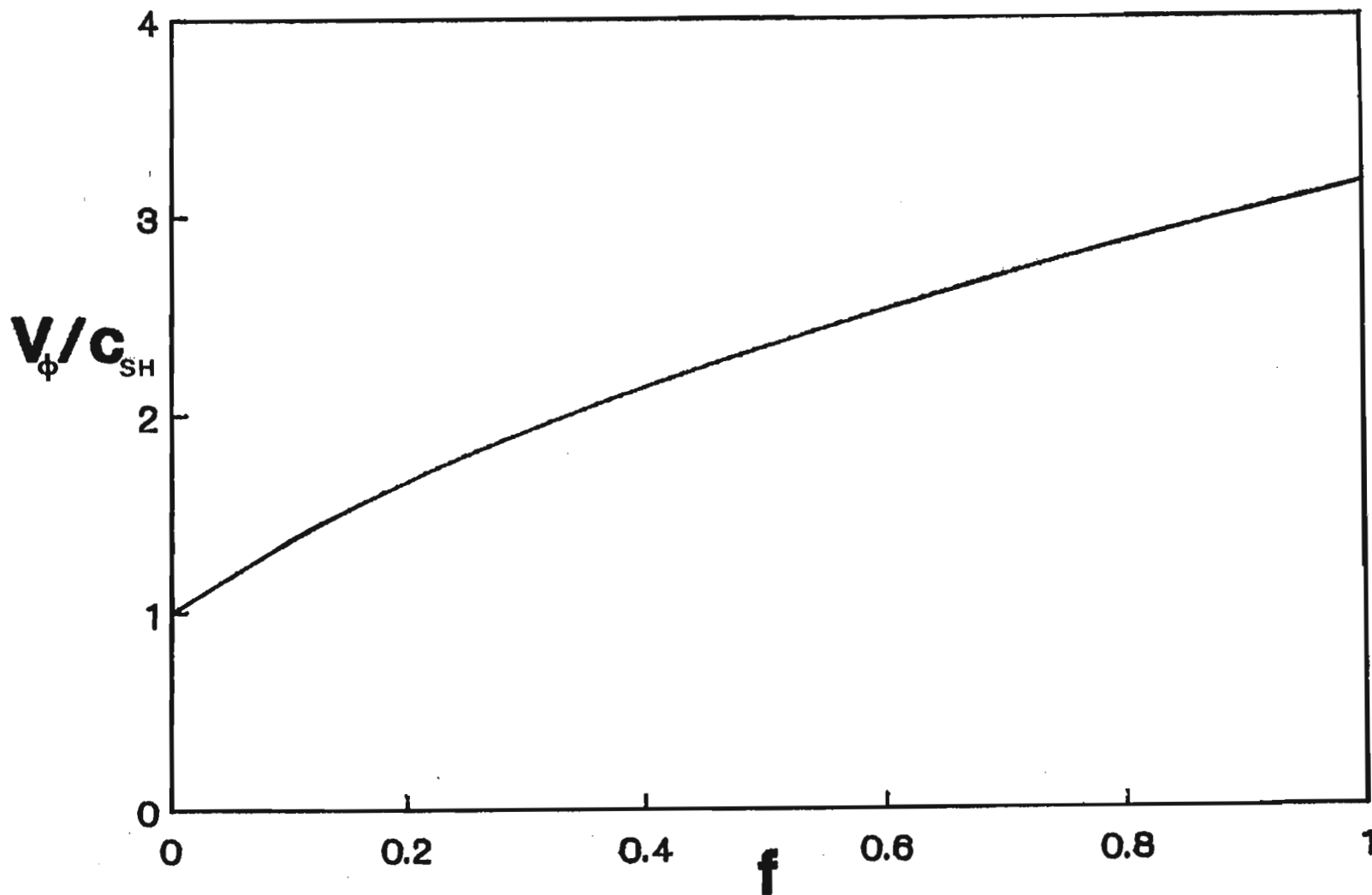
can coincide with the location of maximum slope of the effective electron distribution function and thereby the wave experiences enhanced growth (inverse Landau damping). Since the ions are unmagnetized, their distribution function remains unaffected and hence the ion Landau damping remains unaltered (from the field free case).

### 3.6.2 Variation of the Wave Phase Speed with Light Ion Fraction (f)

Figure 3.7 illustrates the relationship between the normalised phase velocity,  $V_\phi/c_{SH}$ , and the fraction of light ions,  $f$ , as obtained from eqn (3.5.8b). This result is in good agreement with that experimentally found by Nakamura et al. (1975), as shown in Figure 3.8 on page 39.

The graphs show the gradual transition from the heavy ion mode to the light ion mode. Nakamura et al. in subsequent papers (1976a and 1976b) suggested that two waves could be observed simultaneously in a plasma if  $\theta < 2M$ . This was confirmed by Gledhill and Hellberg (1987). For our parameters  $\theta/2M = 1.25$ .

# Fig 3.7



Normalised wave phase velocity as a function of light ion fraction  $f$  for  $M = 10$ ,  $\theta = 25$ .

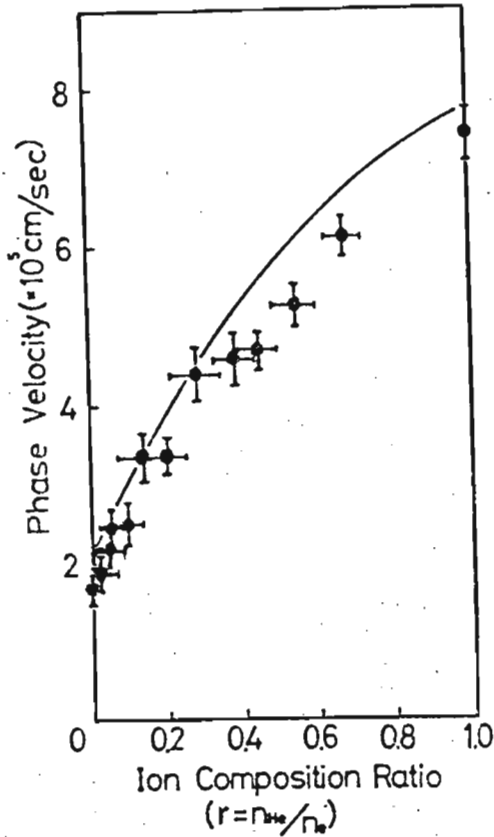


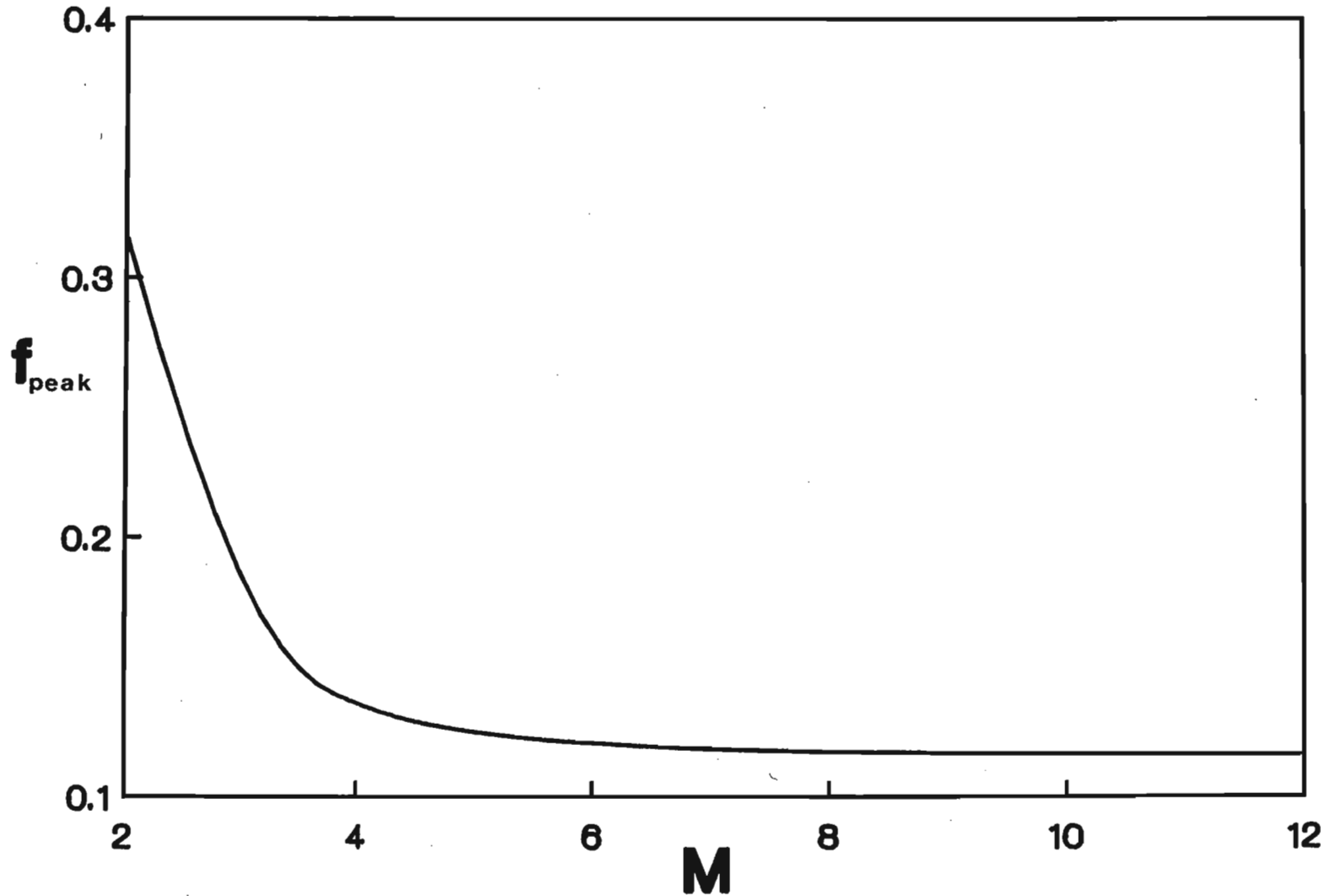
FIG. 3.8. (from Nakamura et al., 1975). Phase velocity of ion acoustic waves in an argon-helium plasma as a function of fraction of light ions for  $\theta = 25$ . Solid curve is the theoretical curve.

### 3.6.3 Variation of $(V_0^C)_{\max}$ with Heavy to Light Ion Mass Ratio (M)

The value of  $f$  at which the critical drift speed ( $V_0^C$ ) reaches a maximum,  $f_{\text{peak}}$ , can be obtained by differentiation of eqn (3.5.9). The variation of  $f_{\text{peak}}$  as a function of  $M$ , the heavy to light ion mass ratio is illustrated in Figure 3.9. Here  $M_H$  was fixed and  $M_L$  varied. We observe that the change in  $f_{\text{peak}}$  is insignificant over the range  $5 < M < 12$ . However, over the range  $2 < M < 5$ ,  $f_{\text{peak}}$  rises sharply from 0.12 to a maximum value of 0.32 for  $M = 2$ . This result warranted a closer examination of the  $M = 2$  case, and Figure 3.10 shows the  $V_0^C$  vs  $f$  curve for  $M = 2$ . Comparison of Figure 3.10 with Figure 3.2 shows that the maximum value of the critical drift speed,  $(V_0^C)_{\max}$ , decreases

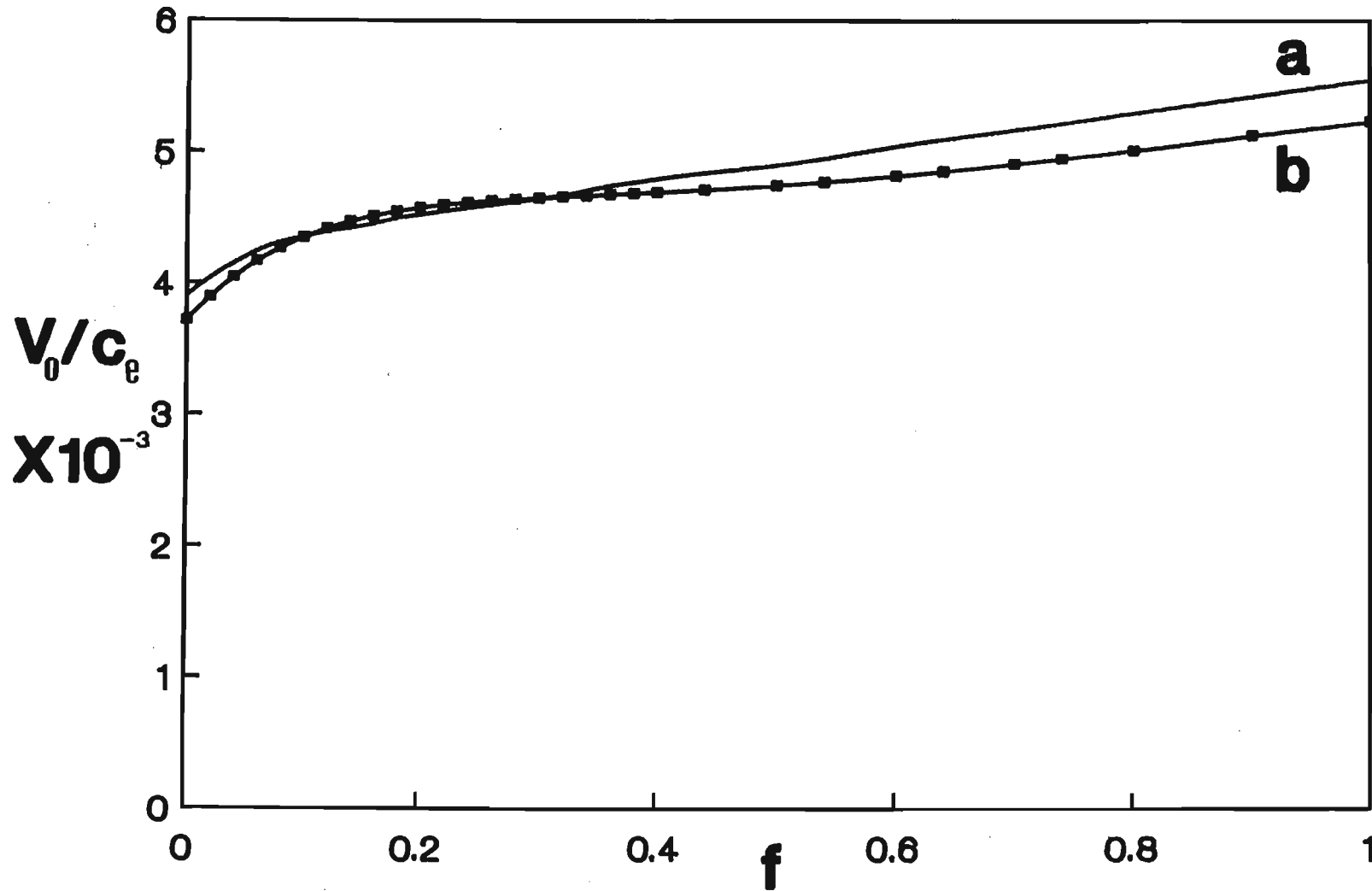


# Fig 3.9



The value of  $f_{\text{peak}}$  (value of  $f$  at which critical drift speed assumes maximum value) as a function of  $M$ , the heavy to light ion mass ratio.  $\theta = 25$ . The approximate dispersion relation, eqn (3.5.9) was used for the plots.

# Fig 3.10



Marginal stability curves for  $M = 2$ ,  $\theta = 25$ . Curve (a) is from the full dispersion relation, eqn (3.4.12) while curve (b) is from the approximate dispersion relation, eqn (3.5.9).

by an order of magnitude for  $M = 2$ . This correlates with the fact that decreasing  $M$  (light ion mass increasing) results in a narrowing of the light ion velocity distribution. Thus fewer ions are available to exchange energy with the wave and the light ion damping becomes weaker. Consequently a smaller electron drift speed is required to drive the instability. In Figure 3.11 we compare the relative positions of the various particle and wave velocities for the  $M = 2$  and  $M = 10$  cases. (These velocities, normalised with respect to the electron thermal speed  $c_e$ , have been calculated from eqns (3.5.8) and (3.5.9)).

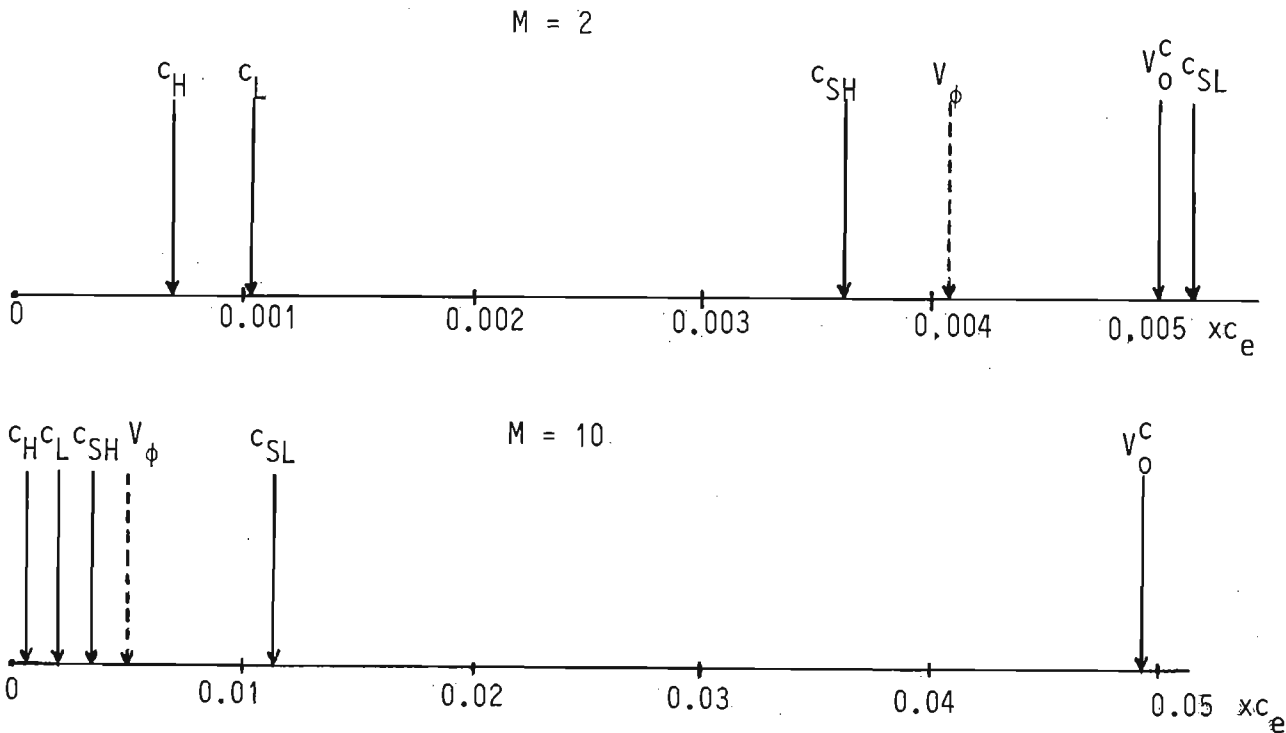


FIG. 3.11

We note that  $(V_O^C)_{\max} / V_\phi = 1.2$  for the  $M = 2$  case is very nearly the instability criterion ( $V_O > V_\phi$ ) for a single-ion plasma. This is not surprising since an ion mass ratio of 2 yields an average total ion distribution which is not too different from a Maxwellian distribution

for a single ion species having a total number of particles

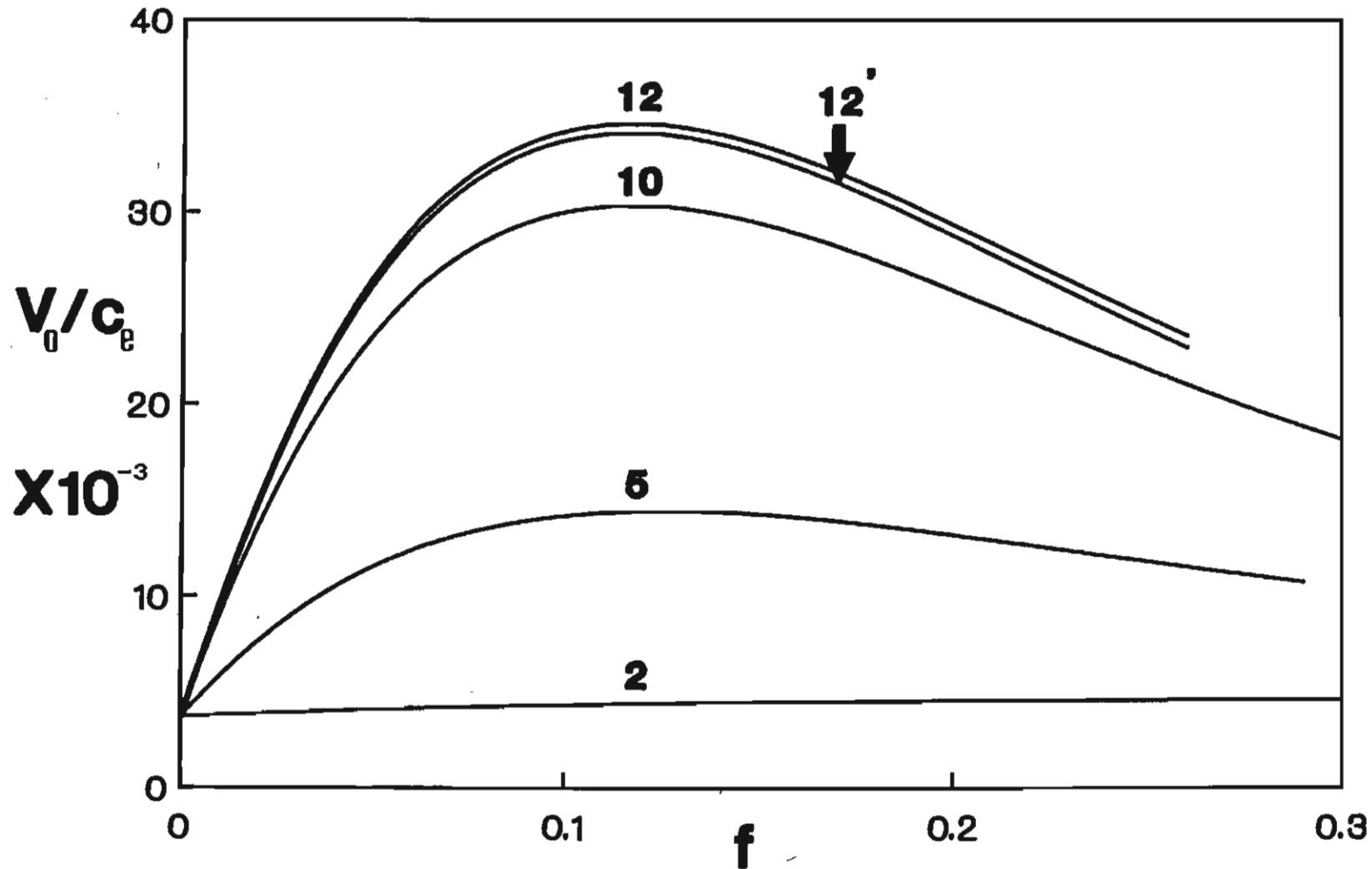
$$n_0 = n_L + n_H \text{ and mass } M_i = \frac{1}{2} (M_L + M_H).$$

From Figures 3.2 and 3.10 it is seen that the approximate analytical solution is in much closer agreement with that of the full dispersion relation for  $M = 2$  than for  $M = 10$ . A numerical evaluation of plasma parameters shows that this is due to the fact that the approximations used in arriving at the results (3.5.8) and (3.5.9) for  $\hat{V}_\phi$  and  $V_0/c_e$ , respectively, are poorly satisfied for the case  $M = 10$  (e.g. from Fig. 3.11 we see that the assumption  $|z_j| \gg 1$  for  $j = L, H$  is more accurately satisfied for  $M = 2$  than  $M = 10$ ).

In Figure 3.12 we show a plot of  $f$  vs  $V_0^C/c_e$  for different  $M$  values. All the curves except  $M = 12$  have been obtained by keeping  $M_H$  fixed and varying  $M_L$ . The approximate expression, eqns (3.5.8) and (3.5.9) were used for the computation. It is seen that an increasing  $M$  (due to  $M_L$  decreasing) is accompanied by an increase in the threshold drift  $(V_0^C)_{\max}$ , required for instability. This is to be expected since a reduction in  $M_L$  causes a broadening of the light ion velocity distribution. Thus there are more light ions in the tail region of the distribution with velocities close to the wave phase velocity. Wave-light ion resonance is enhanced, resulting in an increase in light ion Landau damping. Therefore larger threshold drift velocities are required to drive the instability.

The curve labelled  $M = 12$  has an ion mass ratio of 12 but has been obtained from the  $M = 10$  curve in Figure 3.12 by keeping  $M_L$  fixed and changing  $M_H$ . Increasing  $M_H$  with  $M_L$  fixed causes a decrease in the wave phase speed as given by eqn (3.5.8a). Thus the wave 'sees' a larger negative slope on the light ion velocity distribution resulting in more resonant light ions and an increase in ion Landau damping (as compared to the  $M = 10$  case). Consequently,  $(V_0^C)$  increases.

# Fig 3.12



Marginal stability curves show the effect of varying,  $M$ , the heavy to light ion mass ratio, for  $\theta = 25$ . The parameter labelling the curves is  $M$ . The curve labelled 12' was obtained by keeping  $M_L$  fixed and varying  $M_H$ . All the curves were plotted from the approximate dispersion relation, eqn (3.5.9).

The fact that the two curves  $M = 12$  ( $M_L$  varying,  $M_H$  fixed) and  $M = 12'$  ( $M_L$  fixed,  $M_H$  varying) do not coincide may be due to the light ions for the case  $M = 12$  being lighter and thus having a broader velocity distribution, with a consequent greater light ion Landau damping and corresponding larger  $(V_0^C)_{\max}$ .

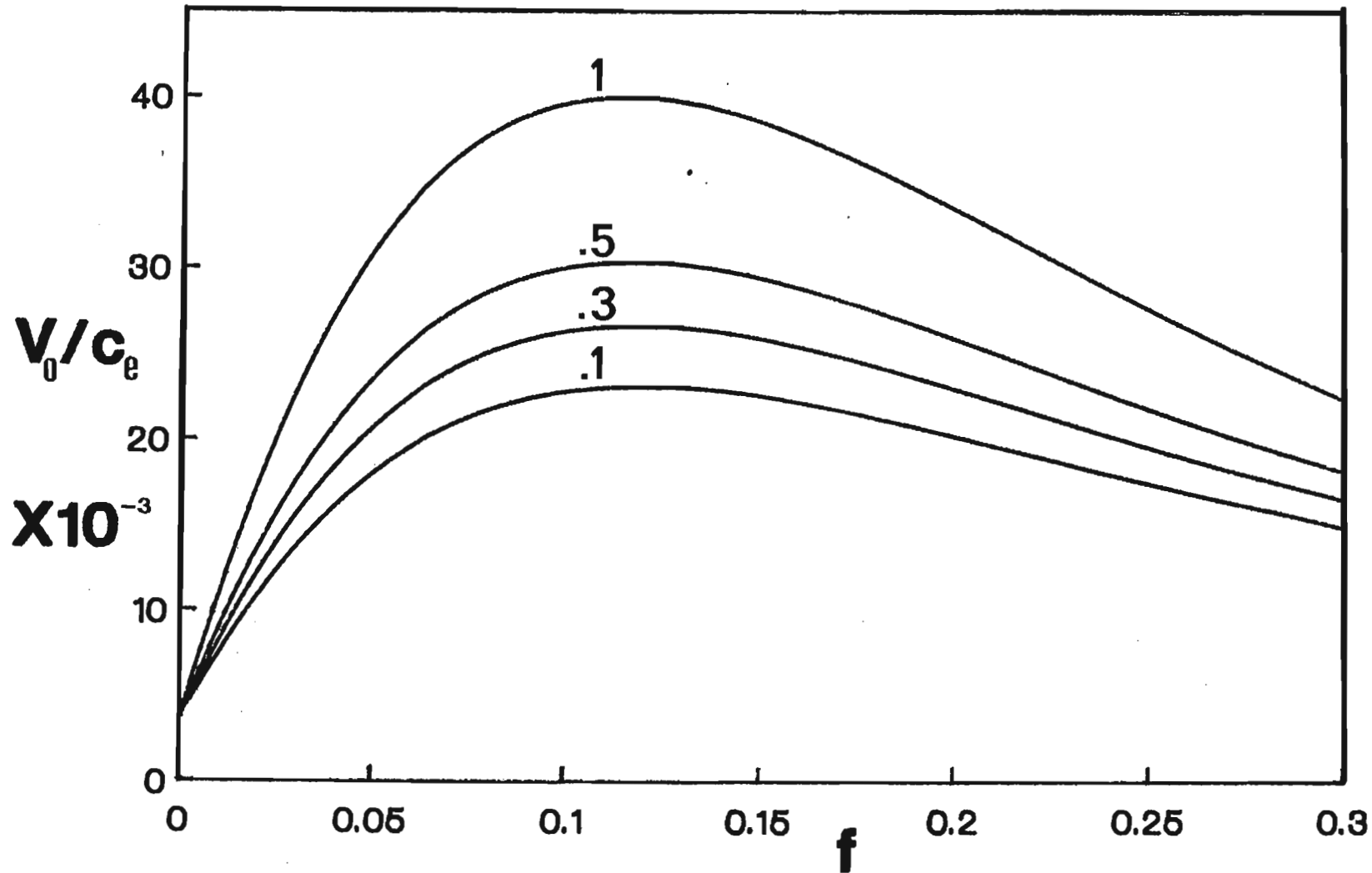
#### 3.6.4 Variation of $(V_0^C)_{\max}$ with Magnetic Field Strength

The effect of changing the magnetic field strength,  $|\vec{B}_0|$ , is shown in Figure 3.13. This corresponds to different values of  $\Gamma_0(b)$  in the expression for  $(V_0^C)/c_e$  since  $b = k_{\perp}^2 c_e^2 / \Omega_e^2$  is inversely proportional to  $|\vec{B}_0|^2$ . The plots have been obtained from the approximate relation, eqns (3.5.8) and (3.5.9). It is seen from the figure that as  $|\vec{B}_0|$  increases ( $b$  decreases, with  $\Gamma_0(b)$  increasing)  $V_0^C/c_e$  decreases for a given  $f$ . This can be explained as follows: since the electrons are tied to the field lines, a stronger field restricts their ability to neutralize any off-parallel potential perturbations. This effectively causes a positive increase in the instability growth rate (Bharuthram and Hellberg, 1974) and thus a smaller threshold velocity is required to drive the instability. The dependence on  $|\vec{B}_0|$  is clearly seen for any two curves in Figure 3.13, e.g., for the curves labelled  $b = 0.5$  and  $b = 1.0$ , we have  $\Gamma_0(1.0)/\Gamma_0(0.5) = 0.72$ , while  $(V_0^C)_{\max}(0.5)/(V_0^C)_{\max}(1.0) = 0.75$ . Thus the maximum threshold velocity is almost inversely proportional to  $\Gamma_0(b)$ .

#### 3.6.5 Variation of $(V_0^C)_{\max}$ with Propagation Angle

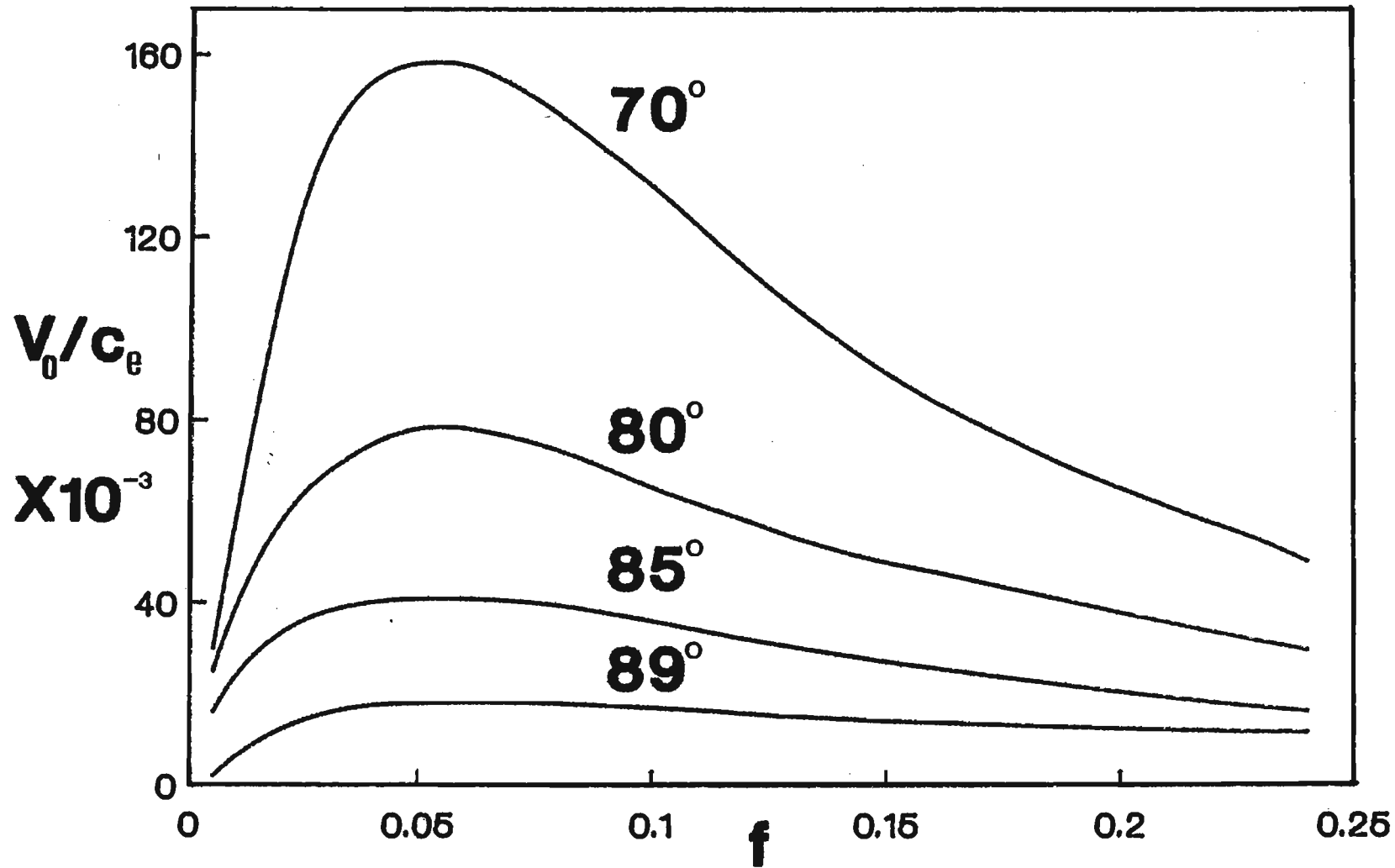
The effect of varying the propagation angle  $\varphi (= \arccos(k_z/k))$  with respect to the magnetic field  $\vec{B}_0$  is shown in Figure 3.14. The full dispersion relation, eqn (3.4.12) was used for the plots. It is seen that

# Fig 3.13



Effect of magnetic field strength on the marginal stability curves for  $M = 10$ ,  $\theta = 25$ . The parameter labelling the curves is  $b (= k_{\perp}^2 c_e^2 / \Omega_e^2)$ , with  $|\vec{B}_0|$  varying. The approximate dispersion relation, eqn (3.5.9) was used for the plots.

# Fig 3.14



Effect of propagation angle  $\phi (= \arccos k_z/k)$  on the marginal stability curves from  $M = 10$ ,  $\theta = 25$ . The parameter labelling curves is  $\phi$ . The full dispersion relation, eqn (3.4.12) was used for the plots.



the threshold drift  $(V_0^C)_{\max}/c_e$  increases with decreasing  $\phi$ , and is consistent with the experimental findings of Hirose et al. (1970). This behaviour can be explained as follows: as  $\phi$  decreases,  $k/k_z$  also decreases for fixed  $k$ . Since for a magnetized plasma the growth rate  $\gamma$  is proportional to  $k/k_z$ , it also decreases. Thus a larger threshold drift speed is needed to excite the instability. Alternatively, as  $\phi$  decreases from  $90^\circ$ , the projection of the particle drift velocity ( $= V_0 \hat{y}$ ) in the propagation direction (as 'seen' by the wave) is reduced in magnitude. However, if this component has to exceed a given value so that the associated free energy will overcome ion Landau damping, it follows that the total drift speed must increase (as  $\phi$  decreases) for wave growth.

In the next Chapter we move away from marginal stability studies and examine the growth rate of the ion acoustic instability. In particular, the effect of inhomogeneities will be studied.

CHAPTER FOUR

THE EFFECT OF INHOMOGENEITIES ON THE CROSSFIELD CURRENT-DRIVEN ION  
ACOUSTIC INSTABILITY IN A TWO-ION PLASMA

In this Chapter we shall study the effect of inhomogeneities in the electron density and temperature and the external magnetic field on the growth rate of the ion acoustic instability in a two-ion plasma.

4.1 DERIVATION OF THE ELECTRON TERM IN THE LINEAR DISPERSION RELATION

The following derivation of the dispersion relation is based on that of Bharuthram (1974). The model considered is essentially the same as in Chapter Three, viz., a collisionless, two-ion plasma embedded in external fields  $\vec{B}_0 = B_0 \hat{z}$ ,  $\vec{E}_0 = -E_0 \hat{x}$ , with the magnetized electrons having an  $\vec{E} \times \vec{B}$  drift,

$$\vec{v}_0 = \left( \frac{cE_0}{B_0} \right) \hat{y} \quad (4.1.1)$$

relative to the stationary unmagnetized ions. In addition to the inhomogeneity in  $\vec{B}_0$  defined by

$$\vec{B}_0(x) = B_0(1 + \epsilon x) \hat{z} \quad , \quad (4.1.2)$$

we include non uniformities in electron density  $n_e$  and perpendicular (to  $\vec{B}_0$ ) electron temperature  $T_{\perp e}$ , given by

$$n_e(x) = n_{0e}(1 + \alpha x) \quad (4.1.3)$$

$$T_{\perp e}(x) = T_{0e}(1 + \delta x) \quad (4.1.4)$$

The associated drift velocities are given by

$$\begin{aligned} \nabla B &: \vec{V}_B = -\frac{\epsilon V_{\perp}^2}{2\Omega_e} \hat{y} = -V_B \hat{y} & (a) \\ \nabla n_e &: \vec{V}_n = -\frac{\alpha T_{oe}}{m_e \Omega_e} \hat{y} = -V_n \hat{y} & (b) \\ \nabla T_{\perp e} &: \vec{V}_T = -\frac{\delta T_{oe}}{m_e \Omega_e} \hat{y} = -V_T \hat{y} & (c) \end{aligned} \quad \left. \vphantom{\begin{aligned} \nabla B \\ \nabla n_e \\ \nabla T_{\perp e} \end{aligned}} \right\} (4.1.5)$$

where  $\Omega_e$  is the electron gyroradius. The Figure 4.1 below indicates the directions of the external fields, inhomogeneities and the associated drift velocities. It is seen that  $\vec{V}_0$  is opposite in direction to the gradient-driven drift velocities.

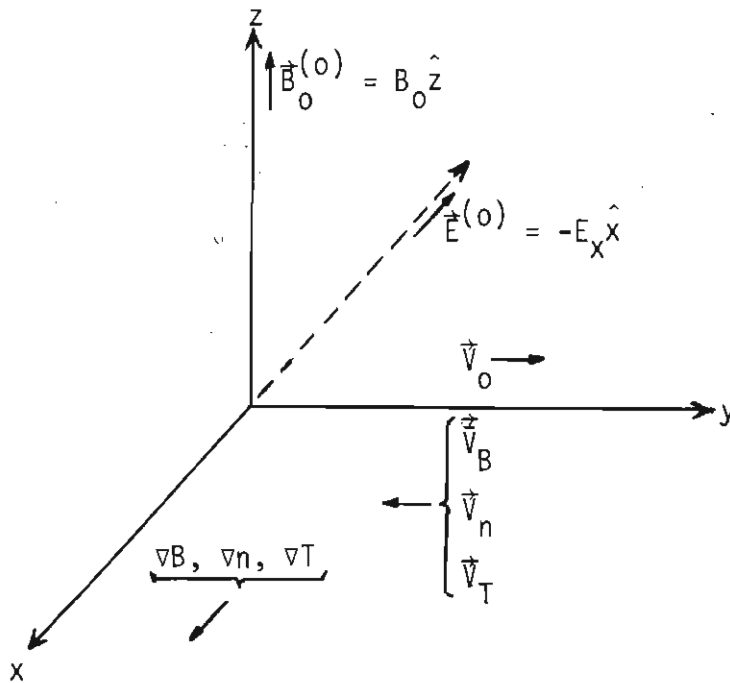


FIG. 4.1

From the electron equations of motion, eqn (3.2.5), we can construct the following constants of motion

$$V_{\perp}^2 = V_x^2 + (V_y - V_0)^2 \text{ and } V_z \text{ (as before) and (to order } \epsilon) \quad \chi = x - \frac{(V_y - V_0)}{\Omega_e}.$$

Thus the steady state electron distribution function is taken to be

$$f_e^{(0)}(V_{\perp}^2, \chi, V_z) = \frac{n_{0e}}{(2\pi c_e^2)^{3/2}} \left\{ 1 + \chi \left[ \alpha + \left\{ \delta \frac{(V_{\perp}^2 - 2c_e^2)}{2c_e^2} \right\} \right] \right\} \exp \left\{ - \frac{(V_{\perp}^2 + V_z^2)}{2c_e^2} \right\} \quad (4.1.6)$$

Since  $f$  is a function of the constants of motion, it is a solution to the linearized Vlasov equation (Krafl and Trivelpiece, 1973).

We also find that the net electron drift is given by

$$\begin{aligned} \vec{V}_D &= \frac{1}{n} \int \vec{V} f_e^{(0)} d^3\vec{V} \\ &= \vec{V}_0 + \vec{V}_n + \vec{V}_T = (V_0 - V_n - V_T) \hat{y} \quad (4.1.7) \end{aligned}$$

We notice that the average  $V_B$  drift does not contribute to the net drift. This is so because in setting up the constants of motion we have ignored the spatial variation in  $\vec{B}$ . It is possible that if  $f(\vec{V})$  was also expressed in terms of the magnetic moment  $\mu = \frac{\frac{1}{2} m_e V_{\perp}^2}{|\vec{B}|}$ , that  $\vec{V}_B$  would appear self consistently in the net drift.

In desiring an expression for the perturbed electron distribution  $f_e^{(1)}$ , it can be seen from eqn (3.2.9) that one requires  $\frac{\partial f_e^{(0)}}{\partial \vec{V}}$ .

For  $f_e^{(0)} \equiv f_e^{(0)}(V_{\perp}^2, \chi, V_z)$ , given by eqn (4.1.6),

$$\begin{aligned}
 \frac{\partial f_e^{(0)}}{\partial \vec{V}} &= \frac{\partial f_e^{(0)}}{\partial V_{\perp}^2} \frac{\partial V_{\perp}^2}{\partial \vec{V}} + \frac{\partial f_e^{(0)}}{\partial x} \frac{\partial x}{\partial \vec{V}} + \frac{\partial f_e^{(0)}}{\partial V_z} \frac{\partial V_z}{\partial \vec{V}} \\
 &= \left[ -\frac{1}{2c_e^2} f_e^{(0)} + n_{oe} (2\pi c_e^2)^{-3/2} \times \frac{\delta}{2c_e^2} \exp\left(-\frac{V^2}{2c_e^2}\right) \right] 2\vec{V}_{\perp} \\
 &+ \left[ n_{oe} (2\pi c_e^2)^{-3/2} \left\{ \alpha + \delta \frac{(V_{\perp}^2 - 2c_e^2)}{2c_e^2} \right\} \exp\left(-\frac{V^2}{2c_e^2}\right) \right] \left(-\frac{1}{\Omega_e} \hat{y}\right) \\
 &- \left[ \frac{V_z}{c_e^2} f_e^{(0)} \right] \hat{z} . \tag{4.1.8}
 \end{aligned}$$

In evaluating eqn (4.1.8) we neglect terms containing the products of gradients since the latter are assumed to be weak. We also make use of the local approximation (Krall and Trivelpiece, 1973) in expanding about  $x = 0$ .

The local approximation requires the spatial variations in the perturbed electric field and distribution function to be nearly harmonic i.e.

$$\begin{aligned}
 \vec{E}^{(1)} &\sim \bar{E}_k \exp \{i(\vec{k} \cdot \vec{x} - \omega t)\} \\
 f_e^{(1)} &\sim \bar{f}_k \exp \{i(\vec{k} \cdot \vec{x} - \omega t)\}
 \end{aligned}$$

where  $\bar{E}_k$  and  $\bar{f}_k$  are constants. Maxwell's equations can then be used to obtain a dispersion relation  $D$  given by

$$D(\vec{k}, \omega, x) = 0.$$

Since the variables vary linearly with  $x$  (cf eqns (4.1.2), (4.1.3), (4.1.4)), the gradients are the same at all points. The dispersion relation  $D(\vec{k}, \omega, x)$  can then be evaluated at any  $x$ . For convenience we select  $x = 0$ . The physical justification for the local approximation, as given by Bharuthram (1974) is as follows:

If the wavelength,  $\lambda$ , of the instability is very much less than the scale lengths of the gradients, e.g.  $\lambda \ll (\frac{1}{n} \frac{dn}{dx})$ , then the drift of the plasma can be regarded as fairly constant. Hence if the variation of the drifts is small over many wavelengths, all other spatial dependence of the equilibrium can be ignored.

The second part of the term [-----]  $2\vec{V}_\perp$  on the right hand side of eqn (4.1.8) may now be approximated as follows:

$$\frac{\delta}{2c_e^2} \left\{ n_{oe} (2\pi c_e^2)^{-3/2} \exp\left(-\frac{V^2}{2c_e^2}\right) \right\} = \frac{\delta}{2c_e^2} f_e^{(0)} \left\{ 1 + \chi \left[ \alpha + \delta \frac{(V_\perp^2 - 2c_e^2)}{2c_e^2} \right] \right\}^{-1} \approx \frac{\delta}{2c_e^2} f_e^{(0)}$$

for weak gradients.

Then eqn (4.1.8) may be written as

$$\frac{\partial f_e^{(0)}}{\partial \vec{V}} \approx \left[ -\frac{(V_y - V_0)}{\Omega_e} \frac{\delta}{2c_e^2} f_e^{(0)} \right] 2\vec{V}_\perp - \frac{1}{\Omega_e} \times \left[ \alpha + \delta \frac{(V_\perp^2 - 2c_e^2)}{2c_e^2} \right] f_e^{(0)} \hat{y} + \frac{(-\vec{V} + \vec{V}_0)}{c_e^2} f_e^{(0)} \quad (4.1.9)$$

with which the perturbed electron velocity distribution  $f_e^{(1)}$  (cf eqn (3.2.16)) becomes

$$f_e^{(1)}(\vec{V}) = \frac{ef_e^{(0)}(\vec{V}') \phi_{k\omega}^{(1)}}{T_{oe}} \left[ 1 + i \left\{ \omega - \vec{k} \cdot \vec{V}_0 + \frac{k_y T_{oe}}{m_e \Omega_e} \times \right. \right. \\ \left. \left. \left[ \alpha + \frac{\delta}{2c_e^2} (V_{\perp}^2 - 2c_e^2) \right] + \frac{2(V_y' - V_0)}{\Omega_e} \left( \frac{T_{oe}}{m_e} \right) \left( \frac{\delta}{2c_e^2} \right) (k_x V_x + k_y [V_y' - V_0]) \right\} \right] \\ \times \int_{-\infty}^0 \exp\{i [\vec{k} \cdot (\vec{r}' - \vec{r}) - \omega t']\} dt'$$

for harmonic perturbations of the form given by eqns (3.2.11) and (3.2.12).

Then upon integrating with respect to time and over velocity space, we obtain the perturbed electron density

$$n_{ek\omega}^{(1)} = \frac{n_{oe} e \phi_{k\omega}^{(1)}}{T_{oe}} \left[ 1 + \sum_{p=-\infty}^{+\infty} \sum_{q=-\infty}^{+\infty} \int_0^{\infty} V_{\perp} dV_{\perp} \int_{-\infty}^{\infty} dV_z \times \right. \\ \left. \frac{J_p \left( \frac{k_{\perp} V_{\perp}}{\Omega_e} \right) J_q \left( \frac{k_{\perp} V_{\perp}}{\Omega_e} \right) \exp\{i(p - q) \phi\}}{[k_z V_z + k_y (V_0 - V_B) - \omega + p\Omega_e]} \times \right. \\ \left. \frac{\exp\left(-\frac{V^2}{2c_e^2}\right)}{(2\pi c_e^2)^{3/2}} \left\{ \left( \omega - k_y V_0 + \frac{k_y T_{oe}}{m_e \Omega_e} \left[ \alpha + \frac{\delta}{2c_e^2} (V_{\perp}^2 - 2c_e^2) \right] \right) \int_0^{2\pi} \exp\{i(p - q) \phi\} d\phi \right. \right. \\ \left. \left. + \frac{2T_{oe}}{m_e \Omega_e} \frac{\delta}{2c_e^2} k_x V_{\perp}^2 \int_0^{2\pi} \exp\{i(p - q) \phi\} \cos \phi \sin \phi d\phi \right. \right. \\ \left. \left. + \frac{2T_{oe}}{m_e \Omega_e} \frac{\delta}{2c_e^2} k_y V_{\perp}^2 \int_0^{2\pi} \exp\{i(p - q) \phi\} \sin^2 \phi d\phi \right\} \right] \quad (4.1.10)$$

where  $V_x = V_{\perp} \cos \phi$ ,  $V_y - V_0 = V_{\perp} \sin \phi$  and the primed notation has been dropped (from the velocities) for convenience.

If we perform the angular integrations, eqn (3.2.21), and introduce the plasma dispersion function, eqn (3.2.22), then eqn (4.1.10) reduces to

$$n_{ek\omega}^{(1)} = n_{oe} e^{\phi_{k\omega}^{(1)}} \left[ 1 + \sum_{p=-\infty}^{+\infty} \frac{1}{\sqrt{2}k_z c_e^3} \int_0^\infty \left\{ \omega - k_y V_o + k_y \left( \frac{\alpha T_{oe}}{m_e \Omega_e} \right) - k_y \left( \frac{\delta T_{oe}}{m_e \Omega_e} \right) + \left( \frac{k_y \delta}{\Omega_e} \right) V_\perp^2 \right\} Z \left\{ \frac{\omega - p\Omega_e - k_y (V_o - V_B)}{\sqrt{2}k_z c_e} \right\} \exp \left( - \frac{V_\perp^2}{2c_e^2} \right) J_p^2 \left( \frac{k_\perp V_\perp}{\Omega_e} \right) V_\perp dV_\perp \right] \quad (4.1.11)$$

As in Chapter Three, for the ion acoustic wave, which is a low frequency mode, we retain only the  $p = 0$  term in the summation above.

Therefore the electron contribution to the full dispersion relation, eqn (3.4.4), with inhomogeneities in external magnetic field, electron density and electron temperature is given by

$$K_e = \frac{k_D^2}{k^2} \left[ 1 + \frac{1}{\sqrt{2}k_z c_e^3} \int_0^\infty \left\{ \omega - k_y V_o + k_y V_n - k_y V_T + k_y \frac{\delta V_\perp^2}{\Omega_e} \right\} \times Z \left\{ \frac{\omega - k_y (V_o - \epsilon V_B)}{\sqrt{2}k_z c_e} \right\} \exp \left( - \frac{V_\perp^2}{2\Omega_e} \right) J_0^2 \left( \frac{k_\perp V_\perp}{\Omega_e} \right) V_\perp dV_\perp \right] \quad (4.1.12)$$

where  $k_D$  is the inverse electron Debye length defined previously, and we note that  $V_B = \epsilon V_\perp^2 / 2\Omega_e$  is a function of  $V_\perp$ .



The integral in eqn (4.1.12) can be written as

$$I = \int_0^{\infty} \left\{ (\omega - k_y V_0 + k_y (V_n - V_T) + \frac{k_y \delta V_{\perp}^2}{\Omega_e}) \right\} Z \left( \frac{\omega - k_y V_0 + \frac{k_y \epsilon V_{\perp}^2}{2\Omega_e}}{\sqrt{2} k_z c_e} \right) \\ \times \exp \left( - \frac{V_{\perp}^2}{2c_e^2} \right) J_0^2 \left( \frac{k_{\perp} V_{\perp}}{\Omega_e} \right) V_{\perp} dV_{\perp} .$$

If we define

$$\bar{\omega} = \omega - k_y V_0 , \\ \omega^* = \bar{\omega} + k_y (V_n - V_T) , \\ \eta = \frac{k_y \delta}{\Omega_e} , \\ \xi = \frac{k_y \epsilon}{2\Omega_e} ,$$

then the integral becomes

$$I = \int_0^{\infty} (\omega^* + \eta V_{\perp}^2) Z \left( \frac{\bar{\omega}}{\sqrt{2} k_z c_e} + \frac{\xi V_{\perp}^2}{\sqrt{2} k_z c_e} \right) \\ \times \exp \left( - \frac{V_{\perp}^2}{2c_e^2} \right) J_0^2 \left( \frac{k_{\perp} V_{\perp}}{\Omega_e} \right) V_{\perp} dV_{\perp} \quad (4.1.13)$$

For weak gradients,

$$|\xi V_{\perp}^2| = |k_y V_B| \ll |\omega - k_y V_0| = |\bar{\omega}| ,$$

and we expand

$$Z \left( \frac{\bar{\omega}}{\sqrt{2} k_z c_e} + \frac{\xi V_{\perp}^2}{\sqrt{2} k_z c_e} \right)$$

as

$$Z \left( \frac{\bar{\omega}}{\sqrt{2} k_z c_e} + \frac{\xi V_{\perp}^2}{\sqrt{2} k_z c_e} \right) = Z \left( \frac{\bar{\omega}}{\sqrt{2} k_z c_e} \right) + Z' \left( \frac{\bar{\omega}}{\sqrt{2} k_z c_e} \right) \frac{\xi V_{\perp}^2}{\sqrt{2} k_z c_e} ,$$

which upon substitution into eqn (4.1.13) yields

$$\begin{aligned}
 I &= \int_0^\infty (\omega^* + nV_\perp^2) \left\{ Z\left(\frac{\bar{\omega}}{\sqrt{2}k_z c_e}\right) + Z'\left(\frac{\bar{\omega}}{\sqrt{2}k_z c_e}\right) \frac{\xi V_\perp^2}{\sqrt{2}k_z c_e} \right\} \\
 &\times \exp\left(-\frac{V_\perp^2}{2c_e^2}\right) J_0^2\left(\frac{k_\perp V_\perp}{\Omega_e}\right) V_\perp dV_\perp \\
 &= \int_0^\infty \omega^* Z\left(\frac{\bar{\omega}}{\sqrt{2}k_z c_e}\right) \exp\left(-\frac{V_\perp^2}{2c_e^2}\right) J_0^2\left(\frac{k_\perp V_\perp}{\Omega_e}\right) V_\perp dV_\perp \\
 &+ \int_0^\infty \omega^* Z'\left(\frac{\bar{\omega}}{\sqrt{2}k_z c_e}\right) \left(\frac{\xi V_\perp^2}{\sqrt{2}k_z c_e}\right) \exp\left(-\frac{V_\perp^2}{2c_e^2}\right) J_0^2\left(\frac{k_\perp V_\perp}{\Omega_e}\right) V_\perp dV_\perp \\
 &+ \int_0^\infty nV_\perp^2 Z\left(\frac{\bar{\omega}}{\sqrt{2}k_z c_e}\right) \exp\left(-\frac{V_\perp^2}{2c_e^2}\right) J_0^2\left(\frac{k_\perp V_\perp}{\Omega_e}\right) V_\perp dV_\perp \\
 &+ \int_0^\infty \frac{n\xi V_\perp^4}{\sqrt{2}k_z c_e} Z'\left(\frac{\bar{\omega}}{\sqrt{2}k_z c_e}\right) \exp\left(-\frac{V_\perp^2}{2c_e^2}\right) J_0^2\left(\frac{k_\perp V_\perp}{\Omega_e}\right) V_\perp dV_\perp \tag{4.1.14}
 \end{aligned}$$

The last term in eqn (4.1.14) contains the factor

$$n\xi = \frac{k_\perp^2 \delta \epsilon}{2\Omega_e^2}$$

which is a product of gradients and hence can be neglected. The first term in eqn (4.1.14) can be written as

$$\begin{aligned}
 & \omega^* Z\left(\frac{\bar{\omega}}{\sqrt{2}k_z c_e}\right) \int_0^\infty \exp\left(-\frac{V_\perp^2}{2c_e^2}\right) J_0^2\left(\frac{k_\perp V_\perp}{\Omega_e}\right) V_\perp dV_\perp \\
 &= \omega^* Z\left(\frac{\bar{\omega}}{\sqrt{2}k_z c_e}\right) c_e^2 e^{-b} I_0(b) \\
 &= \omega^* Z\left(\frac{\bar{\omega}}{\sqrt{2}k_z c_e}\right) c_e^2 \Gamma_0(b) \tag{4.1.15}
 \end{aligned}$$

where we have used the results of eqn (3.4.9) with  $p = 0$ .

The second and third terms in eqn (4.1.14) may be added together to yield

$$\begin{aligned}
 & \left\{ \frac{\omega^* \xi}{\sqrt{2}k_z c_e} Z'\left(\frac{\bar{\omega}}{\sqrt{2}k_z c_e}\right) + \eta Z\left(\frac{\bar{\omega}}{\sqrt{2}k_z c_e}\right) \right\} \int_0^\infty V_\perp^2 \exp\left(-\frac{V_\perp^2}{2c_e^2}\right) J_0^2\left(\frac{k_\perp V_\perp}{\Omega_e}\right) V_\perp dV_\perp \\
 &= \left[ \frac{\omega^* \xi}{\sqrt{2}k_z c_e} Z'\left(\frac{\bar{\omega}}{\sqrt{2}k_z c_e}\right) + \eta Z\left(\frac{\bar{\omega}}{\sqrt{2}k_z c_e}\right) \right] \times 2c_e^4 e^{-b} [(1 - b) I_0 + b I_1(b)] \\
 &= \left[ \frac{\omega^* \xi}{\sqrt{2}k_z c_e} Z'\left(\frac{\bar{\omega}}{\sqrt{2}k_z c_e}\right) + \eta Z\left(\frac{\bar{\omega}}{\sqrt{2}k_z c_e}\right) \right] \times 2c_e^4 S_0, \tag{4.1.16}
 \end{aligned}$$

where we have used the relation (Watson, 1944)

$$\int_0^\infty x^2 \exp(-\alpha x^2) J_0^2(\beta x) x dx = \frac{1}{2\alpha^2} \exp(-\beta^2/2\alpha)$$

$$\times [(1 - \beta^2/2\alpha) I_0(\beta^2/2\alpha) + (\beta^2/2\alpha) I_1(\beta^2/2\alpha)],$$

with  $I_1$  being the modified Bessel function of order 1, and we have defined  $S_0 = (1 - b) \Gamma_0 + b \Gamma_1(b)$  with  $b = \frac{k_\perp^2 c_e^2}{\Omega_e^2}$ .

Substituting eqns (4.1.15) and (4.1.16) into eqn (4.1.14), the integral I becomes

$$I = \omega^* c_e^2 \Gamma_0(b) Z\left(\frac{\bar{\omega}}{\sqrt{2}k_z c_e}\right) + \left\{ \frac{\omega^* \xi}{\sqrt{2}k_z c_e} Z'\left(\frac{\bar{\omega}}{\sqrt{2}k_z c_e}\right) + \eta Z\left(\frac{\bar{\omega}}{\sqrt{2}k_z c_e}\right) \right\} \times 2c_e^4 S_0 \quad (4.1.17)$$

Using this result in eqn (4.1.12), the electron contribution to the dispersion relation becomes

$$\begin{aligned} K_e &= \frac{k_D^2}{k^2} \left[ 1 + \frac{1}{\sqrt{2}k_z c_e^3} \left\{ \omega^* c_e^2 \Gamma_0(b) Z\left(\frac{\bar{\omega}}{\sqrt{2}k_z c_e}\right) + \left[ \frac{\omega^* \xi}{\sqrt{2}k_z c_e} Z'\left(\frac{\bar{\omega}}{\sqrt{2}k_z c_e}\right) + \eta Z\left(\frac{\bar{\omega}}{\sqrt{2}k_z c_e}\right) \right] \times 2c_e^4 S_0 \right\} \right] \\ &= \frac{k_D^2}{k^2} \left[ 1 + \left\{ \left( \frac{\omega^*}{\sqrt{2}k_z c_e} \right) \Gamma_0 + \frac{\eta 2c_e^2}{\sqrt{2}k_z c_e} S_0 \right\} Z\left(\frac{\bar{\omega}}{\sqrt{2}k_z c_e}\right) + \frac{\omega^* \xi}{k_z^2 c_e^2} Z'\left(\frac{\bar{\omega}}{\sqrt{2}k_z c_e}\right) c_e^2 S_0 \right] \\ &= \frac{k_D^2}{k^2} \left[ 1 + \left\{ \frac{(\omega - k_y V_o + k_y V_n) \Gamma_0 - k_y V_T (\Gamma_0 - 2S_0)}{\sqrt{2}k_z c_e} \right\} Z\left(\frac{\omega - k_y V_o}{\sqrt{2}k_z c_e}\right) + \left\{ \frac{\omega - k_y V_o + k_y (V_n - V_T)}{2k_z^2 c_e^2} \right\} k_y \bar{V}_B S_0 Z'\left\{ \frac{\omega - k_y V_o}{\sqrt{2}k_z c_e} \right\} \right] \quad (4.1.18) \end{aligned}$$

where  $\bar{V}_B$  is the average drift speed given by  $\bar{V}_B = \frac{\epsilon \bar{V}_L^2}{2\Omega_e} = \frac{\epsilon c_e^2}{\Omega_e}$ , and we have resubstituted for  $\bar{\omega}$ ,  $\omega^*$ ,  $\eta$  and  $\xi$  as defined in the discussion before eqn (4.1.13). We notice that in the absence of inhomogeneities (i.e.,  $\bar{V}_B = V_n = V_T = 0$ ), eqn (4.1.18) reduces to eqn (3.4.11), as expected.

#### 4.2 THE GENERAL DISPERSION RELATION

The contributions of the two unmagnetized ion species to the dispersion relation are the same as in Chapter 3, and are given by eqns (3.4.5) and (3.4.6). Therefore the dispersion relation for a collisionless two-ion plasma having gradients in external magnetic field, electron density and perpendicular electron temperature is

$$\begin{aligned}
 1 + \frac{k^2}{k_D^2} + \left\{ \frac{(\omega - k_y V_o + k_y V_n) \Gamma_o - k_y V_T (\Gamma_o - 2S_o)}{\sqrt{2} k_z c_e} \right\} Z\left(\frac{\omega - k_y V_o}{\sqrt{2} k_z c_e}\right) \\
 + \left\{ \frac{\omega - k_y V_o + k_y (V_n - V_T)}{2 k_z^2 c_e^2} \right\} k_y \bar{V}_B S_o Z'\left(\frac{\omega - k_y V_o}{\sqrt{2} k_z c_e}\right) \\
 - \frac{\theta}{Z} \left\{ f Z'\left(\frac{\omega}{\sqrt{2} k c_L}\right) + (1 - f) Z'\left(\frac{\omega}{\sqrt{2} k c_H}\right) \right\} = 0 \quad (4.2.1)
 \end{aligned}$$

where, as before, for  $T_L = T_H$  (equal ion temperatures),  $\theta = T_e/T_L = T_e/T_H$ , and  $f = n_{oL}/n_{oH}$  is the fraction of light ions, and  $c_{L(H)} = \sqrt{T_{L(H)}/M_{L(H)}}$  is the light(heavy)ion thermal speed.

In the next section we shall use power series and asymptotic expansions of the Z-function to derive approximate expressions for the real frequency and the growth rate. The results from the full dispersion relation, eqn (4.2.1), would then be compared with the approximate solutions.

#### 4.3 THE APPROXIMATE DISPERSION RELATION

As in section 3.5, for a plasma having warm electrons and cold ions (i.e.,  $T_e \gg T_i$ ) we assume that

$$|z_{oe}| = \left| \frac{\omega - k_y V_o}{\sqrt{2} k_z c_e} \right| \ll 1.$$

Then the power series expansion of the Z-function (eqn 3.5.2), and the relation  $Z'(\lambda) = -2[1 + \lambda Z(\lambda)]$  are used to simplify the electron contribution to the dispersion relation, eqn (4.1.18), to

$$K_e = \frac{k_D^2}{k^2} \left[ 1 + \frac{\left\{ (\omega - k_y V_o) \Gamma_o + k_y (V_n - V_T) \Gamma_o + 2k_y V_T S_o \right\}}{\sqrt{2} k_z c_e} \right] i\sqrt{\pi} - \left\{ \frac{(\omega - k_y V_o) + k_y (V_n - V_T)}{k_z^2 c_e^2} \right\} \times k_y \bar{V}_B S_o \left\{ 1 + \left( \frac{\omega - k_y V_o}{\sqrt{2} k_z c_e} \right) i\sqrt{\pi} \right\} \quad (4.3.1)$$

The term  $k_y^2 (V_n - V_T) \bar{V}_B S_o / k_z^2 c_e^2$  in eqn (4.3.1) can be neglected since it contains products of gradients. Although the factor  $k_y \bar{V}_B / k_z = k_y \epsilon \bar{V}_\perp^2 / 2k_z \Omega_e$  is small, we retain the term  $k_y (\omega - k_y V_o) \bar{V}_B S_o / k_z^2 c_e^2$  in eqn (4.3.1) to examine the correction introduced by the  $\nabla B$  drift. Further, since  $|z_{oe}| \ll 1$ , we set  $(1 + z_{oe} \sqrt{\pi}) \sim 1$  in the last term in eqn (4.3.1).

With the above approximations, eqn (4.3.1) reduces to

$$K_e = \frac{k_D^2}{k^2} \left[ 1 + \left( \frac{\omega - k_y V_o}{\sqrt{2} k_z c_e} \right) i\sqrt{\pi} \Gamma_o - \left( \frac{\omega - k_y V_o}{k_z c_e} \right) \left( \frac{k_y \bar{V}_B}{k_z c_e} \right) S_o + k_y \left( \frac{V_n - V_T}{\sqrt{2} k_z c_e} \right) i\sqrt{\pi} \Gamma_o + \left( \frac{2k_y V_T}{\sqrt{2} k_z c_e} \right) i\sqrt{\pi} S_o \right] \quad (4.3.2)$$

For the ions, which have been assumed to be cold, we once again take

$$|z_{L,H}| = \frac{\omega}{\sqrt{2} k c_{L,H}} \gg 1$$

and use the asymptotic expansion of the Z-function (eqn 3.5.1).

Since we are interested in growth of the instability, we choose

$I_m(z) > 0$  in eqn (3.5.1) to obtain

$$K_L = -k_D^2 f \theta \frac{c_L^2}{\omega^2} \quad (4.3.3)$$

for the light ions, and

$$K_H = -k_D^2 (1 - f) \theta \frac{c_H^2}{\omega^2} \quad (4.3.4)$$

for the heavy ions.

For  $\omega = \omega_R + i\gamma$  and with  $|\gamma| \ll \omega_R$  we can use the approximation

$$\frac{1}{\omega^2} \approx \frac{1}{\omega_R^2} \left( 1 - \frac{2i\gamma}{\omega_R} \right). \quad (4.3.5)$$

Using the results of eqns (4.3.2), (4.3.3), (4.3.4) and (4.3.5) the dispersion relation, eqn (4.2.1), becomes

$$\begin{aligned} 1 + \frac{k^2}{k_D^2} - \frac{k^2 f \theta c_L^2}{\omega_R^2} - \frac{k^2 (1 - f) \theta c_H^2}{\omega_R^2} + \frac{2i\gamma}{\omega_R^3} (k^2 f \theta c_L^2 + k^2 (1 - f) \theta c_H^2) \\ + \left( \frac{\omega_R - k_y V_0}{\sqrt{2} k_z c_e} \right) i\sqrt{\pi} \Gamma_0 + \left( \frac{i\gamma}{\sqrt{2} k_z c_e} \right) i\sqrt{\pi} \Gamma_0 - \left( \frac{\omega_R - k_y V_0}{k_z c_e} \right) \left( \frac{k_y \bar{V}_B}{k_z c_e} \right) S_0 \\ - \left( \frac{i\gamma}{k_z c_e} \right) \left( \frac{k_y \bar{V}_B}{k_z c_e} \right) S_0 + k_y \left( \frac{V_n - V_T}{\sqrt{2} k_z c_e} \right) i\sqrt{\pi} \Gamma_0 + \left( \frac{2k_y V_T}{\sqrt{2} k_z c_e} \right) i\sqrt{\pi} S_0 = 0, \end{aligned}$$

which may be separated into real and imaginary parts as

$$\left[ 1 + \frac{k^2}{k_D^2} - \frac{k^2 \theta \{ f c_L^2 + (1 - f) c_H^2 \}}{\omega_R^2} - \left( \frac{\gamma}{\sqrt{2} k_z c_e} \right) \sqrt{\pi} \Gamma_0 - \left( \frac{\omega_R - k_y V_0}{k_z c_e} \right) \left( \frac{k_y \bar{V}_B}{k_z c_e} \right) S_0 \right]$$

$$\begin{aligned}
 & + i \left[ \frac{2\gamma}{\omega_R^3} k^2 \theta \left\{ f c_L^2 + (1-f) c_H^2 \right\} + \left( \frac{\omega_R - k_y V_0}{\sqrt{2} k_z c_e} \right) \sqrt{\pi} \Gamma_0 - \left( \frac{\gamma}{k_z c_e} \right) \left( \frac{k_y \bar{V}_B}{k_z c_e} \right) S_0 \right. \\
 & \left. + k_y \left( \frac{V_n - V_T}{\sqrt{2} k_z c_e} \right) \sqrt{\pi} \Gamma_0 + \left( \frac{\sqrt{2} k_y V_T}{k_z c_e} \right) \sqrt{\pi} S_0 \right] = 0 \quad (4.3.6)
 \end{aligned}$$

Now, for  $|\gamma| \ll \omega_R$  and  $|(\omega - k_y V_0)/k_z c_e| \ll 1$  (by assumption) we have

$$\left| \frac{\gamma}{k_z c_e} \right| < \left| \frac{(\omega_R - k_y V_0) + i\gamma}{k_z c_e} \right| \ll 1.$$

Also for  $b > 0$  ( $b = k_{\perp}^2 c_e^2 / \Omega_e^2$ ), the function  $|\Gamma_0(b)|$  is always less than 1 (Abramowitz and Stegun, 1965). Hence we can conclude that

$$\left| \frac{\gamma \sqrt{\pi} \Gamma_0}{\sqrt{2} k_z c_e} \right| \ll 1$$

and omit this term from the real part of the left hand of eqn (4.3.6).

For all  $b > 0$ , Bharuthram (1974) has shown that  $|S_0| \lesssim 1$ . Further, for a weakly inhomogenous plasma, we may assume that

$$\bar{V}_B < V_0 \ll c_e.$$

If  $\bar{V}_B/c_e \lesssim k_z/k_y$ , then by the assumption  $|z_{oe}| \ll 1$ , the term

$$\left( \frac{\omega_R - k_y V_0}{k_z c_e} \right) \left( \frac{k_y \bar{V}_B}{k_z c_e} \right) S_0$$

is very small and may be neglected (in comparison with unity) in the real part of the left hand side of eqn (4.3.6). Then setting the real part to zero, we have

$$-1 + \frac{k^2}{k_D^2} - \frac{k^2 \theta}{\omega_R^2} \{ f c_L^2 + (1-f) c_H^2 \} = 0,$$

from which we obtain for the real frequency

$$\omega_R = k \{ f c_{SL}^2 + (1-f) c_{SH}^2 \}^{\frac{1}{2}} \rho \quad (4.3.7)$$



where  $c_{SL(H)} = \sqrt{T_e/M_L(H)}$  is the light (heavy) ion sound speed and  $\rho = (1 + k^2/k_D^2)^{-\frac{1}{2}}$ .

We note that the above expression for the real frequency,  $\omega_R$ , is the same as that found in Chapter Three (eqn 3.5.7) in the absence of inhomogeneities. This may be so since the gradient in the external magnetic field and in the plasma density and temperature are assumed to be weak. Their associated drift speeds influence only the net drift speed, i.e., the amount of free energy available to drive the instability.

The imaginary part of eqn (4.3.6) set to zero yields, for the growth rate,

$$\frac{\gamma}{\omega_R} = \frac{\sqrt{\frac{\pi}{2}} \left(\frac{k}{k_z}\right) \left[ \left(\frac{k_y}{k}\right) \left\{ \left(\frac{V_o}{c_e}\right) - \left(\frac{V_n}{c_e}\right) + \left(\frac{V_T}{c_e}\right) \right\} - \frac{\rho}{c_e} \{ f c_{SL}^2 + (1-f) c_{SH}^2 \}^{1/2} \right] \Gamma_o - 2 \left(\frac{k_y}{k}\right) \left(\frac{V_T}{c_e}\right) S_o}{\left[ 2\rho^{-2} - \left(\frac{k}{k_z}\right) \left(\frac{\rho}{c_e}\right) \{ f c_{SL}^2 + (1-f) c_{SH}^2 \}^{1/2} \left(\frac{k_y}{k_z}\right) \left(\frac{\bar{V}_B}{c_e}\right) S_o \right]}$$

Finally, using  $M = M_H/M_L$  and  $\bar{m} = M_H/m_e$ , we have

$$\frac{\gamma}{\omega_R} = \frac{\sqrt{\frac{\pi}{2}} \left(\frac{k}{k_z}\right) \left[ \left(\frac{k_y}{k}\right) \left\{ \left(\frac{V_o}{c_e}\right) - \left(\frac{V_n}{c_e}\right) + \left(\frac{V_T}{c_e}\right) \right\} - \frac{\rho}{\sqrt{\bar{m}}} \{ 1 + (M-1)f \}^{1/2} \right] \Gamma_o - 2 \left(\frac{k_y}{k}\right) \left(\frac{V_T}{c_e}\right) S_o}{\left[ 2\rho^{-2} - \left(\frac{k}{k_z}\right)^2 \frac{\rho}{\sqrt{\bar{m}}} \{ 1 + (M-1)f \}^{1/2} \left(\frac{k_y}{k}\right) \left(\frac{\bar{V}_B}{c_e}\right) S_o \right]}$$

(4.3.8)

We make the following observations concerning the approximate growth rate given by eqn (4.3.8):

- (i) Equation (4.3.8) does not contain the temperature of the ions in any of its terms, i.e., ion Landau damping is neglected in this analysis. This aspect will be dealt with in the next

section when we consider numerical solutions of the full dispersion relation.

- (ii) In the absence of inhomogeneities ( $\vec{V}_B = V_n = V_T = 0$ ), eqn (4.3.8) gives the growth rate for a homogenous two-ion plasma,

$$\frac{\gamma}{\omega_R} = \sqrt{\frac{\pi}{8}} \left( \frac{k}{k_z} \right) \left[ \frac{k_y}{k} \left( \frac{V_0}{c_e} \right) - \frac{\rho}{\sqrt{m}} \{1 + (M - 1) f\}^{1/2} \right] \Gamma_0 \rho^2 \quad (4.3.9)$$

For a single-ion plasma, this reduces to eqn (4.1.22) of Bharuthram (1974).

- (iii) For typical experimental parameters, Bharuthram and Hellberg (1974) have shown that the instability criterion ( $\gamma > 0$ ) for an inhomogenous single-ion plasma is given by

$$n > \omega_R - \vec{k} \cdot \vec{V}_0 \quad (4.3.10)$$

where 
$$n = 2 \vec{k} \cdot \vec{V}_T \left[ \frac{S_0}{\Gamma_0} - 1 \right] > 0 .$$

#### 4.4 NUMERICAL ANALYSIS OF THE FULL AND APPROXIMATE DISPERSION RELATIONS

In this section we make a graphical study of the normalised growth rate ( $\gamma/\omega_R$ ) as a function of various plasma parameters. Solutions of the full dispersion relation, eqn (4.2.1), are compared with the approximate growth rate given by eqn (4.3.8).

The fixed parameters are the same as those used in Section 3.6. In addition we choose the following standard values:

$$k_D = 17 \text{ cm}^{-1} \Rightarrow \rho^2 = (1 + k^2/k_D^2)^{-1} = 0.9673 \quad ;$$

$$b = k_{\perp}^2 c_e^2 / \Omega_e^2 = 0.5 \Rightarrow \Gamma_0 = 0.64504 \quad ;$$


fraction of light ions,  $f = 0.5$ ;

heavy to light ion mass ratio;  $M = 10$  (which corresponds to a helium-argon plasma).

In all the analyses, the temperature of both ions are assumed to be equal ( $T_L = T_H = T_i$ ).

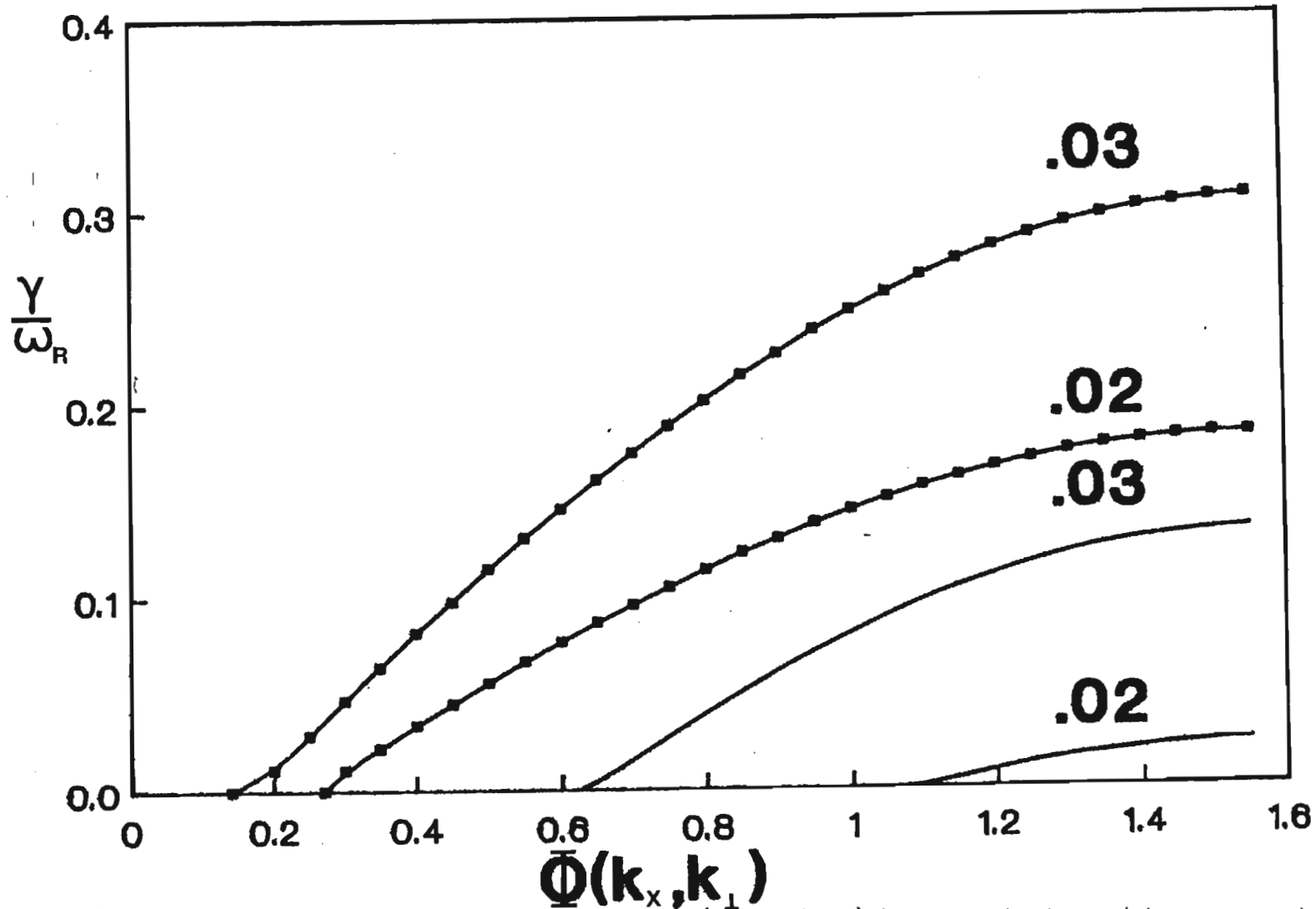
#### 4.4.1 Effect of the Normalised $\vec{E} \times \vec{B}$ Drift ( $V_0/c_e$ )

Figure 4.2 illustrates the relationship between the normalised growth rate ( $\gamma/\omega_R$ ) and the angle  $\phi$  between the  $\vec{k}_x$  and  $\vec{k}_{\perp}$  components of the wave vector  $\vec{k}$ . All inhomogeneities have been excluded (i.e.,  $\bar{V}_B = V_n = V_T = 0$ ). The external magnetic field is kept constant ( $b$  fixed) and an increasing  $V_0$  ( $= cE_0/B_0$ ) can be achieved by increasing the electric field  $E_0$ .

The continuous curves correspond to solutions of the full dispersion relation, eqn (4.2.1), and the curves represented by  to solutions of the approximate expression, eqn (4.3.8).

We observe, from Figure 4.2, that the maximum growth rate increases with increasing normalised electron drift speed ( $V_0/c_e$ ) for a fixed angle  $\phi$ . This may be explained by the fact that an increase in drift speed increases the free energy available to drive the instability. Consequently the growth rate increases.

# Fig 4.2



Normalised growth rate as a function of  $\Phi$ , the angle (in radians) between the  $k_x$  and  $k_\perp$  components of  $\vec{k}$ . The fixed parameters are  $f = 0.1$ ,  $M = 10$ ,  $\theta = 25$ ,  $k_z/k = 0.031$ . The parameter labelling the curves is  $V_0/c_e$ . The two curves marked with points are from the approximate dispersion relation, eqn (4.3.8), while the other two are from the full dispersion relation, eqn (4.2.1).

We also note from the graphs that the maximum growth rate for  $V_0/c_e = 0.03$  and a fixed  $\phi$  is smaller for the full dispersion relation than for the approximate solution by a factor of approximately 0.43. The growth rate is smaller for the full dispersion relation probably because of the light ion Landau damping, as discussed in Section 3.6.1. Since the approximate solution, eqn (4.3.8), does not contain the ion temperature, ion Landau damping is not accounted for. For a value of  $T_e/T_i = 25$ , ion Landau damping could be of significance in solving the full dispersion relation. A closer correlation between the approximate and full dispersion relations is expected for much larger values of  $T_e/T_i$ . This is confirmed in Section 4.4.2.

Another feature of the graphs in Figure 4.2 is that for a given ( $V_0/c_e$ ) the maximum growth rate occurs at  $\phi = 90^\circ$ , at which value the wave propagates almost parallel to the drift velocity  $\vec{V}_0 = V_0 \hat{y}$  ( $k_z$  being negligibly small by choice), and is thus able to draw maximum energy from the drifting electrons.

Analysis of the full dispersion relation indicates that there is a minimum electron drift velocity required for instability. For the temperature ratio  $T_e/T_i = 25$  and  $f = 0.1$ , this value turns out to be  $V_0/c_e = 0.02$  (corresponding to  $V_0 \approx 1.7 c_{SL}$ ). For drift velocities below  $V_0/c_e = 0.02$  inverse electron Landau damping is probably weaker than the light ion Landau damping (the "contaminant" damping of Section 3.6.1). This minimum cut-off drift velocity of 0.02 compares well with the results obtained in Section 3.6.1.

Figure 4.2 indicates that for a given drift speed, there is a cut-off value in the angle  $\phi$  below which there is no growth. Increasing the drift speed increases the range of propagation angles since a greater

amount of free energy is available to drive the instability. We observe that the decrease in cut-off angle with increase in drift speed is much smaller for the approximate dispersion relation than for the full dispersion relation. This may again be due to the absence of ion Landau damping for the former case.

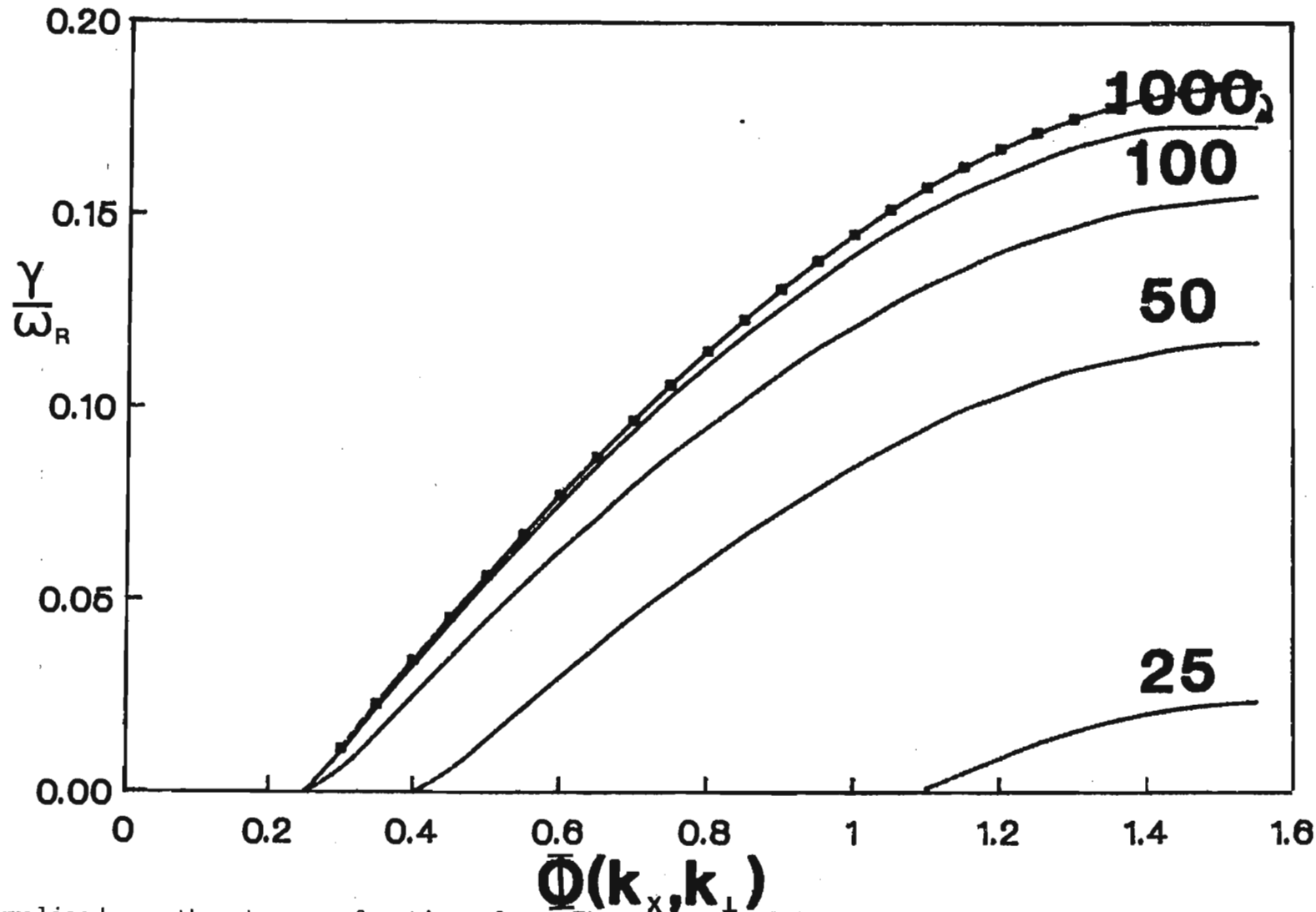
#### 4.4.2 Effect of Increasing $\theta = T_e/T_i$

Figure 4.3 shows the effect of increasing the electron-ion temperature ratio. As before, both ions are assumed to have equal temperatures. The value of  $\theta = T_e/T_i$  was increased by keeping the electron temperature fixed while decreasing the temperature of the ions.

We observe that the growth rate increases with increasing  $\theta$ . When  $\theta$  increases from 25 to 50, the maximum growth rate increases by a factor of about 5. Increasing the temperature ratio beyond 100 results in smaller increases in the maximum growth rate, with little or no change for  $\theta$  around 1000. The increase in growth rate could be attributed to a decrease in ion temperature (as  $\theta$  increases). For small  $T_i$ , there are very few light ions in the tail region of the light ion velocity distribution function to resonate with the wave and produce damping. This could also explain the observed decrease in cut off angle  $\phi$  with an increase in  $\theta$ .

An interesting feature of Figure 4.3 is the very good correlation between the approximate dispersion relation (for which we assume  $\theta \gg 1$ ) and the full dispersion relation for  $\theta = 1000$ . In this case the assumption  $T_e \gg T_i$  for the approximate dispersion relation is much more accurate than for  $\theta = 25$ , for which value the approximate and full dispersion relation results were significantly different (cf Figure 4.2).

# Fig 4.3



Normalised growth rate as a function of  $\bar{\Phi}$ . The parameter labelling the curves is  $\theta = T_e/T_i$ . The other fixed parameters have the same value as in Fig. 4.2. The curve marked with points is from the approximate dispersion relation, eqn (4.3.8), while the others are from the full dispersion relation, eqn (4.2.1).

#### 4.4.3 Effect of Varying the Light Ion Fraction, f

To confirm the "contaminant" damping discussed in Section 3.6.1, a plot of normalised growth rate against light ion fraction  $f$  was made. This is illustrated in Figure 4.4. Here  $k_x = 0$  and only the  $\vec{E} \times \vec{B}$  electron drift was considered, all inhomogeneity-associated drifts being set to zero in eqn (4.2.1).

The minimum in  $\gamma/\omega_R$  at  $f = 0.055$  is in good agreement with the results of Figure 3.2 and consistent with the results obtained by Fried et al. (1971), Nakamura et al. (1975) and Lambert et al. (1976). They find wave damping to be strongest for a  $f$  value close to 0.05.

Figure 4.4 indicates that for the given parameters, maximum growth rate occurs at  $f \approx 0.5$ . Accordingly, we shall use this value of  $f$  when considering inhomogeneities in the following sections.

#### 4.4.4 Effect of Inhomogeneities

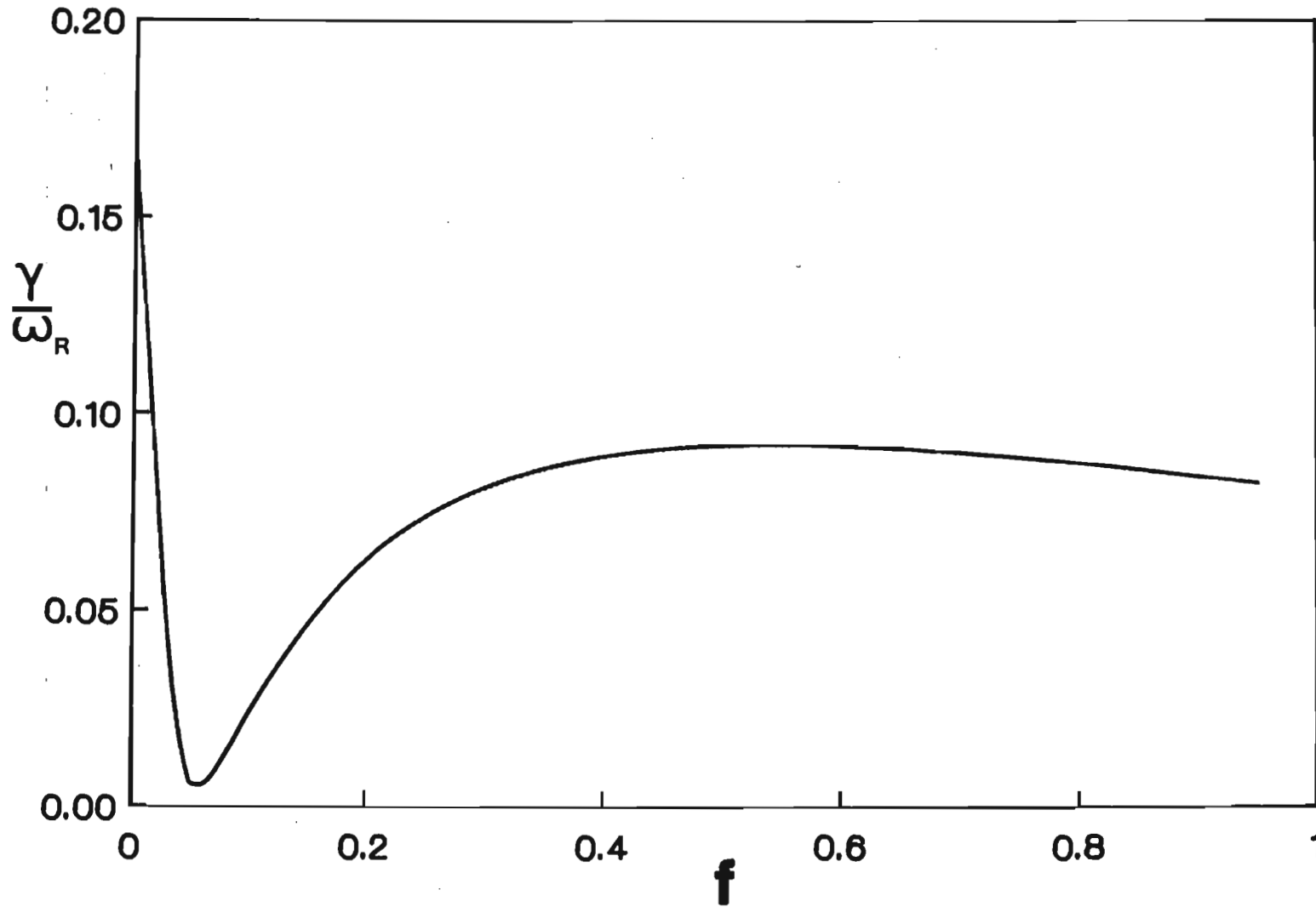
Equation (4.2.1) has been used to draw the graphs of  $(\gamma/\omega_R)$  vs  $\phi$  ( $\vec{k}_x, \vec{k}_\perp$ ) in Figure 4.5. Curve (a) is for the  $\vec{E} \times \vec{B}$  drift alone, while curve (b) is for both the  $\vec{E} \times \vec{B}$  drift and density gradient drift. Curve (c) includes drifts due to all the inhomogeneities. The individual drifts (normalised with respect to the electron thermal speed) have been assigned values independent of each other. Hence the net drift  $V_D$  given by eqn (4.1.7), viz.

$$V_D = (V_0 - V_n - V_T) \hat{y} \quad , \quad (4.1.7)$$

is not kept constant.

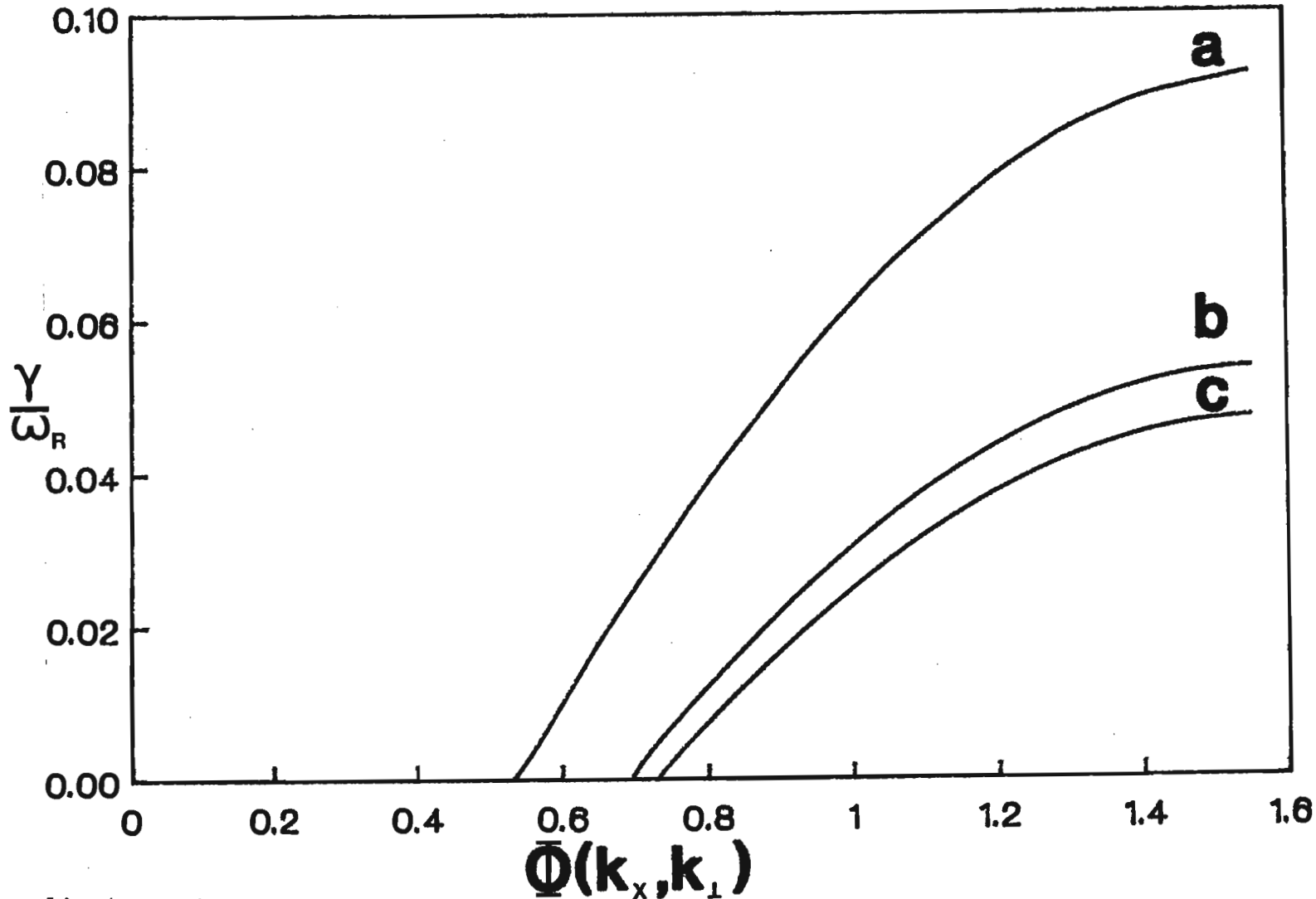


# Fig 4.4



Normalised growth rate as a function of  $f$ , the light ion fraction.  $M = 10$ ,  $\theta = 25$ ,  $k_z/k = 0.031$ ,  $k_x = 0$ ,  $V_0/c_e = 0.02$ . The full dispersion relation, eqn (4.2.1) was used for the plots.

# Fig 4.5



Normalised growth rate as a function of  $\phi$ .  $f = 0.5$  while the other fixed parameters have the same value as in Fig. 4.2. Curve (a) is for the  $\vec{E} \times \vec{B}$  drift alone, with  $V_o/c_e = 0.02$ , while curve (b) includes the density gradient with  $V_n/c_e = 0.004$  and curve (c) includes all the gradients with  $V_n/c_e = 0.004$ ,  $\bar{V}_B/c_e = 0.002$  and  $V_T/c_e = 0.003$ . The full dispersion relation was used.

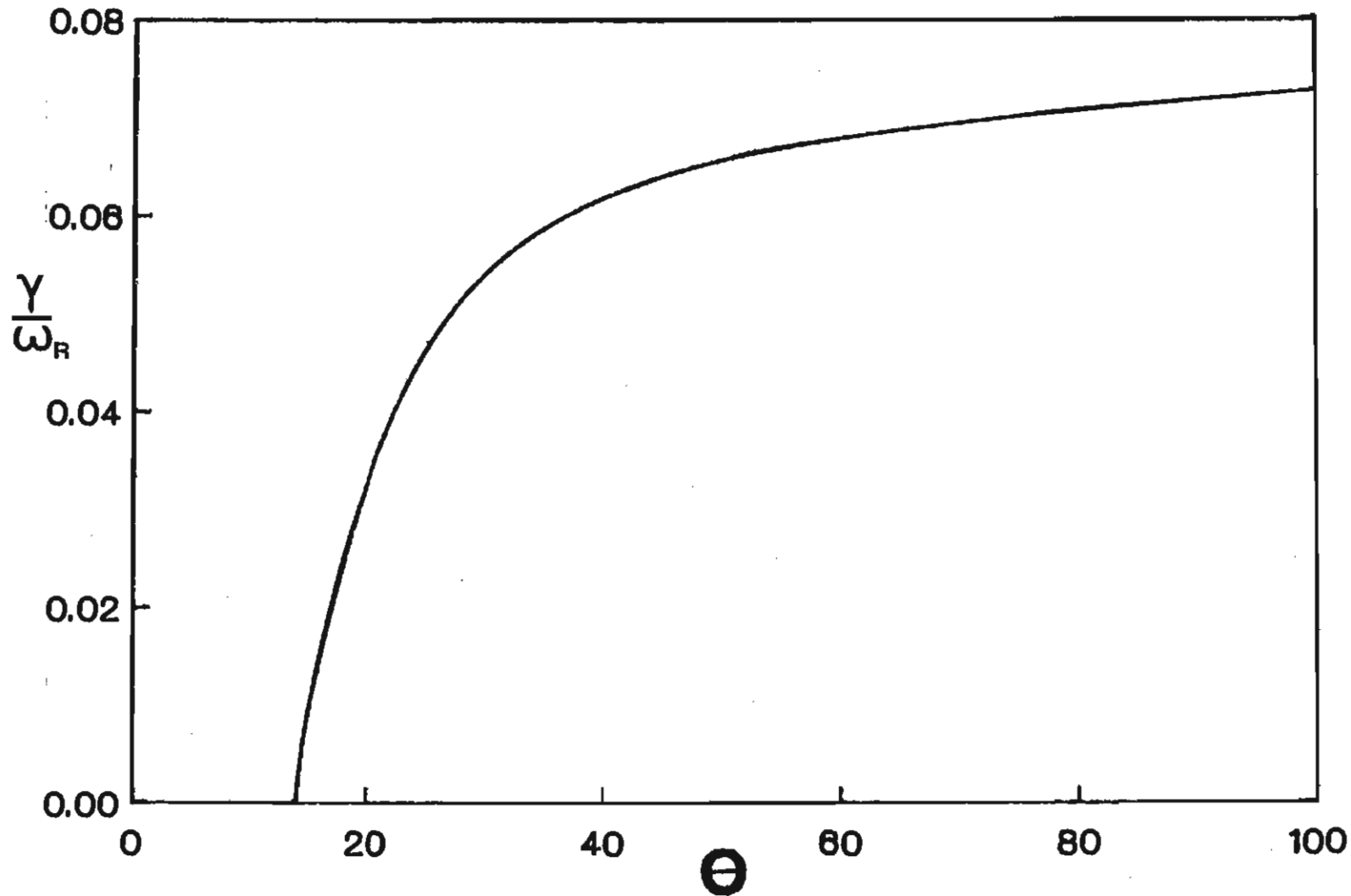
It can be seen from Figure 4.5 that the inclusion of one or more gradient drifts decreases the growth rate. This is consistent with the findings of Bharuthram (1974), and could be explained as follows: the gradient drifts lead to a reduction in the net drift velocity  $V_D$  (eqn (4.1.7)), with a consequent decrease in available free energy to drive the instability. We note, however, that this is not a universal behaviour. For in principle, it is experimentally possible to have an arrangement (e.g., in a Double Plasma device) where the gradient directions are such that the associated drifts enhance the net drift  $V_D$ , resulting in an increased growth rate.

In Figure 4.6, we have plotted the growth rate as a function of  $\theta$ , the electron-ion temperature ratio. Equation (4.2.1) was used for the analysis, with all the drifts being included. We notice that there is a cut-off temperature ratio (of about 14 for the parameters used) below which there is no growth. Light ion Landau damping probably dominates over inverse electron Landau damping for  $\theta < 14$  and the wave is damped. The growth rate increases slowly for temperature ratios of around 100, as was found in the inhomogeneity-free case (Figure 4.3). For such large values of  $T_e/T_i$  the effect of ion Landau damping is small, and the damping continues to decrease as  $\theta$  increases.

#### 4.4.5 Effect of Varying Propagation Angle ( $k_z/k$ )

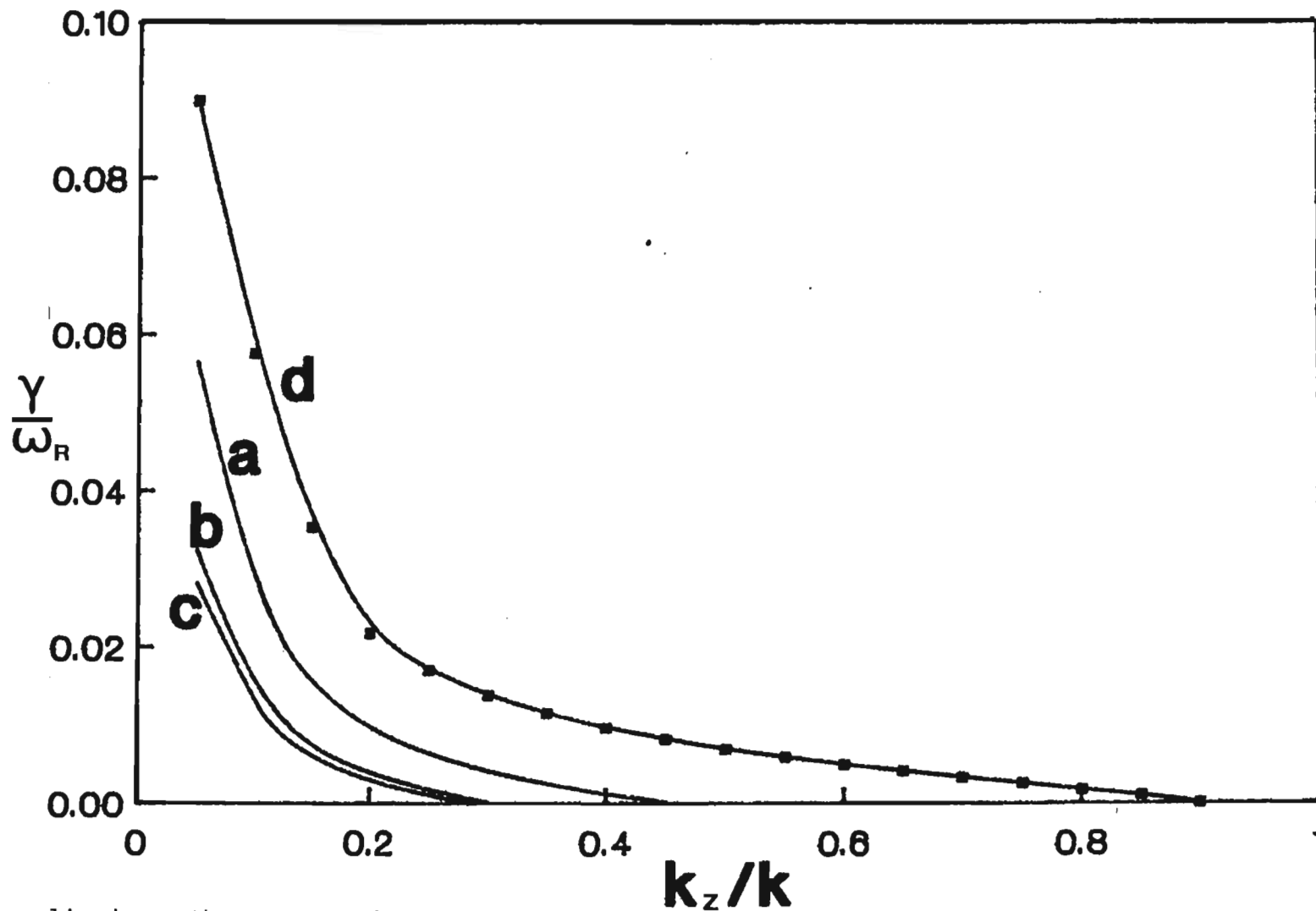
The effect of varying the angle between the wave vector  $\vec{k}$  and the magnetic field  $\vec{B}_0$  was investigated theoretically, and the results are illustrated in Figure 4.7. Here  $k_x$  was set to zero and the values of  $(k_z/k)$  were varied from 0 to 1 by increasing  $k_z$  and fixing  $k$ . Curve

# Fig 4.6



The normalised growth rate as a function of  $\theta$ , the electron-ion temperature ratio.  $f = 0.5$ ,  $M = 10$ ,  $k_z/k = 0.031$ ,  $k_x = 0$ ,  $V_0/c_e = 0.02$ . All drifts due to the inhomogeneities have been included, with  $V_n/c_e = 0.004$ ,  $V_T/c_e = 0.003$  and  $\bar{V}_B/c_e = 0.002$ . The full dispersion relation was used.

# Fig 4.7



Normalised growth rate as a function of  $k_z/k$ .  $\theta = 25$ , with the other fixed parameters having the same values as in Fig. 4.6. Curve (a) is for the  $\vec{E} \times \vec{B}$  drift alone, curve (b) includes the density gradient drift, curve (c) includes all the gradient drifts and curve (d) is for the  $\vec{E} \times \vec{B}$  drift alone, but drawn from the approximate dispersion relation, eqn (4.3.8).

(a) is for  $V_0/c_e$  alone, curve (b) includes the density gradient drift, while curve (c) includes all the drifts due to the inhomogeneities. The continuous curves were drawn from the full dispersion relation, eqn (4.2.1), while the curve represented by  $\text{---}\blacksquare\text{---}\blacksquare\text{---}$  was drawn from the approximate expression, eqn (4.3.8).

It is seen that  $(\gamma/\omega_R) \rightarrow 0$  as  $(k_z/k) \rightarrow 1$ , which corresponds to mode propagation along  $\vec{B}_0$ . As  $(k_z/k) \rightarrow 1$ ,  $(k_y/k) \rightarrow 0$  (with  $k_x = 0$ ) and it is evident from eqn (4.3.8) that  $(\gamma/\omega_R) \rightarrow 0$ . The physical explanation for this is that when the wave travels parallel to the magnetic field, the wave, now being at right angles to the drift velocities, is unable to resonate with the energetic particles and draw energy from them.

We also note that from curves (a) and (d) of Figure 4.7 that the instability exists for a much narrower range of values of  $(k_z/k)$  for results obtained from the full dispersion relation. This can again be attributed to the effect of the light ion Landau damping, which is neglected for the approximate calculations.

For small values of  $(k_z/k)$ , the growth rate increases sharply for all the drift velocities, the full and approximate dispersion expressions yielding similar results. Here  $k_z \rightarrow 0$  (with  $k_x = 0$ ) allows the wave to resonate with the drifting electrons and draw maximum energy from them, resulting in an enhanced growth rate. Similar results were found by Bharuthram and Hellberg (1974) for a single-ion plasma and by Hirose et al. (1970) for a helium-xenon plasma. The lower limit for instability can be determined from the approximation  $|z_{oe}| \ll 1$

i.e.,

$$\left| \frac{\omega_R - k_y V_0}{\sqrt{2} k_z c_e} \right| \ll 1 .$$

For  $V_0 \gg \omega_R/k_y$  (from eqn (4.3.10) with  $V_T = 0$ ) this implies

$k_y V_0 / \sqrt{2} k_z c_e \ll 1$ , from which

$$\frac{k_z}{k} \approx \frac{k_z}{k_y} \gg \frac{V_0}{\sqrt{2} c_e} .$$

Hence the lower limit for instability for  $V_0/c_e = 0.02$  is

$$\frac{k_z}{k} > \frac{1}{\sqrt{2}} \frac{V_0}{c_e} = \frac{0.02}{\sqrt{2}} = 0.014 .$$

Thus our numerical results are not valid for  $k_z/k$  values below this threshold (0.014). This is in close agreement with the lower limit  $k_z/k \sim (m_e/M_f)^{1/2} \approx 0.009$  given by Lashmore-Davies and Martin (1973).

#### 4.4.6 Effect of Magnetic Field

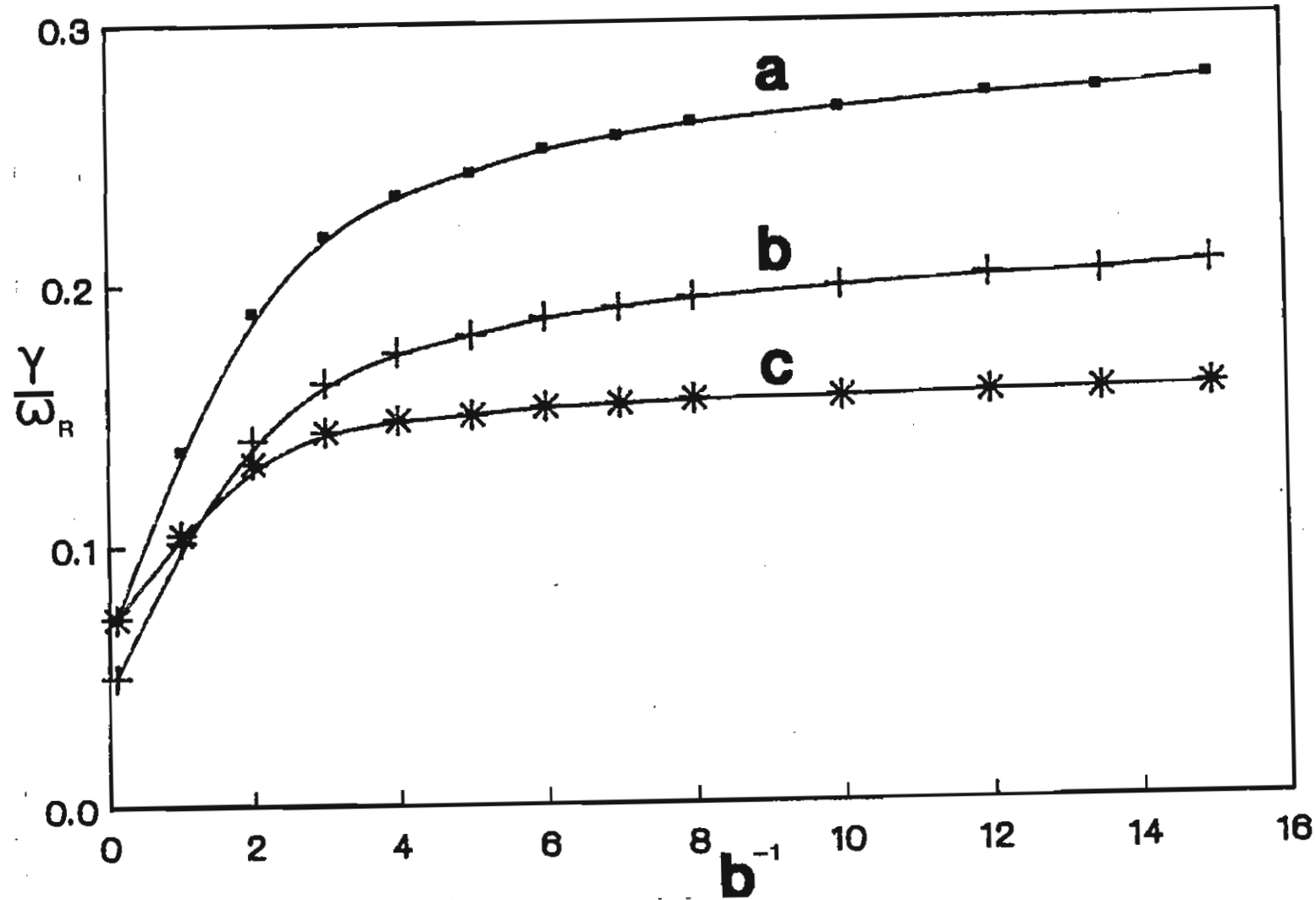
The magnetic field strength was varied by varying the values of  $b$  in the dispersion relation. For our definition of  $b$ , viz.,

$$b = \frac{k_{\perp}^2 c_e^2}{\Omega_e^2} = \frac{k_{\perp}^2 T_{e0} / m_e}{(eB_0 / m_e c)^2} ,$$

we have 
$$b^{-1} = \left( \frac{e^2}{k_{\perp}^2 m_e T_{e0} c^2} \right) B_0^2 .$$

For fixed  $k_{\perp}$  and  $T_{e0}$ ,  $b^{-1}$  was varied, which corresponded to changing the magnetic field strength  $|\vec{B}_0|$ . The normalised growth rate as a function of  $b^{-1}$  is illustrated in Figure 4.8. The approximate expression, eqn (4.3.8), was used with  $k_x = 0$  and  $k_{\perp}$  and  $k_z$  kept fixed. Similar results were obtained by Barrett et al. (1972), Bharuthram and Hellberg (1974) and Hayzen and Barrett (1977).

# Fig 4.8



Normalised growth rate as a function of  $b^{-1}$ ,  $b = k_{\perp}^2 c_e^2 / \omega_e^2$ . The fixed parameters have the same value as in Fig. 4.6 with  $\theta = 25$ . Curve (a) is for the  $\vec{E} \times \vec{B}$  drift alone, curve (b) includes the density gradient drift while curve (c) includes all the drifts due to the inhomogeneities. The approximate dispersion relation, eqn (4.3.8) was used for the plots.



We observe from curves (a) and (b) of Figure (4.8) that the inclusion of a density gradient reduces the growth rate for all values of  $b^{-1}$ . This is attributed to the decrease in net electron drift speed. The addition of a temperature gradient, however, leads to a different behaviour. For values of  $b^{-1} \ll 1$ , the introduction of a temperature gradient results in an increase in growth rate, i.e., it has a destabilising effect. For  $b^{-1} \gtrsim 1$ , the addition of the temperature gradient results in a smaller growth, i.e., it has a stabilising effect. The two-fold effect of the temperature gradient has been discussed by Priest and Sanderson (1972) and Bharuthram (1979), and may be explained as follows:

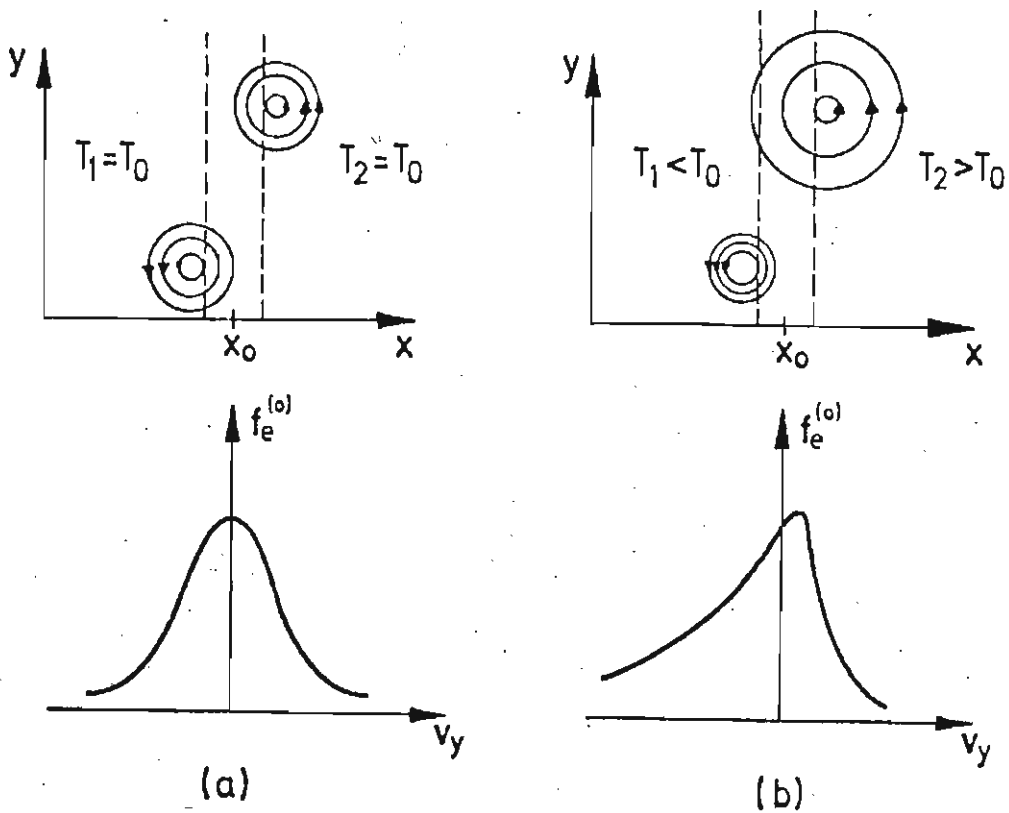


FIG. 4.9. (from Priest and Sanderson, 1972).

In the electron rest frame, the electrons describe circular orbits such that all electrons passing through  $x = x_0$  with guiding centres at  $x > x_0$  ( $x < x_0$ ) have negative  $V_y$  (positive  $V_y$ ) at  $x_0$ . Thus when the electron temperature is the same on both sides of  $x_0$ , Figure 4.9(a), the electron distribution function is symmetric about  $V_y = 0$ . On the other hand, if  $T_e$  is greater for  $V_y < 0$  than for  $V_y > 0$ , then there is a non-symmetric spread in  $V_y$  (Figure 4.9(b)). This temperature gradient distortion of the distribution function increases its slope at the wave phase velocity and this leads to an enhanced growth rate. In the regime  $b^{-1} \gtrsim 1$ , the growth rate decreases with increasing  $|\vec{B}_0|$ . Since the temperature gradient is kept constant, the increase in magnetic field causes a corresponding decrease in electron Larmor radii for both the orbits  $V_y < 0$  and  $V_y > 0$ . These orbits will then have radii smaller than those shown in Figure 4.9(b), although the radius of the orbit for  $V_y < 0$  will still be larger than that for  $V_y > 0$ . Thus the distortion of the electron distribution function will not be as great as in the regime  $b^{-1} \ll 1$ . The corresponding small positive contribution to growth rate would be outweighed by the decrease in net drift velocity produced by the temperature gradient, resulting in a net decrease in the growth rate.

In the next Chapter we transform into the reference frame in which the two ion species have external drifts. The electrons are basically stationary, except for drifts due to inhomogeneities. Using this model the ion acoustic instability is re-examined.

CHAPTER FIVE

THE CROSSFIELD ION ACOUSTIC INSTABILITY IN A TWO-ION PLASMA WITH DRIFTING IONS

5.1 THE PLASMA DISPERSION RELATION FOR DRIFTING IONS

In the previous two chapters we have discussed the ion acoustic instability in a model consisting of drifting electrons and stationary ions. We now turn our attention to a plasma in which the two ion species have external drift velocities  $\vec{v}_L$  and  $\vec{v}_H$  and the electrons are considered to be stationary. The electrons, however, are not entirely stationary - they may experience drifts due to gradients in external magnetic field, electron temperature and electron density, as shown in Figure 5.1 below.

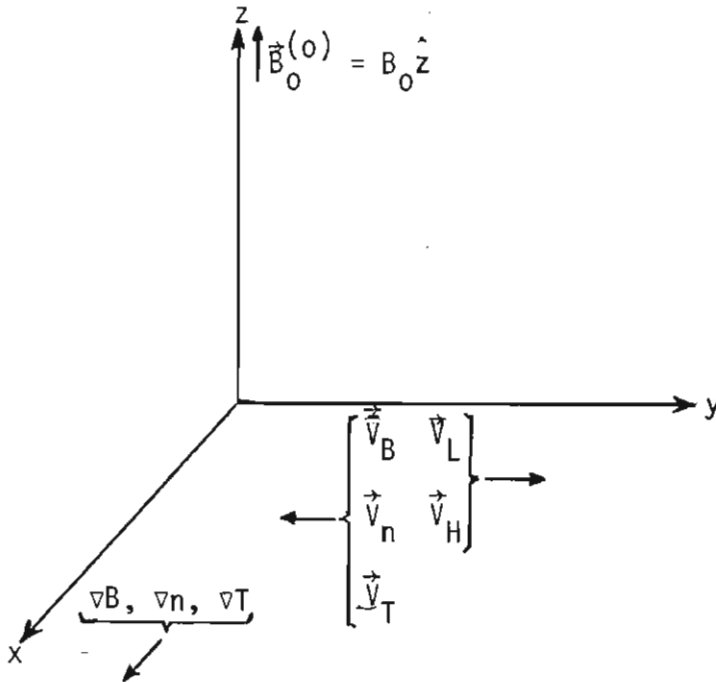


FIG. 5.1

For the case of drifting ions, the dispersion relation, eqn (4.2.1), (with inhomogeneities in external magnetic field, perpendicular electron temperature and electron density) modifies to

$$\begin{aligned}
 1 + \frac{k^2}{k_D^2} + \left\{ \frac{(\omega + k_y V_n) \Gamma_0 - k_y V_T (\Gamma_0 - 2S_0)}{\sqrt{2} k_z c_e} \right\} Z\left(\frac{\omega}{\sqrt{2} k_z c_e}\right) \\
 + \left\{ \frac{\omega + k_y (V_n - V_T)}{2k_z^2 c_e^2} \right\} k_y \bar{v}_B S_0 Z'\left(\frac{\omega}{\sqrt{2} k_z c_e}\right) \\
 - \frac{\theta}{Z} \left[ f Z'\left(\frac{\omega - k_y V_L}{\sqrt{2} k c_L}\right) + (1 - f) Z'\left(\frac{\omega - k_y V_H}{\sqrt{2} k c_H}\right) \right] = 0
 \end{aligned} \tag{5.1.1}$$

where  $V_L$  ( $V_H$ ) is an externally-induced (e.g. electrostatically) drift of the light (heavy) ions, and the other symbols have their usual meaning.

In the limit  $T_e \gg T_i$  ( $\sim 0$ ), asymptotic and power series expansions of the  $Z$ -functions (eqns (3.5.1) and (3.5.2)) can be employed in the usual manner to reduce the real part of eqn (5.1.1) to

$$1 + k^2 \lambda_D^2 = \frac{f k^2 c_{SL}^2}{(\omega_R - k_y V_L)^2} + \frac{(1 - f) k^2 c_{SH}^2}{(\omega_R - k_y V_H)^2}, \tag{5.1.2}$$

where  $\omega = \omega_R + i\gamma$  with  $|\gamma| \ll \omega_R$ , and where all inhomogeneities have been neglected. For  $V_L = V_H = V_0$ , eqn (5.1.2) yields

$$\omega_R = k_y V_0 \pm k \frac{\{f c_{SL}^2 + (1 - f) c_{SH}^2\}^{1/2}}{(1 + k^2 \lambda_D^2)^{1/2}} \tag{5.1.3}$$

The plus (minus) sign in eqn (5.1.3) corresponds to the fast (slow) beam mode. Equation (5.1.3) has the usual form for the ion acoustic frequency in the electron rest frame (Sato et al., 1975).

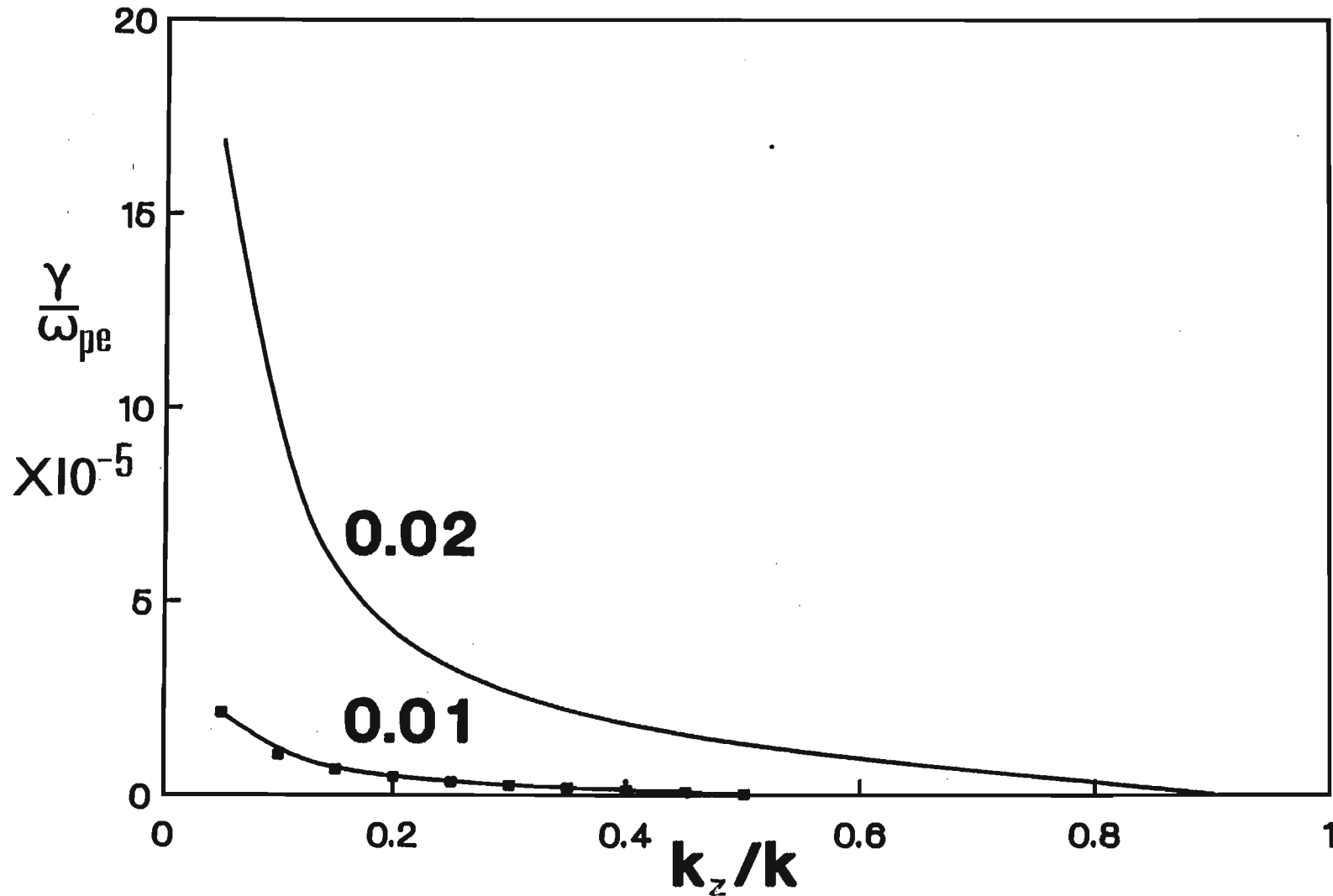
## 5.2 NUMERICAL ANALYSIS

In the numerical analysis that follows, eqn (5.1.1) has been used to solve for the normalised growth rate,  $\gamma/\omega_{pe}$ , where  $\omega_{pe}$  is the electron plasma frequency. As usual, all the particle velocities have been normalised with respect to the electron thermal speed. The standard parameters, e.g.,  $M = 10$ , are the same as those used in Chapter Four. The two ion species are assumed to have equal temperatures, with  $\theta_L = \theta_H = \theta$ . Since  $\theta > 2M$ , it is expected that only a single mode will propagate through the plasma (Nakamura et al., 1976a).

Figure 5.2 illustrates the effect of varying the angle between the wave vector  $\vec{k}$  and the magnetic field  $\vec{B}_0$  on the growth rate. Both ion species have been given the same drift speed, viz.,  $V_L = V_H = V_0$ . Calculations with the use of eqn (5.1.3) reveal that it is the slow beam mode that is unstable in both cases, a finding which is consistent with the experimental observations of Hayzen and Barrett(1977) for a single-ion plasma.

We note that the growth rate decreases as the angle is decreased ( $k_z/k \rightarrow 1$ ), a result similar to that found in Section 4.4 for drifting electrons and stationary ions. The explanation for this decrease in growth rate as the wave travels less obliquely to the magnetic field direction has been discussed in Section 4.4, and is as follows: when the wave travels parallel to the magnetic field, the wave now being at right angles to the drift velocities is unable to resonate with the energetic particles and draw energy from them.

# Fig 5.2



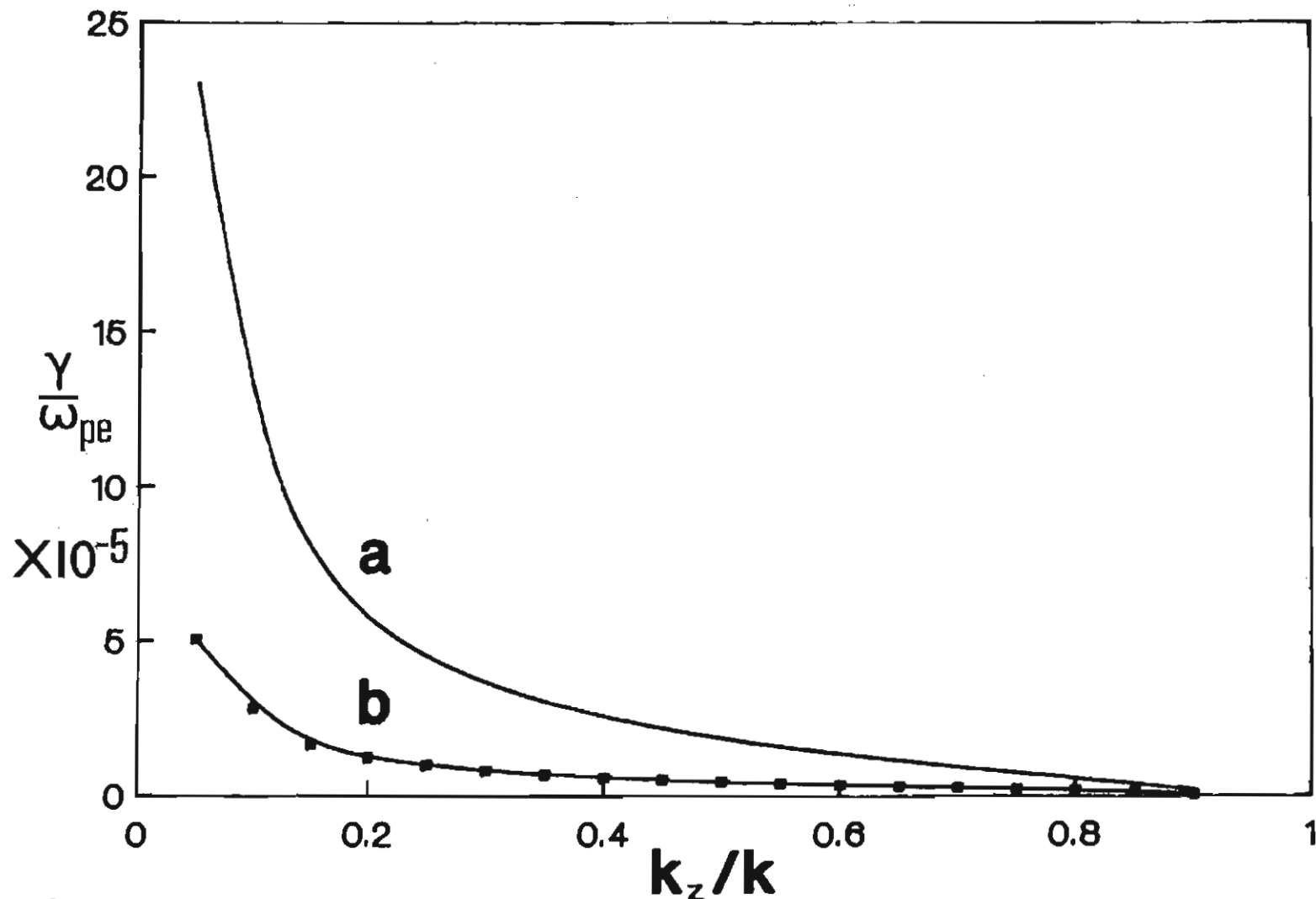
Normalised growth rate for drifting ions as a function of  $k_z/k$ .  $f = 0.5$ ,  $M = 10$ ,  $\theta = 500$ ,  $k_x = 0$ . Parameter labelling the curves is  $V_o/c_e = V_L/c_e = V_H/c_e$ .

As for the increase in  $\gamma/\omega_{pe}$  with  $V_0/c_e$ , an increase in the ion drift speeds results in a greater amount of free energy available to drive the instability - this is seen to enhance both the growth rate and the range of propagation angles (cf  $k_z/k$  cut off).

Figure 5.3 illustrates the effect of unequal ion drift speeds on the growth rate. A comparison has been made between equal drift speeds (curve a) and unequal drift speeds (curve b). In the latter case, both ion species have been given the same kinetic energy and hence the ratio of their speeds is equal to the square root of the ratio of their masses, i.e.  $V_L/V_H = \sqrt{M_H/M_L}$  (e.g. for an applied potential difference  $\phi$ ,  $e\phi = \frac{1}{2} M_L V_L^2 = \frac{1}{2} M_H V_H^2$ ). It can be seen that a decrease in heavy ion drift speed results in a decrease in the growth rate but no appreciable change in the cut-off angle. A study of the distribution functions of the different species offers a possible explanation for this. For both cases ( $V_L = V_H$  and  $V_L \neq V_H$ ) it is the slow beam mode that grows. Such a wave, with  $\omega - \vec{k} \cdot \vec{V}_0 < 0$ , is a negative energy mode (Lashmore-Davies, 1971) and grows when energy is extracted from it, e.g., such a wave will grow when it 'sees' a negative slope on a particle velocity distribution function. It is seen from Figure 5.4b that when  $V_H < V_L$ , the wave phase speed decreases significantly in comparison to the equal drift case (Figure 5.4a). The wave then 'sees' a smaller negative slope on the electron velocity distribution function, with a consequent decrease in growth rate. Ion Landau damping is negligibly small in both cases.

For  $V_H < V_L$ , the normalised phase speed of the unstable mode is found to be  $V_\phi/c_e = 0.0033$  (at  $k_z/k = 0.05$ ), which lies between the modified heavy and light ion sound speeds in the ion rest frame, viz.,

# Fig 5.3



Normalised growth rate for drifting ions as a function of  $k_z/k$ .  $f = 0.5$ ,  $M = 10$ ,  $\theta = 100$ ,  $k_x = 0$ . Drifts due to inhomogeneities in magnetic field and electron temperature and density have been included with  $V_n/c_e = 0.004$ ,  $V_T/c_e = 0.003$  and  $\bar{v}_B/c_e = 0.002$ . Curve (a) is for equal ion drifts  $V_L/c_e = V_H/c_e = 0.02$ , while curve (b) is for unequal ion drifts,  $V_L/c_e = \sqrt{10} V_H/c_e = 0.02$ .



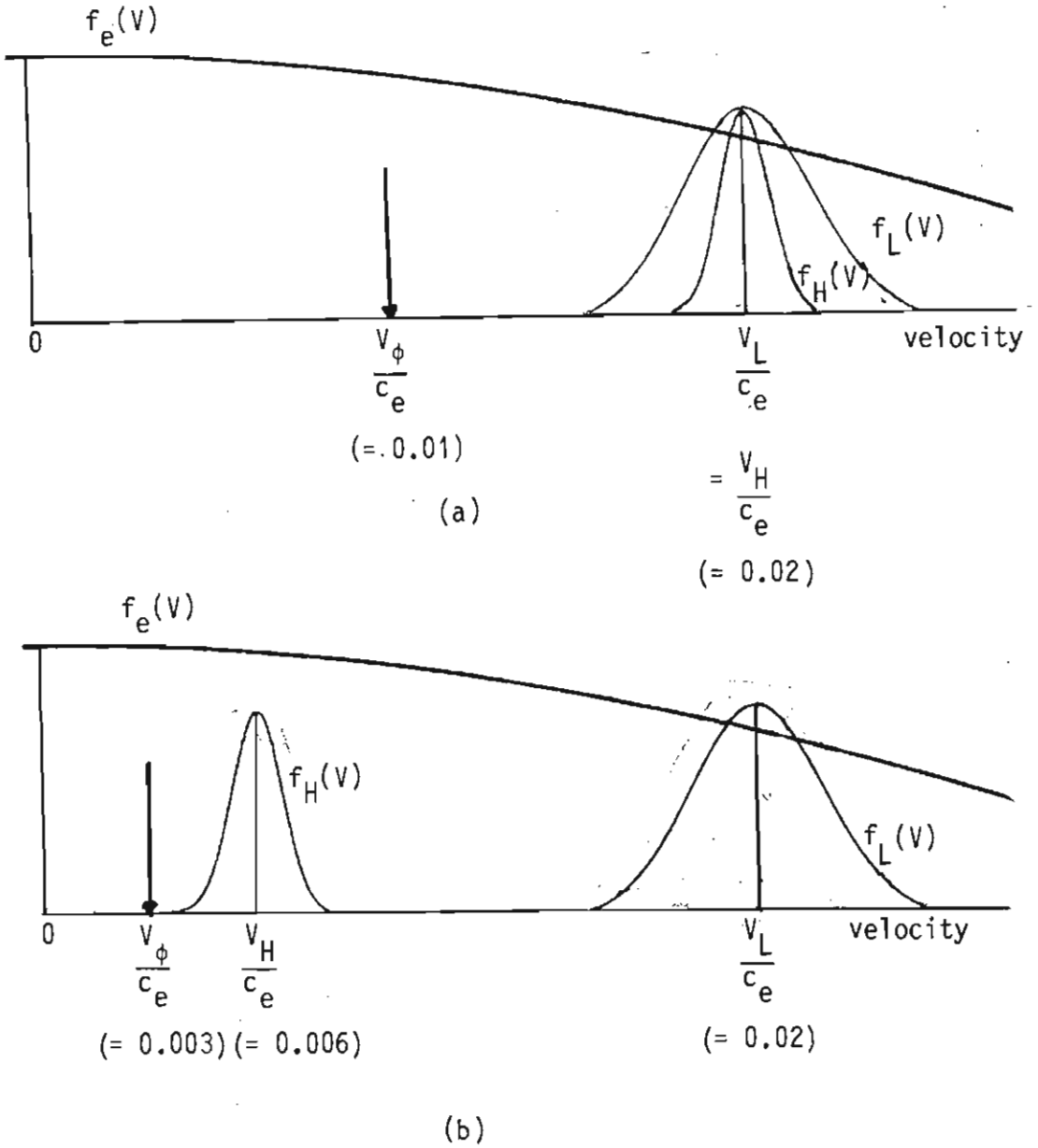


FIG. 5.4 Relative positions of wave phase velocity and particle drifts when  
 (a) both ion species have equal velocities  
 (b) both ion species have equal kinetic energies ( $M = 10$ ).

$$\frac{c_{SL}'}{c_e} = \frac{f^{\frac{1}{2}} c_{SL}}{c_e} = \left( \frac{f m_e M}{M_H} \right)^{1/2} \approx 0.0082 ,$$

and

$$\frac{c_{SH}'}{c_e} = \frac{(1-f)^{\frac{1}{2}} c_{SH}}{c_e} = \sqrt{\frac{(1-f) m_e}{M_H}} \approx 0.0026 ,$$

for  $f = 0.5$  and  $k^2 \lambda_D^2 \ll 1$ . Some insight into this behaviour can be obtained by noting that since  $V_L/V_H = \sqrt{M_H/M_L}$ , we have for  $f = 0.5$ :

$$\frac{f c_{SL}^2}{(1 + k^2 \lambda_D^2) V_L^2} = \frac{(1-f) c_{SH}^2}{(1 + k^2 \lambda_D^2) V_H^2} .$$

Then, if we define a harmonic average velocity (Krall and Trivelpiece, 1973)

$$\frac{1}{V_0} = \frac{1}{2} \left( \frac{1}{V_L} + \frac{1}{V_H} \right) ,$$

an average ion sound frequency

$$\frac{\omega_S^2}{V_0^2} = \frac{k^2 f c_{SL}^2}{(1 + k^2 \lambda_D^2) V_L^2} = \frac{k^2 (1-f) c_{SH}^2}{(1 + k^2 \lambda_D^2) V_H^2} ,$$

and a dimensionless frequency

$$x = \frac{\omega}{\omega_S} \frac{V_L - V_H}{V_L + V_H} ,$$

and express the wave number  $k_y$  in terms of a dimensionless variable  $\bar{y}$  as

$$k_y = \frac{\omega}{V_0} + \bar{y} \frac{\omega_S}{V_0} ,$$

then eqn (5.1.2) transforms to

$$\frac{1}{(x - \bar{y})^2} + \frac{1}{(x + \bar{y})^2} = 1 .$$

It has been shown (Krall and Trivelpiece, 1973) that for a two-stream instability with  $\omega$  real and  $k$  imaginary, this fourth order equation has two real and two imaginary roots for  $k$ , with one growing and the other damped. The frequency at which the growth rate is a maximum is given by

$$\omega_{\max} = \frac{\sqrt{3}}{2} \left( \frac{V_L + V_H}{V_L - V_H} \right) \omega_S .$$

For  $M_H/M_L = 10$ ,

$$\frac{1}{V_0} = \frac{1}{2V_H} \left( 1 + \frac{V_H}{V_L} \right) = \frac{0.66}{V_H} .$$

Then

$$\frac{\omega_S^2}{k^2} \sim 2.3 \frac{(1-f) c_{SH}^2}{(1+k^2 \lambda_D^2)} ,$$

with

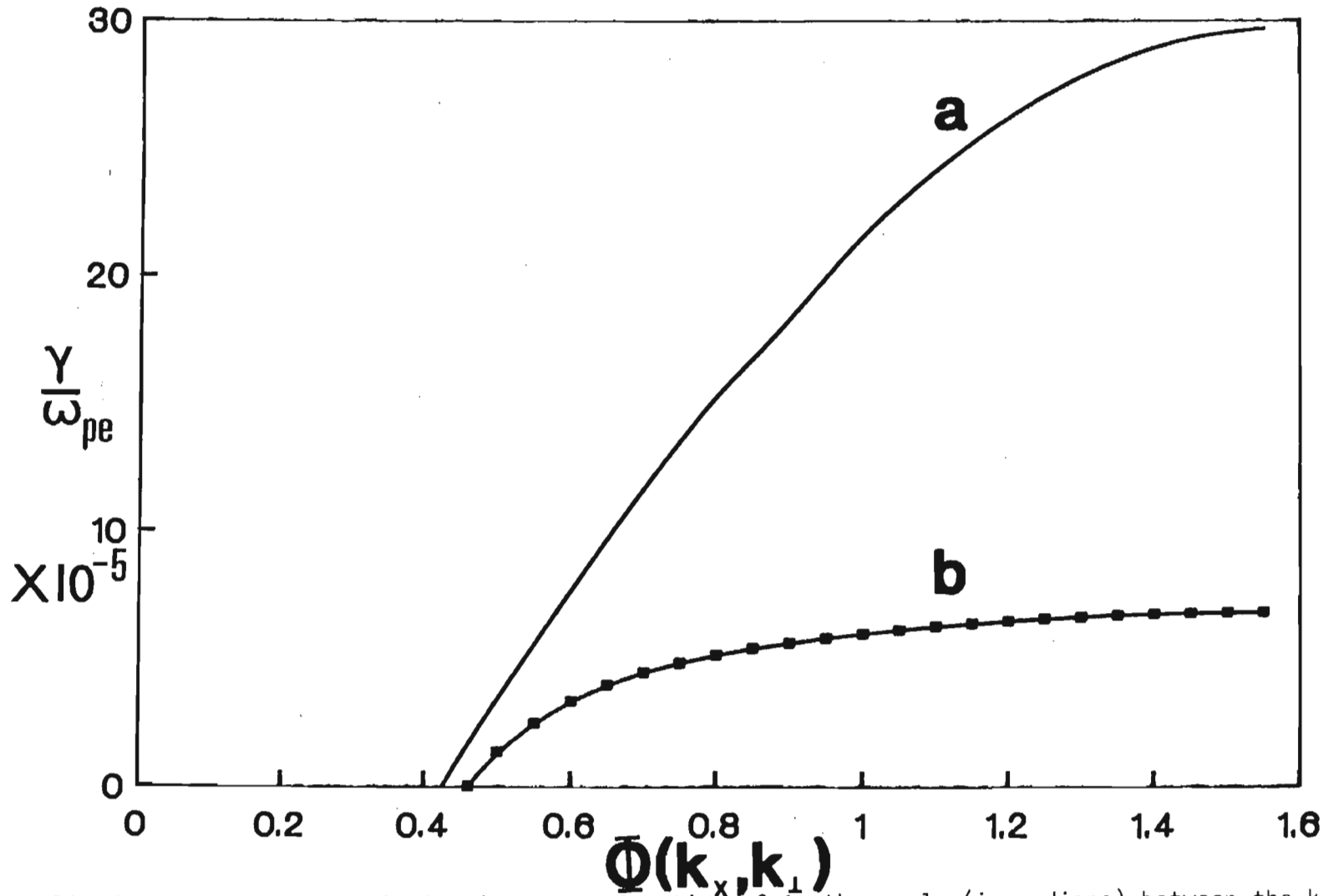
$$\frac{\omega_{\max}}{k} \sim 1.7 \frac{\omega_S}{k} \sim 2.5 c_{SH}' = 0.8 c_{SL}' .$$

It is seen that the wave phase speed corresponding to maximum growth lies between  $c_{SH}'$  and  $c_{SL}'$ , and is much closer to  $c_{SL}'$ . We note that the computed phase speed is, on the other hand, much closer to  $c_{SH}'$ . However, this may not be the value for  $\omega_R$  corresponding to maximum growth.

Figure 5.5 shows a result similar to that of Figure 5.3. Here  $\phi$  is the angle between the  $\vec{k}_x$  and  $\vec{k}_\perp$  components of the wave vector  $\vec{k}$  ( $k_x$  had been set to zero in Figure 5.3). Both curves in Figure 5.5 have a cut-off angle close to 0.4 radians (this is similar to the results of Section 4.4).

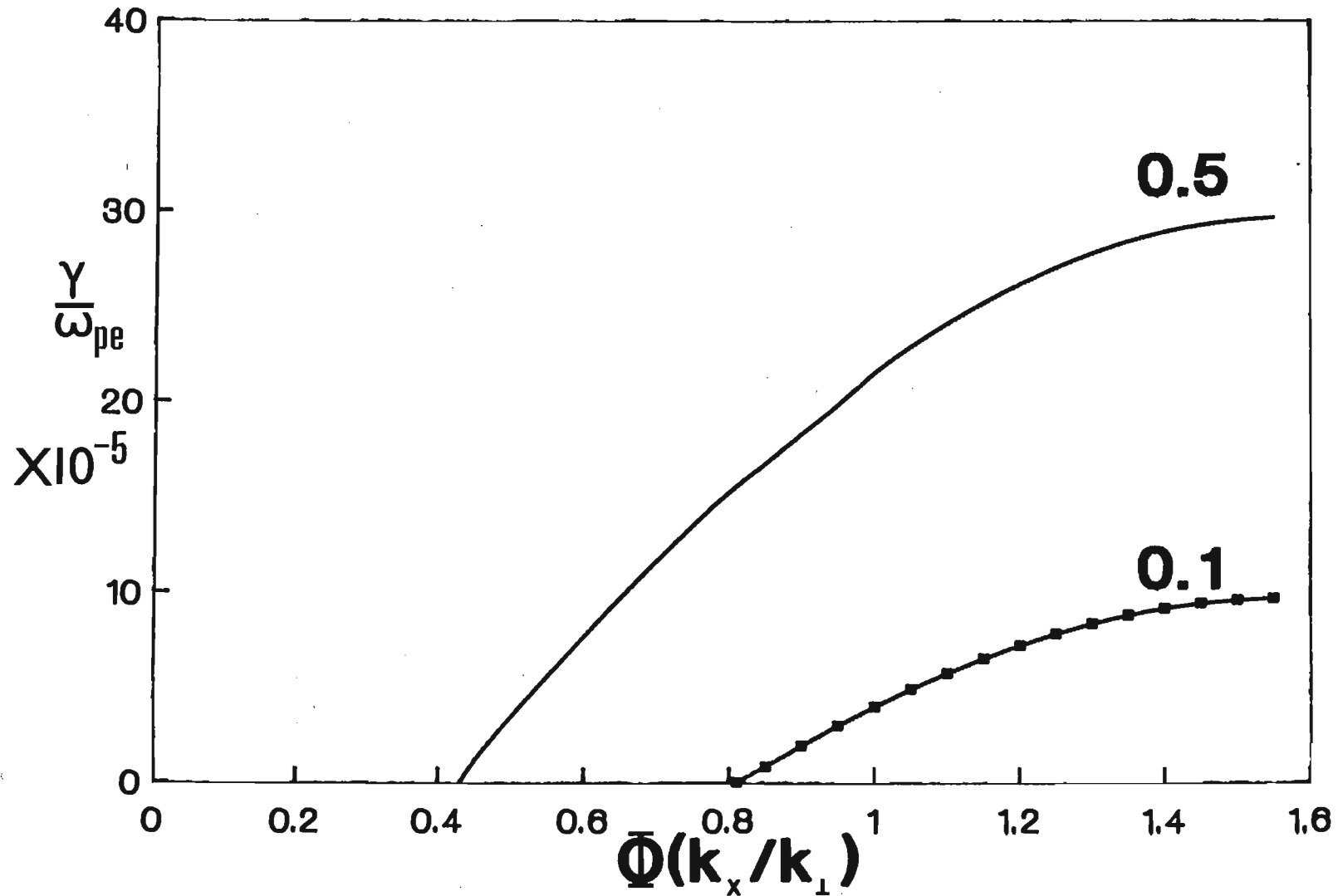
The effect of light ion concentration on the growth rate is shown in Figure 5.6. The growth rate is much smaller for all angles  $\phi$  for

# Fig 5.5



Normalised growth rate for drifting ions as a function of  $\Phi$ , the angle (in radians) between the  $k_x$  and  $k_{\perp}$  components of  $\vec{k}$ .  $\theta = 25$ , with the other fixed parameters having the same value as in Fig. 5.3. Curve (a) is for equal ion drifts,  $V_L/c_e = V_H/c_e = 0.02$ , while curve (b) is for unequal ion drifts  $V_L/c_e = \sqrt{10} V_H/c_e = 0.02$ .

# Fig 5.6



Normalised growth rate for drifting ions as a function of  $\bar{\Phi}$ . The fixed parameters have the same value as in Fig. 5.5. The parameter labelling the curves is  $f$ , the light ion fraction.

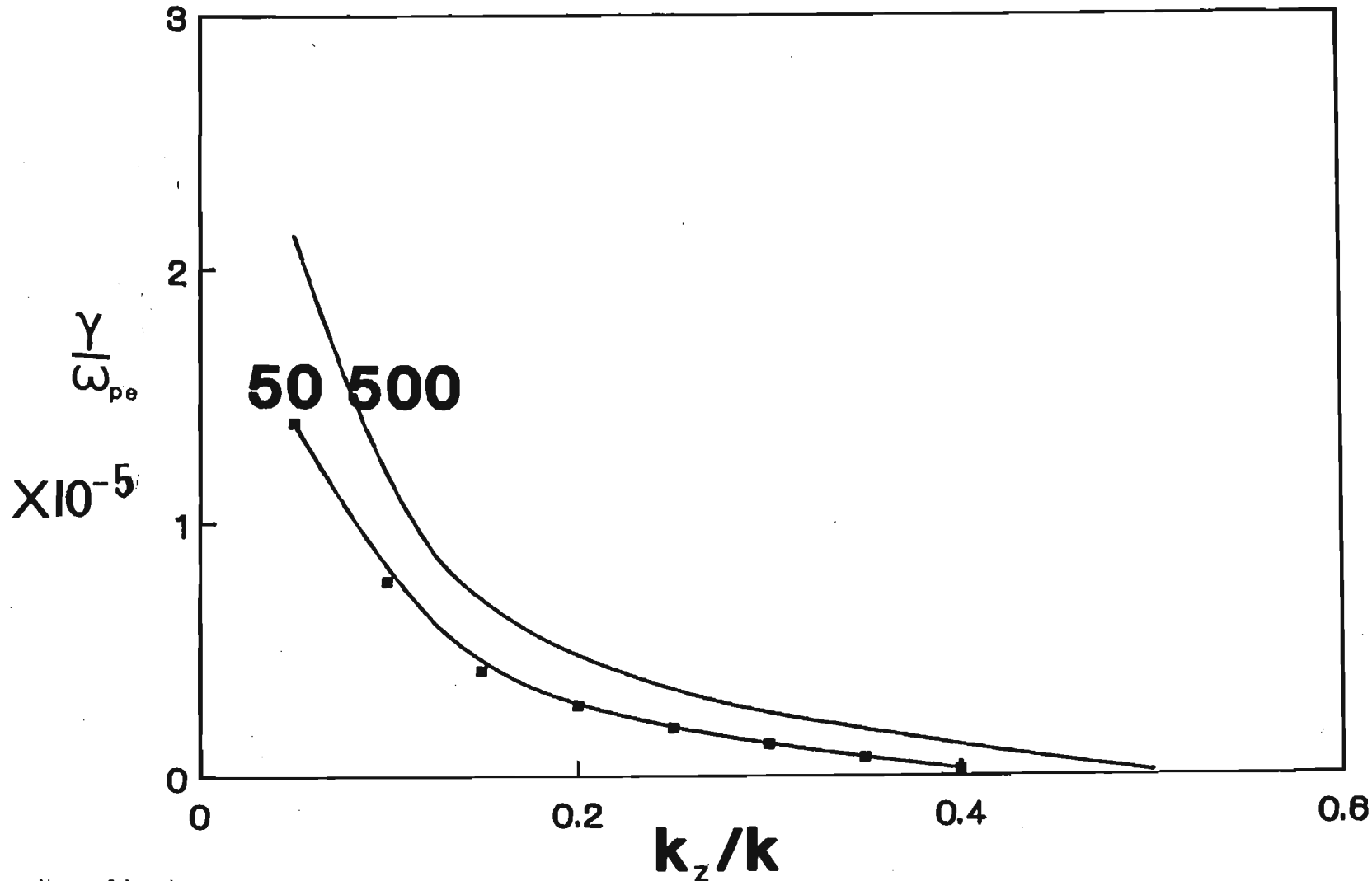
$f = 0.1$  than for  $f = 0.5$ . This is in agreement with the "contaminant" damping discussed in detail in Section 3.6.1.

When the electron-ion temperature ratio is increased (electron temperature kept fixed) there is an increase in both the growth rate and the cut-off angle (Figure 5.7), and this may be associated with a decrease in ion Landau damping. However, for the parameters chosen, there is no substantial increase in growth rate from  $\theta = T_e/T_i = 500$  to  $\theta = 1000$ . This may be due to the ions becoming virtually cold for  $\theta$  values equal to and above 500. Ion Landau damping is then absent.

The effect of inhomogeneities in perpendicular electron temperature, electron density and external magnetic field on the growth rate is illustrated in Figure 5.8. It is interesting to observe that the growth rate is increased by the presence of inhomogeneities, whereas in the external electron drift-stationary ions case (Section 4.4.4) the growth rate decreases. The reason for this is discussed below: Since the electron drift speeds due to the inhomogeneities are along the negative  $y$ -axis (Figure 5.1) while the ions drift in the positive  $y$ -direction, the resultant relative drift velocity between the ions and electrons is increased. This increased velocity provides additional free energy to enhance the instability.

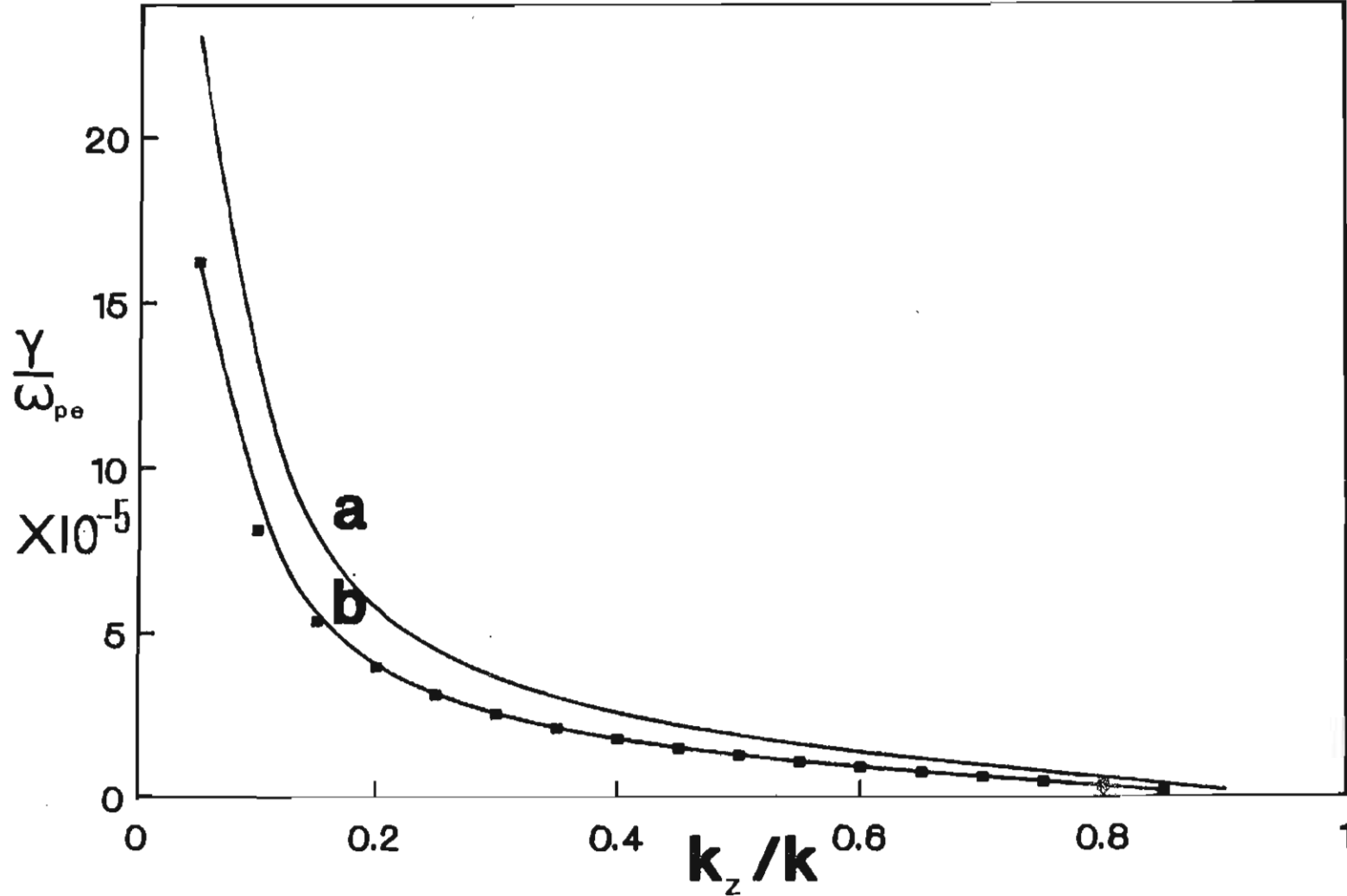
Figure 5.9 shows how the normalised wave speed  $\frac{V_\phi}{\sqrt{2}c_H} \left( = \frac{\omega_R}{\sqrt{2}kc_H} \right)$  varies with  $k_z/k$  for equal ion speeds  $V_0$  in the absence of inhomogeneities. The wave speed decreases to zero and then assumes negative values. The continuity of the values confirms the propagation of a single mode. The graph of the Doppler-shifted wave speed  $\hat{V}_\phi = (\omega_R - k_y V_0)/kc_e$  corresponds to the slow-beam mode in eqn (5.1.3).

# Fig 5.7



Normalised growth rate for drifting ions as a function of  $k_z/k$ .  $f = 0.5$ ,  $M = 10$ ,  $k_x = 0$ ,  $V_L/c_e = V_H/c_e = 0.01$ . Parameter labelling the curves is  $\theta = T_e/T_i$ . The curve for  $\theta = 1000$  was found to be identical to that for  $\theta = 500$ . Note that inhomogeneities have been excluded.

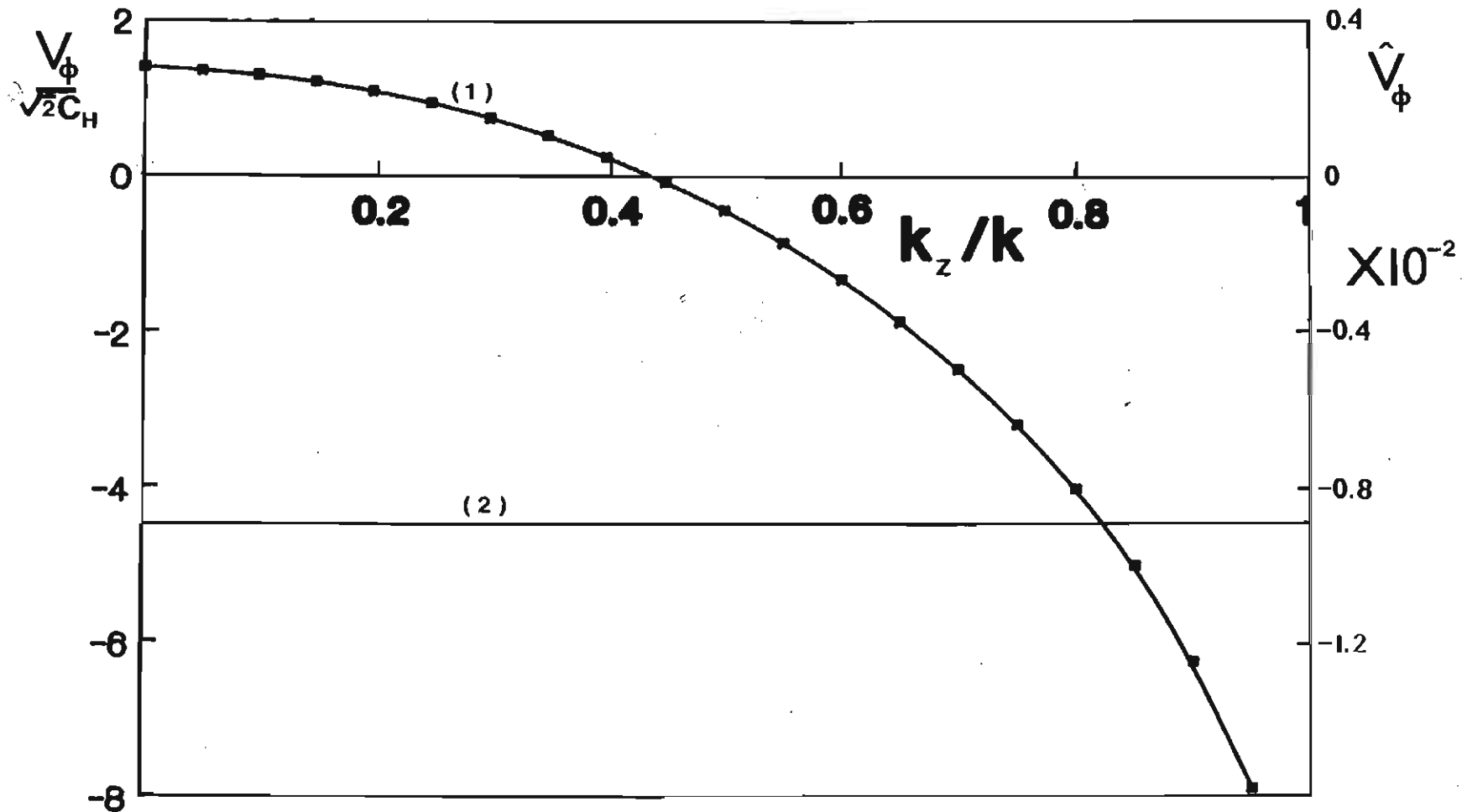
# Fig 5.8



Normalised growth rate for drifting ions as a function of  $k_z/k$ .  $f = 0.5$ ,  $M = 10$ ,  $k_x = 0$ ,  $\theta = 100$ ,  $V_L/c_e = V_H/c_e = 0.02$ . Curve (a) includes all the electron drifts, i.e.  $V_n/c_e = 0.004$ ,  $V_T/c_e = 0.003$ ,  $\bar{V}_B/c_e = 0.002$ , while curve (b) is for zero electron drifts.



# Fig 5.9



Graph (1): Normalised wave speed as a function of  $k_z/k$ .

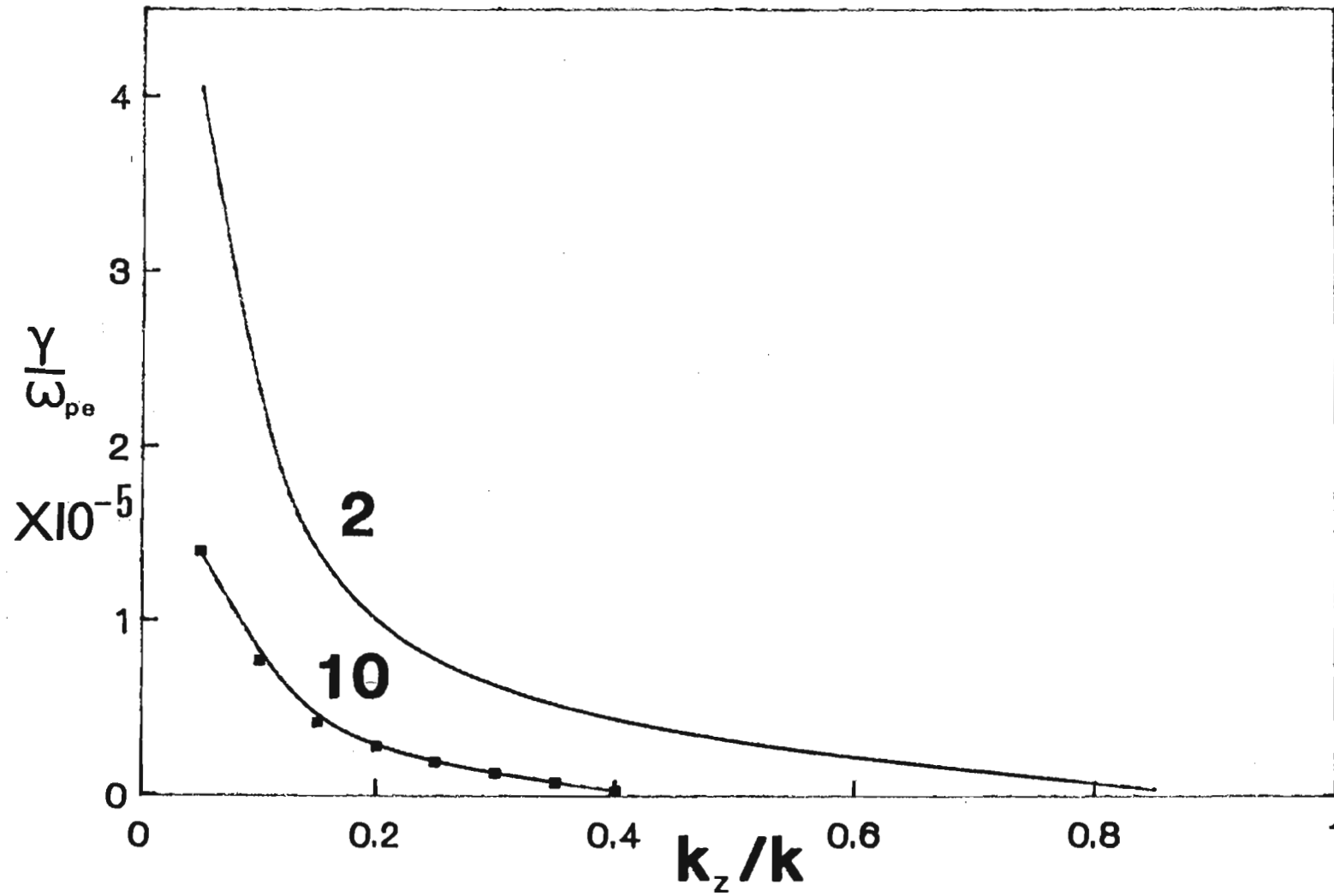
Graph (2): Doppler-shifted wave speed as a function of  $k_z/k$ .

$V_L/c_e = V_H/c_e = V_0/c_e = 0.01$ ,  $\theta = 50$ ,  $M = 10$ , zero electron drift.

The heavy to light ion mass ratio was decreased by increasing the light ion mass and keeping the heavy ion mass fixed. This results in an increase in both the growth rate and the cut-off angle (Figure 5.10). Here the ion drift velocities were taken to be equal and there were no inhomogeneities.

An increase in  $M$  (with  $M_H$  fixed) leads to a decrease in the phase velocity, as can be deduced from eqn (5.1.3), and hence a decrease in growth rate (as the wave now 'sees' a smaller negative slope on the electron velocity distribution function).

# Fig 5.10



Normalised growth rate for drifting ions as a function of  $k_z/k$ .  $\theta = 50$ , and the other fixed parameters are the same as in Fig. 5.7. Parameter labelling the curves is  $M = M_H/M_L$ .

CHAPTER SIX

SUMMARY AND CONCLUSION

Linear kinetic theory has been used to set up the dispersion relation for electrostatic instabilities in a collisionless, magnetized two-ion plasma with crossfield drifts. The initial model consisted of drifting Maxwellian electrons and stationary ions. Previous studies (Nakamura, 1976a; Gledhill, 1982; Gledhill and Hellberg, 1987) have shown that the low frequency ion acoustic wave may propagate in two possible ways in a two-ion plasma. For  $\theta < 2M$ , where  $\theta = T_e/T_i$ ,  $M = M_H/M_L$ , two independent modes may co-exist, one being the principal mode associated with the heavy ions and the other the principal mode associated with the light ions. However, for  $\theta > 2M$  only one mode is possible, with a phase speed increasing continuously from the heavy ion sound speed to the light ion sound speed as the light ion fraction is increased from 0 to 1. In all our studies we have  $\theta > 2M$ .

Marginal stability studies have been made to investigate the effect of the light ion fraction,  $f$ , on the critical  $\vec{E} \times \vec{B}$  electron drift speed  $V_0^C$ , required to produce wave growth for the ion acoustic instability. It was found that  $V_0^C$  assumed a maximum value,  $(V_0^C)_{\max}$ , for a small percentage ( $f \sim 5\%$ ) of light ions. This "contaminant" damping behaviour agrees quite well with other similar investigations, e.g. Fried et al. (1971), and is associated with Landau damping of the principal heavy ion mode produced by the small fraction of light ions. The value of  $(V_0^C)_{\max}$  was found to be considerably smaller than that for the field-free plasma as investigated by Dell (1984). This may be

due to the fact that in a magnetized plasma, the electrons are free to move only along the external magnetic field  $\vec{B}_0$ . Thus their general freedom of motion in neutralizing any potential perturbations is restricted, thereby making it easier to excite an instability in a direction oblique to  $\vec{B}_0$ . Associated with this is the well known  $k/k_z$  enhancement in instability growth rate (Barrett and Hayzen, 1976).

Approximate analytic solutions have also been used to make comparisons with results from the full dispersion relation. The agreement between the two solutions is found to be better for smaller values of  $M$ .

The value of  $f$  at which the critical electron drift velocity assumes a maximum,  $f_{\text{peak}}$ , was found to rise sharply from 0.12 to 0.32 over the range  $2 < M < 5$ . This behaviour could be of significance in fusion oriented devices where the deuterium-tritium reaction is of importance. The ion Landau damping associated with the light ions is found to be the primary factor influencing wave growth.

Other parameter studies indicated that  $(V_0^C)_{\text{max}}$  increased as the heavy to light ion mass ratio ( $M$ ) was increased, while  $(V_0^C)_{\text{max}}$  decreased with an increase in propagation angle and magnetic field strength  $|\vec{B}_0|$ . However, no appreciable change in  $f_{\text{peak}}$  (the value of  $f$  for which  $(V_0^C)_{\text{max}}$  occurred) was observed.

Investigations of the dependence of the ion acoustic instability growth rate on the electron drift speed confirm the existence of a minimum drift speed required for instability growth. The results also show that there is a minimum value of  $\theta$  (the electron-ion temperature ratio) for which growth occurs. For the parameters used, this minimum value of  $\theta$  is approximately equal to 14. Results from

the full dispersion relation showed that the change in growth rate was insignificant for values of  $\theta$  above 100, a result also found by Lambert et al. (1976). This may be due to the fact that ion Landau damping becomes negligibly small at such large  $\theta$  values.

Inhomogeneities in external magnetic field, perpendicular electron temperature and electron density were found to produce a decrease in the growth rate. This is probably due to a decrease in the net electron drift produced by the associated gradient drifts in our model, and is consistent with the findings of Bharuthram (1974) for a single ion plasma.

For  $\theta < 100$ , the growth rates as obtained from the approximate analytic solutions of the dispersion relation are found to be generally larger than that for the full dispersion relation. This may be due to the total absence of ion Landau damping in the approximate solutions.

The effect of the magnetic field on the growth rate reveals that although the inhomogeneities in electron density and external magnetic field have a stabilising effect on the plasma for all values of  $b^{-1}$  ( $b = k_{\perp}^2 c_e^2 / \Omega_e^2$ ), the addition of a temperature gradient has a destabilising effect for  $b^{-1} \ll 1$ . Other authors (Priest and Sanderson, 1972 and Bharuthram, 1979) have also reported on this two-fold effect of the temperature gradient for a single-ion plasma.

Studies using a model consisting of drifting ions and stationary electrons in a two-ion plasma reveal that it is the slow mode with real frequency

$$\omega_R = k_y V_0 - k \{ f c_{SL}^2 + (1 - f) c_{SH}^2 \}^{1/2} (1 + k^2 \lambda_D^2)^{-1/2}$$

that becomes unstable. We note that since  $\omega_R - \vec{k} \cdot \vec{V}_0 < 0$ , this is a negative energy mode. The choice of parameters ( $\theta > 2M$ ) resulted in the propagation of a single mode whose growth rate increased with an increase in the ion beam velocities. Results using both equal and unequal ion velocities were obtained. In particular, it was found that the growth rate decreased when the heavy ion beam was given a velocity smaller than that of the light ion beam.

The effect of the light ion concentration on the growth rate for a plasma with drifting ions (the "contaminant" damping) was similar to that previously found for drifting electrons. For this model, the introduction of inhomogeneities in external magnetic field, perpendicular electron temperature and electron density tended to increase the growth rate. This was due to the electron gradient drifts being directed such that the relative ion-electron drift speed was increased. An increase in heavy to light ion mass ratio,  $M$ , (with the heavy ion mass fixed) resulted in a decrease in both the phase speed and the growth rate. This was associated with a decrease in electron Landau damping (which reduces the growth rate of a negative energy mode).

In discussing possible extensions to the work undertaken in this thesis, we note that all the studies have been done for  $\theta > 2M$ , for which value only a single ion acoustic mode propagates in the two-ion plasma. Thus a natural extension is to consider the region  $\theta < 2M$  and investigate the behaviour of the two independent ion acoustic modes which may coexist. Further, since we have dealt with a common

ion temperature,  $T_i$ , one may consider the case of unequal ion temperatures which is more realistic for ion-beam heating experiments.

The nonlinear evolution of plasma instabilities and their saturation are topics of much interest. Quasilinear theory could be used to study the saturation of the crossfield ion acoustic instability in a two-ion plasma. As regards to the nonlinear regime, solitons and double layers associated with such instabilities, especially in a magnetized plasma, are problems worthy of investigation.



REFERENCES

ABRAMOWITZ, M. and STEGUN, I.A. (1965).

Handbook of Mathematical Functions, New York: Dover Publications.

ALEXEFF, I., JONES, W.D. and MONTGOMERY, D. (1967).

Phys. Rev. Lett., 19, 422.

BARRETT, P.J., FRIED, B.D., KENNEL, C.F., SELLEN, J.M. and  
TAYLOR, R.J. (1972).

Phys. Rev. Lett., 28, 337.

BHARUTHRAM, R. (1974).

University of Natal, M.Sc. Thesis.

BHARUTHRAM, R. (1979).

University of Natal, PhD. Thesis.

BHARUTHRAM, R. and HELLBERG, M.A. (1974).

Plasma Phys. and Contr. Nucl. Fusion Research, 2, 693 (IAEA:  
Vienna).

BHARUTHRAM, R. and HELLBERG, M.A. (1982).

J. Plasma Phys., 28, 267.

BOYD, T.J.M. and SANDERSON, J.J. (1969).

Plasma Dynamics; Nelson.

CHEN, F.F. (1974).

Introduction to Plasma Phys., New York: Plenum Press.

DELL, M.P. (1984).

University of Natal, M.Sc. Thesis.

FRIED, B.D. and CONTÉ, S.D. (1961).

The Plasma Dispersion Function New York: Academic Press

FRIED, B.D., WHITE, R.B. and SAMEC, T.K. (1971).

Phys. Fluids, 14, 2388.

GABL, E.F. and LONNGREN, E.E. (1984).

Plasma Phys. and Contr. Fusion, 26, 799.

GARY, S.P. (1970).

J. Plasma Phys., 4, 753.

GARY, S.P. and BISKAMP, D. (1971).

J. of Phys. A, 4, 27.

GARY, S.P. and OMIDI, N. (1987).

J. Plasma Phys., 37, 45.

GARY, S.P. and SANDERSON, J.J. (1970).

J. Plasma Phys., 4, 739.

GLEDHILL, I.M.A. (1982).

University of Natal, PhD. Thesis.

GLEDHILL, I.M.A. and HELLBERG, M.A. (1987).

J. Plasma Phys., 36, 76.

HAYZEN, A.J. (1977).

University of Natal, PhD. Thesis.

HAYZEN, A.J. and BARRETT, P.J. (1977).

Phys. Fluids, 20, 1713.

HIROSE, A., ALEXEFF, I. and JONES, W.D. (1970).

Phys. Fluids, 13, 1290.

HIROSE, A., LONNGREN, K.E. and SKARSGARD, H.M. (1972).

Phys. Rev. Lett., 28, 270.

JACKSON, J.C. (1986).

Plasma Phys. and Contr. Fusion, 28, 669.

KRALL, N.A. and BOOK, D.L. (1969).

Phys. Fluids, 12, 347.

KRALL, N.A. and TRIVELPIECE, A.W. (1973).

Principles of Plasma Physics, New York: McGraw-Hill.

LAMBERT, A.J.D., SLUIJTER, F.W. and SCHRAM, D.C. (1976).

Physica, 84C, 394.

LAMBERT, A.J.D., SLUIJTER, F.W. and SCHRAM, D.C. (1977).

Physica, 85C, 357.

LASHMORE-DAVIES, C.N. (1971).

Phys. Fluids, 14, 1481.

LASHMORE-DAVIES, C.N. and MARTIN, T.J. (1973).

Nucl. Fusion, 13, 193.

LONNGREN, K.E., KHAZEI, M., GABL, E.F. and BULSON, J.M. (1982):

Plasma Phys., 24, 1483.

MAJESKI, R.P., KOEPKE, M. and ELLIS, R.F. (1984).

Plasma Phys. and Contr. Fusion, 26, 373.

NAKAMURA, M., ITO, M., NAKAMURA, Y. and ITOH, T. (1975).

Phys. Fluids, 18, 651.

NAKAMURA, Y., NAKAMURA, M. and ITOH, T. (1976a).

University of Tokyo, Institute of Space and Aeronautical Science,  
Research Note RN13.

NAKAMURA, Y., NAKAMURA, M. and ITOH, T. (1976b).

Phys. Rev. Lett., 37, 209.

PRIEST, E.R. and SANDERSON, J.J. (1972).

Plasma Phys., 14, 951.

RAYCHAUDHURI, S., GABL, E.F., TSIKIS, E.K. and LDNNGREN, K.E. (1984).

Plasma Phys. and Contr. Fusion, 26, 1451.

SATO, N., SUGAI, H. and HATAKEYAMA, R. (1975).

Phys. Rev. Lett., 34, 931.

SEKAR, A.N. and SAXENA, Y.C. (1985).

Plasma Phys. and Contr. Fusion, 27, 181.

TRAN, M.Q. and COQUERAND, S. (1975a).

Helv. Phys. Acta, 48, 477.

TRAN, M.Q. and COQUERAND, S. (1975b).

Helv. Phys. Acta, 48, 488.

TRAN, M.Q. and COQUERAND, S. (1976).

Phys. Rev., 14A, 2301.

WATSON, G. (1944).

A Treatise on the Theory of Bessel Functions, 2nd Ed.,

Cambridge: Cambridge University Press.

WONG, A.Y. and D'ANGELO, N. (1964).

Phys. Rev., 133, 436.

YAGURA, S., FUJITA, H. and ITOH, H. (1985).

Plasma Phys. and Contr. Fusion, 27, 827.